Technische Universität München

Wissenschaftszentrum Weihenstephan für Ernährung, Landnutzung und Umwelt
Experimentelle Radioonkologie und Strahlentherapie

Utilizing Heat Shock Protein 70 (Hsp70) as a Tumor-Specific Blood Biomarker and for the Isolation of Circulating Tumor Cells (CTCs)

Stephanie Breuninger, M.Sc.

Vollständiger Abdruck der von der Fakultät Wissenschaftszentrum Weihenstephan für Ernährung, Landnutzung und Umwelt der Technischen Universität München zur Erlangung des akademischen Grades eines Doktors der Naturwissenschaften genehmigten Dissertation.

Vorsitzender:	Prof. Dr. Bernhard Küster
Prüfer der Dissertation:	1. Prof. Dr. Gabriele Multhoff
	2. Priv.-Doz. Dr. Thomas E. Schmid

Die Dissertation wurde am 21.12.2017 bei der Technischen Universität München eingereicht und durch die Fakultät Wissenschaftszentrum Weihenstephan für Ernährung, Landnutzung und Umwelt am 06.03.2018 angenommen.

Table of Content

Abbreviations

°C	degrees Celsius
ATP	adenosine triphosphate
AUC	area under the curve
BSA	bovine serum albumine
CD	cluster of differentiation
CFSE	Carboxyfluorescein succinimidyl ester
CI	confidence interval
CK	cytokeratin
cm	centimeter
CSC	cancer stem cell
CTC	circulating tumor cell
CTM	circulating tumor microemboli
ctrl	control
CV	coefficient of variation
DAPI	4',6-diamidino-2-phenylindole
DEP	dielectrophoresis
dl	deciliter
DMSO	Dimethyl sulfoxide
DNA	deoxyribonucleic acid
e.g.	exempli gratia
EDTA	ethylenediaminetetraacetic acid
ELISA	Enzyme-Linked Immunosorbent Assay
EMT	epithelial-to-mesenchymal transition
EpCAM	epithelial cell adhesion molecule
ER	endoplasmic reticulum
FACS	fluorescence-activated cell sorting
FCS	fetal calf serum
FDA	Food and Drug Administratio
FITC	fluorescein isothiocyanate
FSMW	functionalized structured medical wire
Gb3	globoyltriaosylceramide
GTV	gross tumor volume

h	hour
H_2O dd	double-distilled water
HB	herringbone
HRP	horseradish peroxidase
HSBP1	heat shockfactor binding protein 1
Hsc	heat shock cognate protein
HSF	heat shock factor
Hsp	heat shock protein
Ig	immunoglobulin
ISET	isolation by size of epithelial tumor cells
kDa	kilodalton
lip	liposomal
LoB	limit of blank
LoD	limit of detection
M	molar
mA	milliampere
mAb	monoclonal antibody
MET	mesenchymal-to-epithelial transition
MET ≙ HGFR	hepatocyte growth factor receptor
mg	milligram
min	minutes
miRNA	micro ribonucleic acid
ml	milliliter
mm	millimeter
MVB	multivesicular body
µg	microgram
µl	microliter
µm	micrometer
NK cells	natural killer cells
nm	nanometer
NSCLC	non-small cell lung cancer
OD	optical density
PBMC	peripheral blood mononuclear cell
PBS	phosphate buffered saline

pg	picogram
POPC	1-palmitoyl-2-oleoyl-*sn*-glycero-3-phosphocholine
POPS	1-palmitoyl-2-oleoyl-*sn*-glycero-3-phospho-L-serine
Rab-4	
RBC	red blood cell
ROC	receiver operating characteristics
rpm	revolutions per minute
RT	room temperature
scFv	single-chain variable fragment
SDS-PAGE	sodium dodecyl sulfate polyacrylamide gel electrophoresis
sec	seconds
TGN	trans-golgi network
V	volt

Summary

Heat shock protein 70 (Hsp70) plays a key role in protein homeostasis, being involved in assisting protein folding, preventing protein aggregation and transporting proteins across membranes. Tumor cells frequently overexpress Hsp70 under physiological conditions and, in contrast to normal cells, present it on their plasma membrane, which is associated with increased malignancy and resistance to chemo- and radiotherapy. However, membrane-bound Hsp70 can also serve as a target for imaging and capturing of tumor cells. In addition to that, Hsp70 is actively released into the extracellular environment by viable tumor cells via exosomes, making it a promising blood biomarker for the detection and monitoring of cancer. Our group has developed the monoclonal Hsp70 antibody cmHsp70.1, which is able to detect free and lipid-bound Hsp70 on the membrane of tumor cells and on exosomes. This makes it a valuable tool for the detection of Hsp70 in various body fluids and for the isolation of Hsp70-positive tumor cells.

In this project, the cmHsp70.1 antibody was used to develop a novel ELISA optimized for the detection of free as well as lipid-bound Hsp70 in serum and plasma samples (= lipHsp70 ELISA). Validation experiments showed a high assay precision and linearity. Spiking experiments revealed a significantly better recovery of Hsp70 in buffer and serum using the lipHsp70 ELISA compared to a widely used commercial ELISA. The lipHsp70 ELISA was equally suited for the analysis of serum and plasma samples and was not impacted by food intake of the proband, repeated freezing and thawing of the sample and moderate hemolysis. After successful establishment of the lipHsp70 ELISA, the Hsp70 serum levels of 114 healthy human volunteers and 197 cancer patients from six different tumor entities were analyzed. Significantly higher Hsp70 levels could be found in the serum of cancer patients of all entities.

Studying circulating tumor cells (CTCs) can help to understand the mechanisms of metastasis and they can serve as biomarkers for tumor progression and therapy monitoring. Most CTC detection methods rely on the epithelial cell adhesion molecule (EpCAM) as a target molecule. However, many CTCs undergo epithelial-to-mesenchymal transition (EMT) and might therefore be lost in these approaches. Therefore, a novel approach was pursued taking advantage of the unique binding capabilities of the cmHsp70.1 antibody to develop a CTC capturing method. To be

able to compare the performance of EpCAM- versus Hsp70-based isolation techniques, cancer cell lines with differential expression of both markers were selected. In a first approach, a magnetic bead-based method was developed. The recovery fractions of tumor cell lines from buffer and after spiking into blood of healthy donors were in line with the Hsp70 membrane status of the respective cell lines.

An inherent problem of most CTC isolation techniques is the limited volume of the analyzed blood samples. Therefore, the next step was to combine the cmHsp70.1 antibody with the GILUPI CellCollector®, a functionalized medical wire suitable for direct insertion into the patient's blood stream, which is currently used together with EpCAM antibodies.

The newly developed Hsp70 wire had a similar capacity to capture tumor cells with comparable Hsp70 and EpCAM expression like the EpCAM wire. The amount of tumor cells captured by the Hsp70 wire was associated with the intensity of the Hsp70 membrane expression, indicating reliability of the Hsp70 wire. Further optimization and an increased sample size are necessary to reveal significant differences between tumor cells with low and high Hsp70 membrane expression.

Zusammenfassung (Summary in German)

Das Hitzeschockprotein 70 (Hsp70) spielt eine entscheidende Rolle für die zelluläre Proteinhomöostase. Es ist beteiligt an der Proteinfaltung, verhindert die Aggregation von Proteinen und assistiert bei deren Transport über Membranen hinweg. Tumorzellen weisen bereits unter physiologischen Bedingungen eine erhöhte Hsp70-Expression auf. Darüber hinaus exprimieren Tumorzellen im Gegensatz zu normalen Zellen Hsp70 häufig auch auf der Plasmamembran. Studien zeigen, dass eine erhöhte Hsp70-Membranexpression mit erhöhter Malignität und Resistenz gegenüber Chemo- und Radiotherapie einhergeht. Membran-Hsp70 kann aber auch als Target für Tumor-Imaging oder die Isolierung von Tumorzellen dienen. Außerdem können Tumorzellen Hsp70 aktiv über Exosomen in den extrazellulären Raum abgeben. Hsp70 ist daher ein vielversprechender Tumorbiomarker. Unsere Gruppe hat den monoklonalen Hsp70-Antikörper cmHsp70.1 entwickelt, mit dem sowohl freies als auch lipidgebundenes Hsp70 auf Zellmembranen und in Exosomen detektiert werden kann. Der Antikörper ist daher sowohl für die Detektion von Hsp70 in verschiedenen Körperflüssigkeiten, als auch für die Isolierung Hsp70-positiver Tumorzellen vielseitig einsetzbar.

In diesem Projekt wurde der cmHsp70.1-Antikörper dazu verwendet, einen neuartigen ELISA zu entwickeln, der sowohl freies als auch lipidgebundenes Hsp70 in Serum und Plasma detektiert (= lipHsp70-ELISA). Validierungsexperimente konnten eine hohe Präzision und Linearität des Assays zeigen. Rekombinantes Hsp70-Protein konnte in Puffer- oder Serumproben mittels lipHsp70-ELISA signifikant besser detektiert werden als durch einen weit verbreiteten kommerziellen ELISA. Der lipHsp70-ELISA war gleichermaßen für die Untersuchung von Serum- und Plasmaproben geeignet und wurde nicht durch Nahrungsaufnahme des Probanden, wiederholtes Einfrieren und Auftauen der Probe, und moderate Hämolyse beeinflusst. Nach erfolgreicher Etablierung des lipHsp70-ELISAs wurden die Hsp70-Serumkonzentrationen von 114 gesunden Freiwilligen und von 197 Patienten mit sechs verschiedenen Tumorentitäten verglichen. In allen sechs Tumorentitäten wurden signifikant höhere Hsp70-Serum konzentrationen gefunden.

Die Erforschung zirkulierender Tumorzellen (CTCs) hilft, die Mechanismen der Metastasierung besser zu verstehen. Gleichzeitig können CTCs als Biomarker für

Tumorprogression und Therapie-Monitoring dienen. Die meisten Detektionsmethoden für CTCs basieren auf dem Epithelialen Zelladhäsionsmolekül (epithelial cell adhesion molecule, EpCAM). Allerdings durchlaufen viele CTCs die Epithelial-mesenchymale Transition (EMT) und könnten dadurch bei EpCAM-basierten Methoden der Detektion entgehen. Daher war das Ziel dieses Projekts, die einzigartigen Eigenschaften des cmHsp70.1-Antikörpers zu nutzen, um eine neue CTC-Detektionsmethode zu entwickeln. Um die Leistungsfähigkeit von EpCAM-basierten mit Hsp70-basierten Detektionsmethoden zu vergleichen, wurden Zelllinien mit unterschiedlich starker Expression beider Marker ausgewählt. In einem ersten Ansatz wurde eine auf magnetischen Beads basierende Methode entwickelt. Die Rückgewinnungsrate von Tumorzellen aus Puffer und nach Spiking in Blut von gesunden Spendern entsprach der jeweiligen Hsp70-Membranexpression der Zelllinien.

Eines der größten Probleme der meisten CTC-Isolierungsmethoden ist das eingeschränkte Volumen der Blutproben. Zur Weiterentwicklung der Methode wurde daher der cmHsp70.1-Antikörper mit dem GILUPI CellCollector® kombiniert, einem funktionalisierten medizinischen Draht, der direkt in ein Blutgefäß des Patienten eingeführt werden kann. Die derzeit erhältliche Version des CellCollectors verwendet EpCAM-Antikörper für die Zellisolierung. Der neu entwickelte Hsp70-Draht hatte eine ähnliche Kapazität Tumorzellen mit vergleichbarer Hsp70- und EpCAM-Expression zu binden wie der EpCAM-Draht.

Die Anzahl der mittels Hsp70-Draht isolierten Tumorzellen entsprach der Intensität der Hsp70-Membranexpression und bestätigt die Funktionsfähigkeit der neuen Methode. Eine weitere Optimierung und eine erhöhte Anzahl an Experimenten sind notwendig, um signifikante Unterschiede in Abhängigkeit vom Hsp70-Membranstatus zu zeigen.

1 Introduction

1.1 Biomarkers and Cancer

Cancer is among the leading causes of mortality worldwide with approximately 14 million new cases and 8.2 million deaths in 2012 (Stewart & Wild, 2014). In Germany, 25% of all deaths in 2013 were cancer-related, making cancer the second leading cause of death behind cardiovascular diseases (Statistisches Bundesamt, 2015). Successful treatment of cancer depends on the patient's response to the respective therapy. Due to tumor heterogeneity even within a single tumor entity, therapy response can vary significantly between patients, depending on tumor stage, the molecular characteristics of the tumor and the patient's characteristics including genetic disposition and the immune system (Kirkwood *et al.*, 2012). Therefore, today's therapy approach moves away from general treatment strategies for all patients towards a personalized treatment strategy for each individual patient. In order to identify and select patients for different treatment strategies, as well as for early tumor detection and disease monitoring, appropriate biomarkers are needed (Duffy & Crown, 2008).

A biomarker refers to any substance (genetic/epigenetic, proteomic, glycomic, enzymatic, pathological, molecular signatures, cells) or process that serves as an indicator of normal biological processes, pathogenic processes or pharmacologic responses to a therapeutic intervention and can be objectively measured and evaluated. A tumor biomarker is indicative for the presence of tumor cells in the body. Clinical practice guidelines for the use of tumor biomarkers are provided by the American Society of Clinical Oncology (ASCO) and the National Academy of Clinical Biochemistry (NACB) (American Society of Clinical Oncology, 2016; National Academy of Clinical Biochemistry, 2016). According to the National Cancer Institute, tumor biomarkers are defined as any substance found in the blood, urine, stool, tumor tissue, other tissues, or any other body fluids of patients with cancer that are produced by the cancer or by other body cells in response to the cancer (National Cancer Institute, 2016). In cancer, biomarkers can be used in screening for early malignancies, cancer detection, diagnosis and prognosis, as well as for the prediction of drug response or resistance and therapy monitoring (Duffy, 2001, 2007). In any

case, an ideal biomarker should have a strong predictive value, should be detectable by a simple and standardized assay and should be obtained with minimally invasive methods (Duffy, 2013). A variety of cancer biomarkers is already in clinical use or under investigation, one of the most commonly known probably being the kallikrein member prostate-specific antigen (PSA) (Bratt & Lilja, 2015). Kallikreins can be markers for the detection and monitoring of therapeutic outcome in patients with prostate, testicular, breast or ovarian cancer (Diamandis & Yousef, 2002). Another prominent example for a therapy-predictive marker is the human epidermal growth factor receptor 2, which is routinely used to select breast cancer patients for treatment with trastuzumab (Herceptin) (Moelans *et al.*, 2011). However, many biomarkers in cancer have been criticized for their lack of specificity or selectivity (Grunnet & Sorensen, 2012; Hayes & Barry, 2014; Loeb, 2014). In addition, it has proven to be very difficult to find a universal yet specific marker for the detection and prediction of different cancer types.

1.2 Heat Shock Protein 70 (Hsp70)

1.2.1 Structure and Function

The heat shock response was first described by Ritossa in 1962, when he discovered the upregulated expression of heat shock proteins (HSPs) in *Drosophila melanogaster* salivary gland cells after their exposure to elevated temperatures (Ritossa, 1962). In addition to heat, HSPs can be upregulated by various other stress stimuli including oxidative stress, hypoxia, altered pH, irradiation and chemical compounds like heavy metals and cytostatic drugs (Lindquist & Craig, 1988; Murphy, 2013).

According to their molecular weight ranging from 20 to over 100 kDa, HSPs are divided into different families. They are evolutionary highly conserved and play key roles in maintaining protein homeostasis, transport, degradation and protection against environmental stress. The HSP70 family is the best studied class of HSPs. As molecular chaperones, they mediate many different cell functions under physiological as well as under stress conditions. After exposure to external stress stimuli, Hsp70 proteins prevent protein aggregation by binding to hydrophobic residues of denatured client proteins and assist in their refolding or degradation

(Hartl, 1996; Lindquist & Craig, 1988). Under physiological conditions they are involved in the folding of nascent polypeptides and in transporting proteins across membranes, e. g. into mitochondria or the nucleus (Hartl & Hayer-Hartl, 2002; Stuart *et al.*, 1994). They are also potent inhibitors of apoptosis by neutralizing several proapoptotic effectors and signaling molecules (Garrido *et al.*, 2001).

Members of the HSP70 family consist of a ~43-kDa N-terminal nucleotide binding domain with ATPase activity, a highly conserved linker region, a ~15-kDa substrate binding domain, which interacts with hydrophobic amino acids in proteins and peptides, and a ~10-kDa C-terminal domain, which mediates co-chaperone binding (Bertelsen *et al.*, 2009; Flaherty *et al.*, 1990; Mayer, 2013; Zhu *et al.*, 1996).

The HSP70 family currently has eight identified human members, which are highly homologous and can be categorized by differences in localization (e. g. in the cytosol, mitochondria or endoplasmic reticulum), tissue-specific expression and stress-induced expression (Murphy, 2013). There are two major representatives of the HSP70 family: the heat shock cognate protein 70 (Hsc70) and the major stress-inducible heat shock protein 70 (Hsp70). They are present in all nucleated eukaryotic cells and show a high sequence homology of 86% (Daugaard *et al.*, 2007). Hsc70 is constitutively expressed in all cells and only moderately induced by stress (De Maio, 1999). It is therefore believed to carry out the majority of housekeeping functions of the HSP70 family (Murphy, 2013). In contrast, Hsp70 is highly upregulated after a variety of different stress stimuli (Lindquist & Craig, 1988) and is believed to play an important role in maintaining cell survival after stress (Murphy, 2013).

Hsp70 expression is induced by heat shock transcription factors (HSF), the main activator being HSF1. When activated by stress, HSF1 trimerizes and translocates to the nucleus where it binds to heat shock elements in the HSP genes and activates their transcription (Calderwood *et al.*, 2010; Wu, 1995). Inhibition of Hsp70 transcription occurs by negative feedback when Hsp70 binds to HSF1 (Shi *et al.*, 1998) or by binding of HSF1 to the heat shock factor binding protein 1 (HSBP1) (Satyal *et al.*, 1998).

In contrast to normal cells, Hsp70 has been shown to be highly upregulated in cancer cells already under physiological conditions (Jaattela, 1999). It protects the tumor

from cell death and correlates with tumor grade, proliferation, invasion, poor prognosis and drug resistance (Ciocca & Calderwood, 2005; Murphy, 2013).

1.2.2 Hsp70 on the Membrane of Tumor Cells

In addition to their upregulated cytosolic Hsp70 expression, tumors have been shown to frequently present Hsp70 on their plasma membrane (Multhoff *et al.*, 1995). This Hsp70 membrane-positivity has been found in a large variety of different tumor entities such as head and neck, lung, colorectal, pancreas, breast carcinomas and hematological malignancies, but not on the corresponding normal tissues (Hantschel *et al.*, 2000; Pfister *et al.*, 2007).

Experiments where tumor cells were treated with high salt, acid or basic conditions did not alter the Hsp70 surface expression (M. Gehrmann, Liebisch*, et al.*, 2008; Vega *et al.*, 2008). These results suggest that Hsp70 is not merely associated with other membrane proteins but rather interacts directly with the lipid bilayer of the plasma membrane, even though it does not possess a transmembrane domain. Lipid profiling revealed the interaction partners of Hsp70 in the membrane. Under non-stress conditions, Hsp70 interacts with the tumor-specific lipid component globoyltriaosylceramide (Gb3) in cholesterol-rich microdomains. Gb3-positive tumor cells were also able to bind soluble Hsp70 protein from outside; the interaction could be blocked with a Gb3-specific antibody or the depletion of Gb3 (M. Gehrmann, Liebisch*, et al.*, 2008). In addition, Hsp70 was found to interact with phosphatidylserine with high preference in artificial membranes as well as on stressed viable tumor cells (Arispe *et al.*, 2004; Schilling *et al.*, 2009; Vega *et al.*, 2008).

Our group has developed a unique mouse monoclonal antibody (mAb) cmHsp70.1, which detects the lipid-associated, membrane-bound form of Hsp70 on viable tumor cells. This antibody is highly specific for the stress-inducible Hsp70 and does not cross-react with the highly homologous constitutive Hsc70. It recognizes a non-conserved 8-mer epitope (453-460 NNLLGRFE) within the C-terminal oligomerization domain of Hsp70 (Stangl *et al.*, 2011), which is not recognized by other Hsp70 antibodies (Botzler, Li*, et al.*, 1998; Multhoff & Hightower, 2011). Regarding these findings, it is assumed that only a small part of the C-terminus, which is recognized by cmHsp70.1, is accessible or exposed to the extracellular milieu of tumor cells.

The membrane expression of Hsp70 on tumor cells is elevated after irradiation (M. Gehrmann *et al.*, 2005), treatment with tubulin-interacting chemotherapeutics (M. Gehrmann *et al.*, 2002) and under hypoxia (Schilling *et al.*, 2009). This finding is particularly important because all three conditions play a major role in tumor biology and treatment. Unfortunately, membrane Hsp70 also protects tumor cells against radiation- and chemotherapy-induced apoptosis (M. Gehrmann, Radons*, et al.*, 2008; Murakami *et al.*, 2015). When metastases were compared to the corresponding primary tumor, higher levels of membrane Hsp70 were found on the metastases in mouse tumor models as well as in samples from human patients (Botzler, Schmidt*, et al.*, 1998; Farkas *et al.*, 2003). All these data suggest that Hsp70-positivity indicates a more aggressive and treatment-resistant tumor type. In agreement with that, a membrane Hsp70-positive phenotype in patients with lower rectal carcinoma, squamous cell carcinoma of the lung (Pfister *et al.*, 2007) or malignant melanoma (Farkas *et al.*, 2003) was associated with a less favorable prognosis and significantly lower survival rate compared to Hsp70-negative tumor patients.

In contrast to this, Hsp70 on the membrane of tumor cells can also act as a recognition structure of the innate immune system. IL-2-activated natural killer (NK) cells display a higher lytic activity against Hsp70-positive tumor cells (Botzler *et al.*, 1996; Multhoff *et al.*, 1997). An incubation of the NK cells with Hsp70 protein or a 14-mer peptide (TKD), originating from the substrate binding domain of Hsp70, in combination with low-dose IL-2 has shown an enhanced cytolytic activity against Hsp70 membrane-positive tumors (Gastpar *et al.*, 2004; Multhoff *et al.*, 1999). This stimulation can be used for tumor patients who show a very low cytolytic activity against Hsp70 membrane-positive tumor cells. After promising results both *in vitro* and *in vivo* and a successful phase I study (Krause *et al.*, 2004), the effect of this immunotherapy as an adjuvant treatment after radiochemotherapy is currently under investigation in a phase II randomized clinical trial with non-small cell lung cancer (NSCLC) patients (Gunther *et al.*, 2015; Specht *et al.*, 2015).

Another approach to utilize Hsp70 as a target structure on tumor cells for therapy is currently investigated by Prof. Franz Rödel's group in Frankfurt. They loaded nanoparticles with miRNA directed against survivin, which is an inhibitor of apoptosis and is associated with increased proliferation and survival. Overexpression of survivin in cancer is known to enhance aggressiveness, metastatic potential and

therapy resistance. In order to direct these nanoparticles towards the tumor cells, they were coated with the cmHsp70.1 antibody (Stangl *et al.*, 2011). Treatment with these nanoparticles led to a reduction of survivin expression, induction of apoptosis and an enhanced response to irradiation of Hsp70-positive tumor cells *in vitro* (Gaca *et al.*, 2013).

In addition, membrane Hsp70 has been successfully used as a marker for *in vitro* and *in vivo* imaging of tumors with cmHsp70.1 in combination with fluorescence (M. Gehrmann, Stangl*, et al.*, 2014; Stangl *et al.*, 2014), gold nanoparticles (M. K. Gehrmann *et al.*, 2015) and superparamagnetic iron oxide nanoparticles (Shevtsov *et al.*, 2015).

In summary, membrane Hsp70 on tumor cells provides a tumor-specific molecular marker as well as a promising target for targeted therapies.

1.2.3 Hsp70 Release by Tumor Cells

Tumor cells not only present Hsp70 on their plasma membrane. In contrast to normal cells, they also release large amounts of Hsp70 into the extracellular environment. Accordingly, Hsp70 levels were found to be elevated in the serum of cancer patients (De Maio, 2011).

Presently, two major pathways are discussed as possible mechanisms for the release of Hsp70 by tumor cells. Hsp70 can be released from the cytosol by dying cells. However, evidence is accumulating that a major proportion of extracellular Hsp70 is actively released by living tumor cells with an intact plasma membrane via vesicular export (Gastpar *et al.*, 2005). Protein profiling of tumor-derived lipid vesicles revealed the presence of cytosolic (e.g. Hsp70) and endosomal proteins (e.g. Rab-4) in these vesicles. In contrast, endoplasmic reticulum (ER)-derived proteins were absent. In line with these findings, ER/Golgi-perturbing drugs like monensin and brefeldin A did not negatively impact the release of Hsp70-containing vesicles from tumor cells (Bausero *et al.*, 2005). According to their biophysical characteristics, such as their floating properties on a sucrose gradient, their small size of 50-100 nm and their high acetylcholinesterase activity, these vesicles could be identified as exosomes (Gastpar *et al.*, 2005).

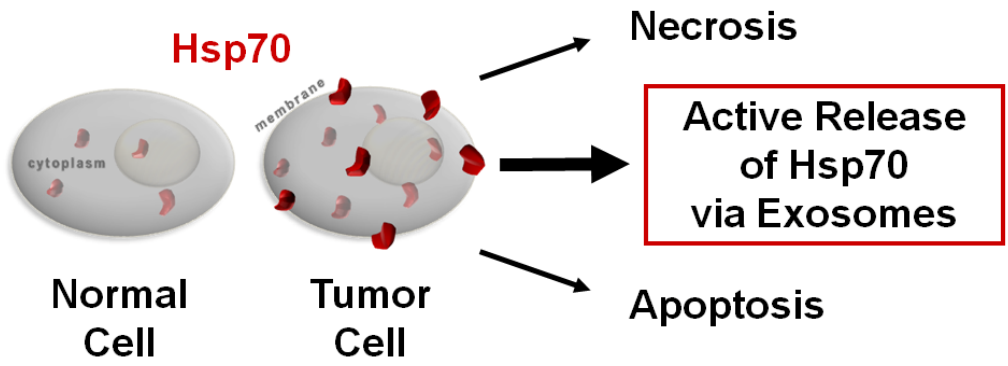

Figure 1: Pathways of Hsp70 release by tumor cells. Normal cells express low levels of Hsp70 in their cytosol. Tumor cells express higher cytosolic levels and, in contrast to normal cells, also frequently express it on their plasma membrane. Hsp70 can be released into the extracellular space during cell death. However, it has been shown that a major proportion of Hsp70 is actively released by living tumor cells via exosomes.

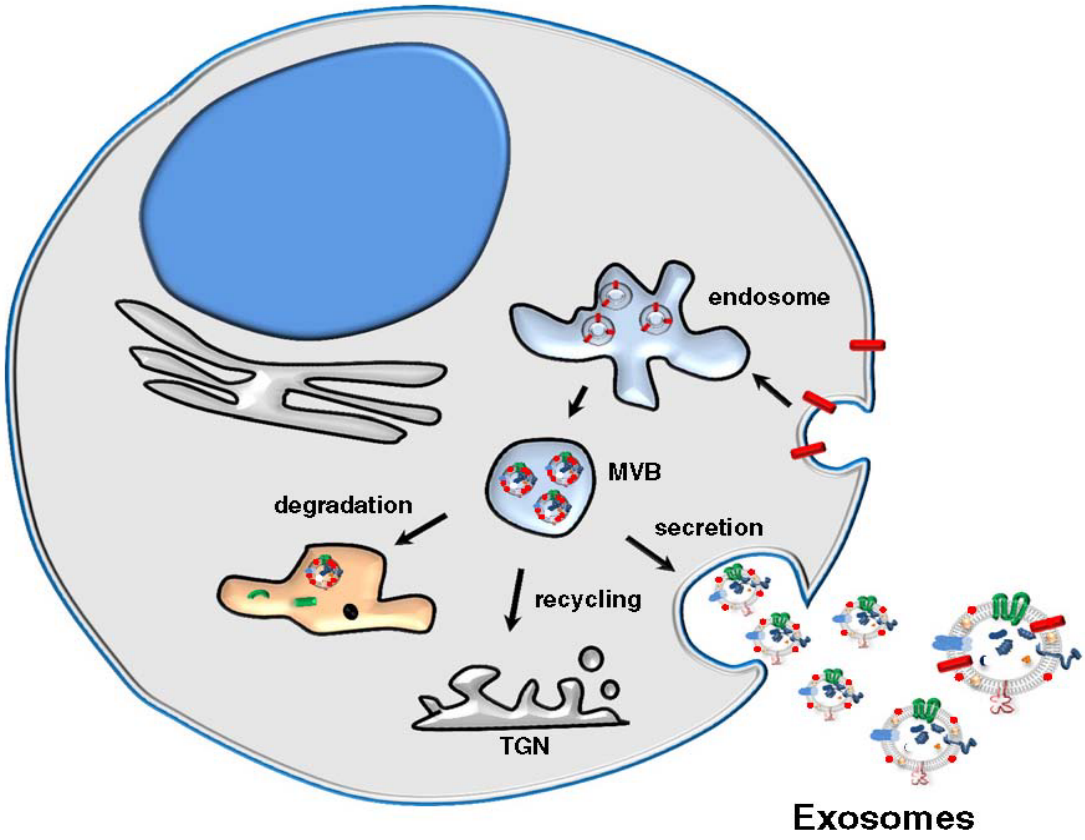

Figure 2: The mechanism of exosome formation. Exosomes are produced by a double inversion of the plasma membrane. First, multivesicular bodies (MVBs) are formed by an inward budding of the endosomal membrane. When these MVBs fuse with the plasma membrane of the cell, the smaller vesicles inside, the exosomes, are released into the extracellular space. TGN: trans-golgi network, MVB: multivesicular bodies. (Kharaziha *et al.*, 2012)

The formation of exosomes involves multivesicular bodies (MVBs), which are formed by an inward budding of the endosomal membrane (Mathivanan *et al.*, 2010). This results in vesicles that carry smaller vesicles in their lumen. When these MVBs fuse with the plasma membrane, the smaller vesicles, or exosomes, are secreted into the extracellular space (Thery *et al.*, 2009). Apart from tumor cells, a variety of cell types has been described to release exosomes, including different hematopoietic cells, intestinal epithelial cells, Schwann cells, neuronal cells, adipocytes and fibroblasts (Anand, 2010; Record *et al.*, 2011). Therefore, exosomes can be found in several different biological fluids like serum, plasma, urine, breast milk, ascites, synovial fluid and broncho-alveolar lavage fluid (Record *et al.*, 2011).

Since exosomes are produced by a double inversion of the plasma membrane, protein content and orientation of proteins in the exosomal membrane reflect that of the plasma cell membrane from which they are derived (Kharaziha *et al.*, 2012). As a result, tumor cells that express Hsp70 on their plasma membrane secrete exosomes that also exhibit Hsp70 on their surface (Gastpar *et al.*, 2005). Similarly, the protein composition in the exosomal lumen reflects that of the cytosol of the respective cell. It is therefore assumed that exosomes derived from normal cells carry low amounts of Hsp70, whereas exosomes from tumor cells with a high cytosolic Hsp70 content contain high amounts of Hsp70 in their lumen and additionally present it on their lipid surface (Mathivanan *et al.*, 2010).

Taken together, these results suggest that Hsp70 is a promising biomarker for tumor detection, which could be determined in patient blood using Enzyme-Linked Immunosorbent Assay (ELISA) techniques. However, depending on the ELISA test system that was used, the detected Hsp70 levels vary from pg/ml (Fredly *et al.*, 2012; Lebherz-Eichinger *et al.*, 2012; Lichtenauer *et al.*, 2014) and ng/ml (Lee *et al.*, 2015) to several µg/ml (Pockley *et al.*, 1998). This might be due to the fact that most commercially available Hsp70 ELISA kits are optimized and validated for the detection of free Hsp70 in aqueous buffer solutions but not serum. Furthermore, in case of undiluted serum (Njemini *et al.*, 2005), matrix effects need to be considered, which might negatively influence the detection of Hsp70 by the ELISA test. In conclusion, there is need for an improved system for the detection of Hsp70 as a biomarker in the blood of cancer patients.

1.3 Circulating Tumor Cells

1.3.1 Origin and Relevance

Apart from free proteins and exosomes, the peripheral blood offers other sources of cancer-derived material, such as circulating tumor DNA and circulating tumor cells (Speicher & Pantel, 2014). Circulating tumor cells (CTCs) are generated when cells are shed from the primary tumor and enter the blood stream. This process can start already very early during tumor development, long before metastases actually occur and even before the patient is diagnosed with cancer (Husemann *et al.*, 2008; Sanger *et al.*, 2011). It is widely accepted that the intravasation of tumor cells involves epithelial-to-mesenchymal transition (EMT) and that the reverse process, mesenchymal-to-epithelial transition (MET), supports the extravasation at distant sites (Hanahan & Weinberg, 2011). This, and the implications of single CTCs versus CTC clusters, will be described in more detail in 1.3.2.

CTCs are being extensively studied because they can provide additional information in several different respects: prognostic information such as risk for metastatic relapse or progression, therapy monitoring, identification of therapeutic targets and resistance mechanisms and understanding metastasis development in cancer patients (Alix-Panabieres & Pantel, 2012). For metastases to form, CTCs have to survive a hostile environment, which requires a series of stochastic events: cancer cell migration, local invasion, entry into the circulation, survival in the periphery of the body, arrest at secondary sites, extravasation and colonization, which involves the formation of micrometastases, possibly a long lasting latency phase and finally the formation of macrometastases (Vanharanta & Massague, 2013). This process is highly inefficient, especially the survival in the circulation and the colonization of distant organs (Chambers *et al.*, 2002). Even though CTCs are usually very rare, with a typical frequency of <10 CTCs in 1 ml of blood (Kraan *et al.*, 2011), some tumors release thousands of cells into the circulation each day, resulting in comparatively huge numbers of CTCs (Baccelli *et al.*, 2013; Nagrath *et al.*, 2007; Stott, Lee*, et al.*, 2010). The CTC count has been shown to correlate with decreased progression-free and overall survival in patients with breast, lung and colorectal cancer (Cohen *et al.*, 2009; Cristofanilli *et al.*, 2004; Krebs *et al.*, 2011). However, the probability for these cells to form a metastatic colony is very small, as they would have to overcome

endothelial barriers, an adversary immune system and the lack of survival signals (Vanharanta & Massague, 2013).

Nevertheless, some CTCs will survive and succeed to overcome endothelial barriers. A better understanding of the molecular characteristics and the mechanisms of CTCs will enable the development of new therapies. This fact and their contribution to cancer prognosis and therapy monitoring make the detection and characterization of circulating tumor cells a valuable tool in cancer research and therapy.

1.3.2 CTC Biology and Molecular Characterization

Circulating tumor cells can be found in the circulation not only as single cells but also as cell clusters, which consist of two to more than 50 CTCs (Cho *et al.*, 2012; Liotta *et al.*, 1976). These large clusters are called circulating tumor microemboli (CTM). Traveling in clusters can provide the tumor cells with a survival benefit through sustainment of cell-cell contacts, survival signals and protection from shear forces (Aceto *et al.*, 2014; Hou *et al.*, 2012).

Aceto *et al*. have recently characterized these clusters in more detail. They could show that CTC clusters are not generated by the proliferation of a single CTC or aggregation in the blood stream but are cell aggregates that are directly shed from the primary tumor. In mouse experiments, these clusters had a 50-times higher metastatic potential than single cells, even though they comprised only 2.6% of all detected events. In accordance with these findings, breast and prostate cancer patients with CTC clusters had a significantly reduced overall survival compared to patients with only single CTCs. They identified the overexpression of plakoglobin, a component of desmosomes and adherence junctions, as the main mediator in the formation of CTC clusters. (Aceto *et al.*, 2014)

Most tumors are of epithelial origin. Therefore, the corresponding CTCs mostly express epithelial markers like EpCAM (epithelial cell adhesion molecule), and cytokeratins like CK8, CK18 and CK19 (Jolly *et al.*, 2015). These markers are often used to isolate and identify CTCs (see 1.3.3). However, many studies have shown that the intravasation of CTCs involves epithelial-to-mesenchymal transition (EMT), which can lead to the loss of these markers. The mesenchymal state makes cells more motile and invasive, which of course enhances their ability to spread to distant

sites (Jolly *et al.*, 2015). Yu *et al.* found that benign and pre-invasive tumor tissue is exclusively epithelial, while invasive breast cancer tissue contains rare cells and clusters that are positive for epithelial as well as mesenchymal markers. They isolated CTCs with a predominantly mesenchymal phenotype in patients with a more aggressive type of breast cancer. After therapy, patients with progressive disease had an increased number of mesenchymal CTCs, while patients with a good therapy response had less mesenchymal CTCs (Yu *et al.*, 2013). It has also been shown that CTC clusters with a partial EMT, which show both epithelial and mesenchymal markers, often correlate with increased migratory behavior, invasiveness, metastatic potential, poor survival and drug resistance (Jolly *et al.*, 2015). These cells are also the most likely to gain “stemness” and become so-called cancer stem cells (CSCs), which are thought to be major mediators in metastasis (Grosse-Wilde *et al.*, 2015). Proposed CTC markers for these partial EMT cells include CD24 (epithelial marker), CD44 (mesenchymal, stem cell marker) (Zhang *et al.*, 2011) and P-cadherin (cell adhesion and cellular movement) (Ribeiro & Paredes, 2014). Baccelli *et al*. found CD44 and CD47 (immune evasion) on all CTCs in breast cancer patients. They also identified a subpopulation of MET-positive CTCs (hepatocyte growth factor receptor; associated with migration/invasion), which correlated with an increased number of metastatic sites and a decreased survival (Baccelli *et al.*, 2013).

In addition to being markers for prognosis and therapy monitoring, circulating tumor cells can teach us about metastasis, if we analyze them from a molecular and mechanistic point of view. This is particularly important because they represent a missing piece in the whole picture of cancer research. It has been shown that there can be major discrepancies in marker expression between the primary tumor and CTCs/metastasis (Vignot *et al.*, 2012). This in turn means that there is a need for new targeted therapies. However, only relatively few metastases are resected and analyzed. The reasons for this include limited accessibility and discomfort or pain for the patient. The isolation of circulating tumor cells is therefore an interesting alternative, serving as a “liquid biopsy” of the cancer patient that might predict characteristics of future metastases (Saucedo-Zeni *et al.*, 2012).

1.3.3 Detection Methods for CTCs

Detection and isolation methods for circulating tumor cells can be roughly divided into methods that utilize the physical properties of the cells, like size, density, electric charges and deformability, and methods that utilize the biological properties, like the expression of specific markers.

Density gradient centrifugation, e.g. with Ficoll, uses the floating properties of different cell types based on their differences in density. Several filtration methods are based on the usually larger size of CTCs compared to blood cells, e.g. the ISET filter (isolation by size of epithelial tumor cells) (Vona *et al.*, 2000) or a three-dimensional microfilter (Zheng *et al.*, 2011). The disadvantage of filtration-based methods is that smaller CTCs can get lost, while larger blood cells can get stuck in the filter. A special biochip combines differences in size with differences in deformability, as CTCs are normally stiffer than blood cells (Tan *et al.*, 2010). Several assays combine the dielectrophoresis (DEP) cell separation technique with different microfluidic chip systems, which use differences in membrane capacitance of the cells (Fuchs *et al.*, 2006; Gascoyne *et al.*, 2009; Moon *et al.*, 2011).

Methods based on biological properties of the cells predominantly make use of antibodies that are directed against different cell surface molecules. The antibodies are either immobilized a chip or coupled to magnetic beads or particles that are then collected with magnetic separation techniques. Some techniques use negative selection with antibodies directed towards the common leukocyte antigen CD45 (Liu *et al.*, 2011; Yang *et al.*, 2009), though most currently available techniques make use of markers on the tumor cells for positive selection.

Although many different antibody-based separation techniques have been developed, the vast majority is based on the epithelial cell adhesion molecule EpCAM. Among these, the CellSearch® system is seen as a “gold standard”, as it is the only isolation method that has been approved by the FDA (U.S. Food and Drug Administration) (Pantel *et al.*, 2009). Blood is collected in a 7.5 ml tube and processed in a half-automated system. First, blood plasma is removed and EpCAM antibody-coupled ferrofluids are added to the cells. After magnetic separation, the cells are stained with DAPI for the nucleus and antibodies directed against different cytokeratins. Finally, the cells are fixed, transferred to an analysis cartridge and analyzed with the microscope (Coumans & Terstappen, 2015).

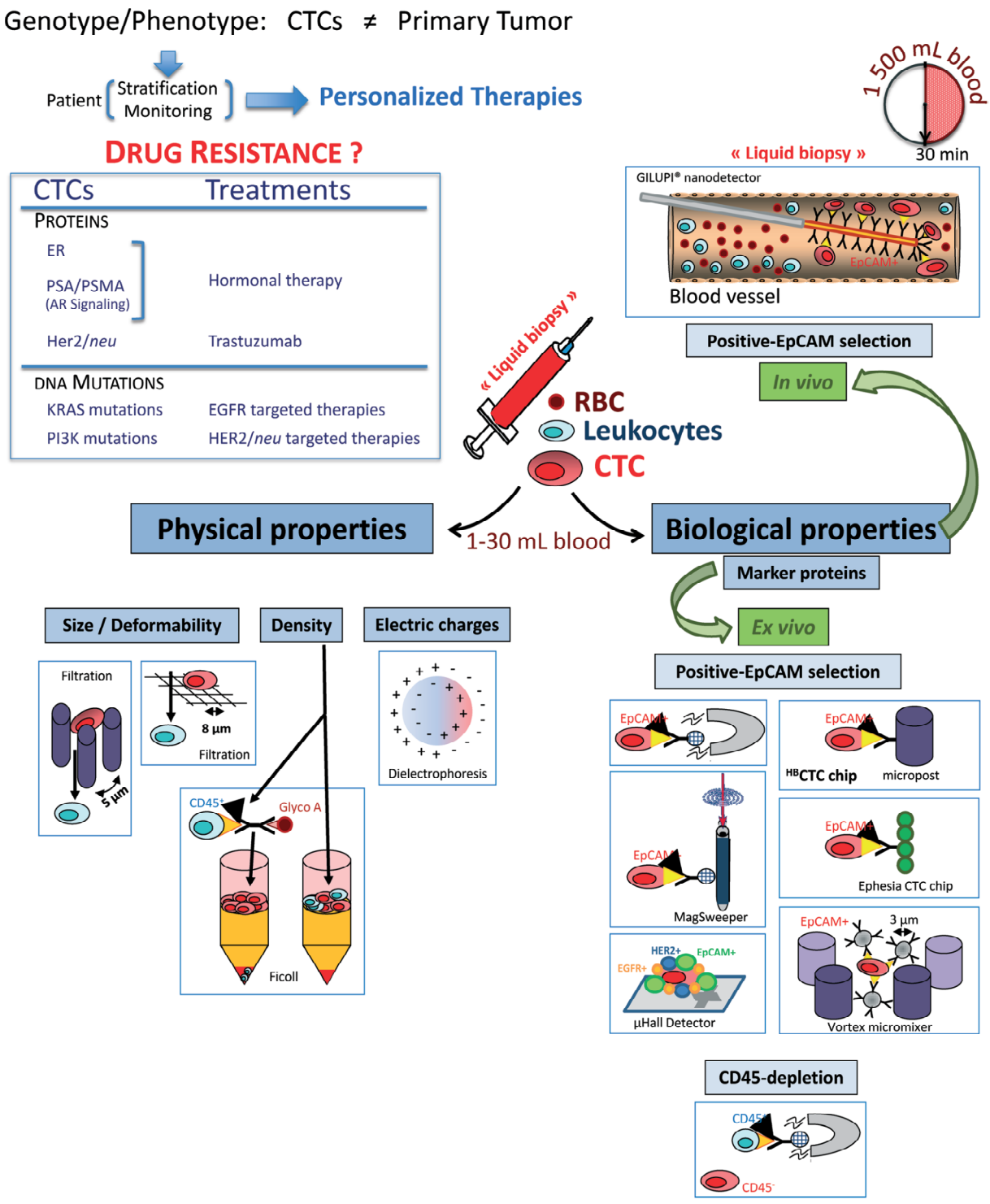

Figure 3: Existing methods for the detection of circulating tumor cells (CTCs). CTC detection methods can be roughly divided into methods based on the physical properties of the cells, like size, deformability, density and electric charges, and methods based on their biological properties. The latter include negative selection by removing CD45-positive blood cells as well as positive selection, which most commonly uses the epithelial cell adhesion molecule (EpCAM) to detect tumor cells. All these methods are limited in the volume of blood they analyze ex vivo. The GILUPI CellCollector® also uses EpCAM selection, but due to its direct placement in the blood vessel a much larger blood volume can be analyzed. Insights gained from analyzing CTCs can help our understanding of metastasis formation and present us with new targets for personalized therapies. (Alix-Panabieres & Pantel, 2014)

An example for a chip-based approach is the herringbone- or HB-chip. In this device, the anti-EpCAM antibodies are immobilized on a microfluidic array of channels. When a cell suspension is applied to the chip, the setup of these channels leads to the generation of microvortices that increase the number of contacts between the target cells and the antibody-coated surface of the chip. The cells are then stained directly on the chip (Stott, Hsu*, et al.*, 2010).

An inherent problem of most of these isolation techniques is the limited blood volume that is analyzed. Blood is usually collected in conventional blood collection tubes, with a capacity of a few milliliters (2.5 to 9 ml). As CTCs occur at very low frequencies, this limits the sensitivity of these systems significantly (Tibbe *et al.*, 2007). To address this issue, GILUPI developed the CellCollector®.

1.3.4 GILUPI CellCollector®

The GILUPI CellCollector® is designed to collect CTCs directly from the bloodstream. It is based on a Seldinger guidewire, a stainless steel medical wire of 0.5 mm diameter normally used for angiography or central venous catheters (Barber, 1989). To create the functionalized structured medical wire (FSMW), the first 20 mm of the wire are plated with a 2 µm gold layer covered by a hydrogel. Antibodies directed against EpCAM can then be coupled covalently to this hydrogel.

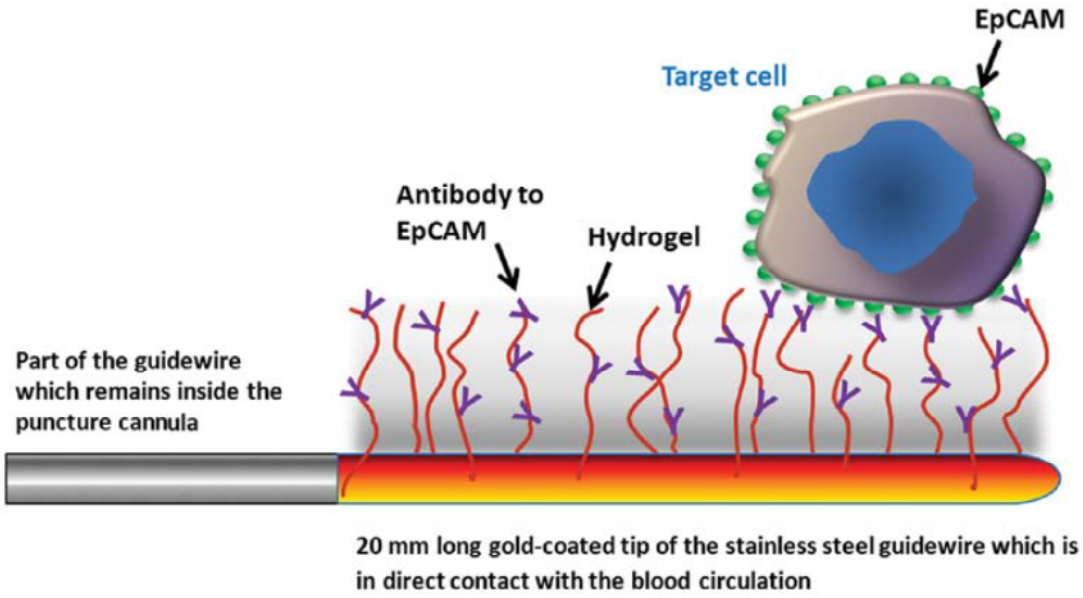

Figure 4: Setup of the GILUPI CellCollector®. The CellCollector® is based on a stainless steel Seldinger guide wire with a diameter of 0.5 mm, which is plated with a 2 µm gold layer. The gold is covered by a hydrogel, which can be covalently coupled to antibodies directed against cell surface molecules like EpCAM. (Saucedo-Zeni *et al.*, 2012)

To collect CTCs, the CellCollector® is inserted into the patient's cubital vein through an intravenous cannula. The wire remains in the bloodstream for 30 min. During this time, between 1.5 and 3 liters of blood pass the functionalized surface of the device and EpCAM-positive CTCs are captured and bound by the antibodies. The CellCollector® is then removed from the vein and cells can be stained directly on the wire, usually for cytokeratins and CD45 as a control (Saucedo-Zeni *et al.*, 2012).

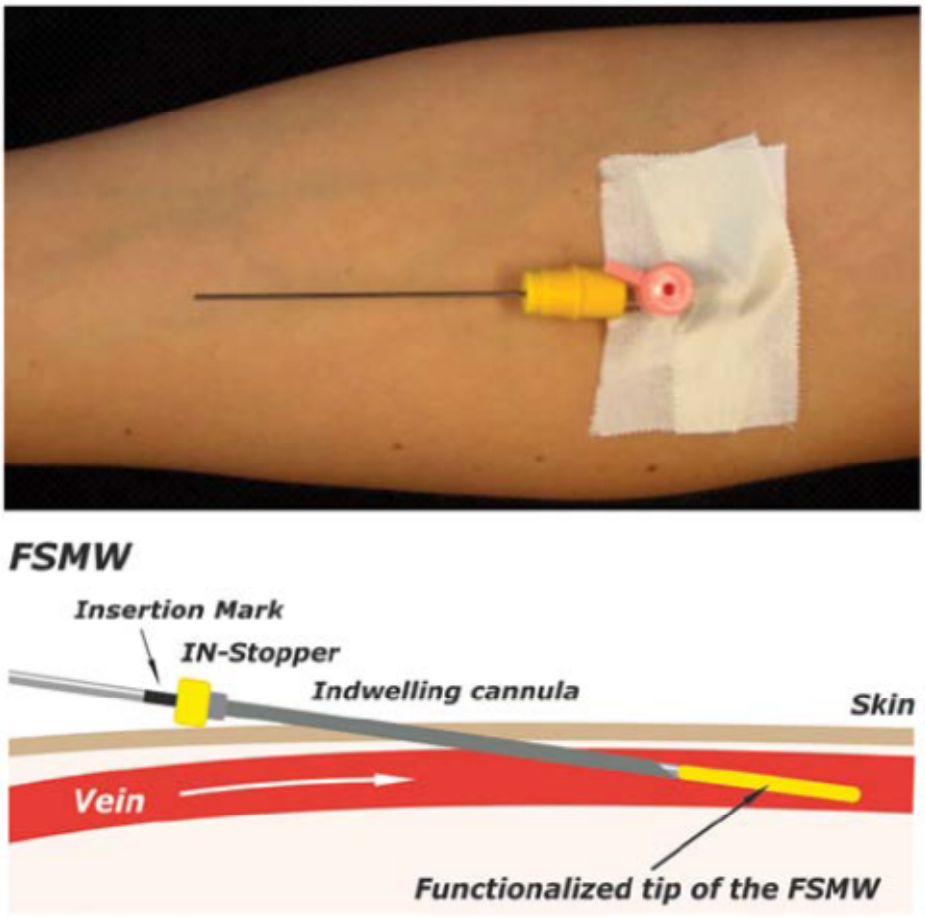

Figure 5: Application of the CellCollector® *in vivo*. The detector is inserted into the patient's cubital vein through an intravenous cannula and can remain in the blood stream for 30 min. While 1.5 to 3 liters of blood pass the wire, EpCAM-positive cells are captured on the functionalized surface. FSMW: functionalized and structured medical wire. (Saucedo-Zeni *et al.*, 2012)

As a CE-certified sterile medical device, the CellCollector® is well tolerated by patients and does not cause any adverse events. During *in vivo* application of the CellCollector® in patients with breast or non-small cell lung cancer (NSCLC), CTCs were collected in 91.6% of the patients. The number of collected cells ranged from 1-50 cells in breast cancer and from 2-515 in NSCLC with a median of 9.7 and

16 CTCs, respectively. No CTCs were captured in healthy control individuals (Saucedo-Zeni *et al.*, 2012).

1.4 Aim of the Study

There is a great need for biomarkers for the diagnosis, prognosis and therapy monitoring of cancer. However, most currently available biomarkers lack selectivity, specificity, sensitivity and, most importantly, universality. Blood-borne markers are often only applicable in a certain type of cancer. Similarly, methods to isolate circulating tumor cells as a cellular biomarker of cancer mostly rely on EpCAM antibodies as a capturing tool. However, cells with a downregulated or absent EpCAM expression after EMT cannot be captured. Hsp70 has been shown to be present on the cell surface of a wide variety of different tumor entities. In addition to that, Hsp70 is also released into the extracellular environment by many different tumors. It therefore has the potential to serve as a blood biomarker and a target for the isolation of CTCs.

The Hsp70 antibody cmHsp70.1 provides a valuable tool for the detection of Hsp70 and the isolation of Hsp70-positive tumor cells, as it offers the advantage of detecting not only soluble but also lipid-bound Hsp70.

The aim of this thesis was to use the cmHsp70.1 antibody for the development of

1. a novel ELISA for the detection of Hsp70 in the blood of cancer patients.
2. a new isolation technique for CTCs by combining the concept of the GILUPI CellCollector® and Hsp70 as a universal tumor cell marker.

2 Material and Methods

2.1 Material

2.1.1 Chemicals and Reagents

Chemical/Reagent	Company
2-Propanol (100%)	Carl Roth, Karlsruhe, Germany
Aceton	Carl Roth, Karlsruhe, Germany
Ammonium persulfate (APS)	Sigma-Aldrich, St. Louis, USA
Ammonium sulfate	Sigma-Aldrich, St. Louis, USA
Boric acid	Merck Millipore, Billerica, USA
Bovine serum albumin (BSA)	Sigma-Aldrich, St. Louis, USA
Bromphenole blue (BPB)	Sigma-Aldrich, St. Louis, USA
Dimethyl sulfoxide (DMSO)	Sigma-Aldrich, St. Louis, USA
Dithiothreitol (DTT)	Carl Roth, Karlsruhe, Germany
Glycerol	Sigma-Aldrich, St. Louis, USA
Glycine	Sigma-Aldrich, St. Louis, USA
Hoechst 33342	Thermo Fisher Scientific, Waltham, USA
Hydrochloric acid (32%)	Carl Roth, Karlsruhe, Germany
Imidazole	Carl Roth, Karlsruhe, Germany
Methanol	Carl Roth, Karlsruhe, Germany
Milk powder	Carl Roth, Karlsruhe, Germany
Nonidet P40	Sigma-Aldrich, St. Louis, USA
POPC (1-palmitoyl-2-oleoyl-*sn*-glycero-3-phosphocholine)	Avanti Polar Lipids, Alabaster, USA
POPS (1-palmitoyl-2-oleoyl-*sn*-glycero-3-phospho-L-serine)	Avanti Polar Lipids, Alabaster, USA
Propidium iodide (PI)	Merck Millipore, Billerica, USA
Protease inhibitor tablets	Roche, Basel, Switzerland
Rotiphorese Gel 40	Carl Roth, Karlsruhe, Germany
Sodium bicarbonate	Sigma-Aldrich, St. Louis, USA
Sodium carbonate	Merck Millipore, Billerica, USA

Sodium chloride	Carl Roth, Karlsruhe, Germany
Sodium dodecyl sulfate (SDS)	Carl Roth, Karlsruhe, Germany
Sodium hydrogen carbonate	Merck Millipore, Billerica, USA
Sodium hydroxide	Merck Millipore, Billerica, USA
Sodium phosphate	Merck Millipore, Billerica, USA
Sytox Red Dead Cell Stain	Thermo Fisher Scientific, Waltham, USA
Tetramethylethylendiamine (TEMED)	Carl Roth, Karlsruhe, Germany
Triton-X 100	Sigma-Aldrich, St. Louis, USA
Trizma Base (TRIS)	Sigma-Aldrich, St. Louis, USA
Tween 20	Merck Millipore, Billerica, USA

2.1.2 Solutions

Solution	Company
Coomassie solution Roti-Blue	Carl Roth, Karlsruhe, Germany
CrossDown Buffer	AppliChem, Darmstadt, Germany
Dulbecco's modified eagle's medium	Sigma-Aldrich, St. Louis, USA
Dulbecco's phosphate buffered saline (PBS)	Sigma-Aldrich, St. Louis, USA
Ethylenediaminetetraacetic acid (EDTA) (0.5 M)	Thermo Fisher Scientific, Waltham, USA
FACS lysing solution	BD Biosciences, San Jose, USA
Fetal calf serum (FCS)	Sigma-Aldrich, St. Louis, USA
HEPES (1 M)	Thermo Fisher Scientific, Waltham, USA
L-glutamine (200 mM)	Sigma-Aldrich, St. Louis, USA
Lymphocyte Separation Medium LSM 1077	GE Healthcare, Chalfont St. Giles, UK
Non-essential amino acids (NEAA)	Sigma-Aldrich, St. Louis, USA
Penicillin/streptomycin (10,000 U/ml PenNa, 10,000 µg/ml StrepSulfate)	Sigma-Aldrich, St. Louis, USA
Quick Start Bradford 1x Dye Reagent	Bio-Rad, Hercules, USA
RPMI 1640	Sigma-Aldrich, St. Louis, USA
Sodium pyruvate (100 mM)	Sigma-Aldrich, St. Louis, USA
TNM-FH insect cell medium	Allele Biotechnology, San Diego, USA

Trypan Blue (0.4%)	Sigma-Aldrich, St. Louis, USA
Trypsin/EDTA (0.05% Trypsin, 0.02% EDTA)	Sigma-Aldrich, St. Louis, USA
β-mercaptoethanol	Thermo Fisher Scientific, Waltham, USA

2.1.3 Buffers

Buffer	Composition	Solvent	Application
Bicarbonate buffer	0.1 M Na_2CO_3 (buffer A), 0.1 M $NaHCO_3$ (buffer B), (x parts of A) + ((100-x) parts of B), pH 9.6	dd	ELISA: coating
Blocking buffer (ELISA)	2% milk powder	PBS	ELISA: blocking
Wash buffer	0.05% Tween 20	PBS	ELISA: washing
Running buffer	25 mM Tris pH 8.3,190 mM Glycin, 0.1% SDS	dd	Gel electrophoresis
Transfer buffer	25 mM Tris pH 8.3,190 mM Glycin, 0.02% SDS	dd	Western Blot: transfer to NC membrane
TPBS	0.5% Tween 20	PBS	Western Blot: washing
Blocking buffer (WB)	5% Milk powder	PBS	Western Blot: blocking
Stacking gel buffer	0.5 M Tris pH 6.8	dd	Gel electrophoresis
Separating gel buffer	1.5 M Tris pH 8.8	dd	Gel electrophoresis
Loading buffer 4x (Lämmli)	200 mM Tris pH 6.8, 100 mM DTT, 8% SDS, 40% Glycerol, 0.1% BPB	dd	Gel electrophoresis
Coomassie staining solution	20% Roti-Blue, 20% MeOH	dd	Coomassie staining
Coomassie destaining solution	25% MeOH	dd	Coomassie destaining
Gel drying solution	10% Glycerol, 20% EtOH	dd	Gel drying

Sodium borate buffer pH 9.5	0.1 M H_3BO_3, pH adjustment: 5 M NaOH	dd	Beads: coating
Ammonium sulfate buffer	3 M $(NH_4)_2SO_4$	0.1 M sodium borate	Beads: coating
Blocking buffer (beads)	0.5% BSA, 0.05% Tween 20	PBS	Beads: blocking
Washing/Storage buffer	0.1% BSA, 0.05% Tween 20	PBS	Beads: washing/storage
FACS buffer	10% FCS	PBS	FACS: washing
IC Diluent #1	1% BSA	PBS	R&D ELISA
IC Diluent #4	1 mM EDTA, 0.5% Triton X-100	PBS	R&D ELISA
Insect cell lysis buffer	50 mM Tris pH 7.8, 150 mM NaCl, 1% Nonidet P40 2 Tablets protease inhibitor	dd	Hsp70 purification: lysis of Sf9 cell
Binding buffer	20 mM Na_3PO_4, 0.5 M NaCl, pH 7.4	dd	Hsp70 purification: binding to column
Elution buffer	20 mM Na_3PO_4, 0.5 M NaCl, 0.5 M imidazole	dd	Hsp70 purification: elution from column
Lymphocyte lysis buffer	10 mM $KHCO_3$, 155 mM NH_4Cl, 0.1 mM EDTA	dd	Lysis of lymphocytes
Rehydration buffer	25 mM Tris/HCl pH 7.4, 250 mM NaCl	dd	Lipid rehydration

2.1.4 Media

Cell line	Composition	Solvent
CT26	10% FCS, 1% Pen/Strep, 2 mM L-glutamine, 1% NEAA, 50 µM β-Mercaptoethanol	RPMI
A549, LN-229, SK-BR-3, U-87	10% FCS, 1% Pen/Strep, 2 mM L-glutamine, 1 mM sodium pyruvate	DMEM
cmHsp70.1, EPLC-272H, H1339, HeLa	10% FCS, 1% Pen/Strep, 2 mM L-glutamine, 1 mM sodium pyruvate	RPMI 1640
HCT-15, MIA PaCa	10% FCS	RMPI 1640
MCF7, MDA-MB-231, PANC-1, T47D	10% FCS, 1% Pen/Strep, 2 mM L-glutamine, 1 mM sodium pyruvate, 10 mM HEPES	RPMI 1640
Freezing medium	20% DMSO	RPMI 1640

2.1.5 Kits

Kit	Company
DuoSet Human/Mouse/Rat Total Hsp70	R&D Systems, Minneapolis, USA
Dynabeads MyOne Tosylactivated	Thermo Fisher, Waltham, USA
FluoReporter FITC Protein Labeling Kit	Thermo Fisher, Waltham, USA
MycoAlert Mycoplasma Detection Kit	Lonza, Basel, Switzerland
Pierce BCA Protein Assay Kit	Thermo Fisher, Waltham, USA
Pierce BSA standard	Thermo Fisher, Waltham, USA
Pierce ECL Detection Kit	Thermo Fisher, Waltham, USA
PKH26 Red Fluorescent Cell Linker Kit	Sigma-Aldrich, St. Louis, USA
Substrate Reagent Pack	R&D Systems, Minneapolis, USA
Vybrant CFDA SE Cell Tracer Kit	Thermo Fisher, Waltham, USA

2.1.6 Antibodies

Antibody (Clone)	Host	Isotype	Conjugate	Company
Anti-mouse	Rabbit	IgG	HRP	Dako, Glostrup, Denmark
EpCAM/CD326 (HEA125)	Mouse	IgG1	FITC	Acris, San Diego, USA
CK7 (LP5K)	Mouse	IgG2b	FITC	Millipore, Billerica, USA
CK19 (A53-B/A2)	Mouse	IgG2a	AF488	Exbio, Vestec, Czech Republic
CD45 (MEM-28)	Mouse	IgG1	AF647	Exbio, Vestec, Czech Republic
CD45	Mouse	IgG1	APC	Thermo Fisher, Waltham, USA
Mouse IgG1	Mouse	IgG1	APC	Thermo Fisher, Waltham, USA
Mouse IgG1	Mouse	IgG1	FITC	BD Biosciences, San Jose, USA
HLA Class I (W6/32)	Mouse	IgG2a	FITC	Sigma-Aldrich, St. Louis, USA
Hsp70	Rabbit	-	-	Davids Biotechnologie GmbH, Regensburg, Germany
cmHsp70.1	Mouse	IgG1	-	multimmune, Munich, Germany
cmHsp70.1	Mouse	IgG1	FITC	multimmune, Munich, Germany
panCK (4, 5, 6, 8, 10, 13, 18) (C11)	Mouse	IgG1	AF488	Exbio, Vestec, Czech Republic

2.1.7 Proteins and Standards

Protein or Standard	Company
EZ-Link Sulfo-NHS-LC-Biotin	Thermo Fisher, Waltham, USA
Full-Range Rainbow MW marker	GE Healthcare, Chalfont St. Giles, UK
Hsc70 (NSP-751)	Enzo Life Sciences, Farmingdale, USA
Hsp70 (ESP-555)	Enzo Life Sciences, Farmingdale, USA
Hsp70 (NSP-555)	Enzo Life Sciences, Farmingdale, USA
Streptavidin-HRP	Thermo Fisher, Waltham, USA

2.1.8 Consumables

Consumables	Company
96 well plates	TPP, Trasadingen, Switzerland; Costar, Tewksbury, USA
Amersham Hyperfilm ECL High Performance chemiluminescence film	GE Healthcare, Chalfont St. Giles, UK
Cell culture dishes	TPP, Trasadingen, Switzerland
Cell culture flasks (25, 75, 162 cm^2)	Corning, Amsterdam, Netherlands
Cellophane sheets	Sigma-Aldrich, St. Louis, USA
Chamber slides	Nalgen Nunc, Rochester, USA
Cover slips	Thermo Fisher, Waltham, USA
Cryo tubes (2 ml)	TPP, Trasadingen, Switzerland
FACS tubes (5 ml)	Sarstedt, Nürmbrecht, Germany
HisTrap HP column (5 ml)	GE Healthcare, Chalfont St. Giles, UK
Injection needle	B. Braun, Melsungen, Germany
Injection needle 18G x 2”1.2 x 50 mm	B. Braun, Melsungen, Germany
Micro insertion tubes	MedChrom, Flörsheim-Dalsheim, Germany
Microscope slides	Thermo Fisher, Waltham, USA
Microscopy slides, poly-lysine coated	Thermo Fisher, Waltham, USA
Nitrocellulose membrane	GE Healthcare, Chalfont St. Giles, UK
PAP Pen	Sigma-Aldrich, St. Louis, USA
Parafilm	Sigma-Aldrich, St. Louis, USA
Pipette tips (10, 200, 300, 1000 µl)	Sarstedt, Nürmbrecht, Germany; Eppendorf, Hamburg, Germany
Pipettes (1, 2, 5, 10, 25, 50 ml)	Greiner, Frickenhausen, Germany
Polycarbonate membranes	Avanti Polar Lipids, Alabaster, USA
Reaction tubes (0.5 ml)	Eppendorf, Hamburg, Germany
Reaction tubes (1, 2 ml)	Sarstedt, Nürmbrecht, Germany
Reaction tubes (15, 50 ml)	Greiner, Frickenhausen, Germany
Reservoirs	VWR International, Radnor, USA
Safety Multifly Set	Sarstedt, Nürmbrecht, Germany
SealPlate	TPP, Trasadingen, Switzerland

Silicone stoppers with turn-up lip	Carl Roth, Karlsruhe, Germany
S-Monovette 7.5 ml Z	Sarstedt, Nürmbrecht, Germany
S-Monovette 9 ml K3E	Sarstedt, Nürmbrecht, Germany
Spectra/Por 1 Dialysis Tubing 6-8 kDa MWCO, 3.3 ml/cm	Spectrum Labs, Rancho Dominguez, USA
Syringe filters (0.22 µm)	TPP, Trasadingen, Switzerland
Syringes (5, 10, 50 ml)	B. Braun, Melsungen, Germany
Whatman blotting paper	GE Healthcare, Chalfont St. Giles, UK
Zeba Spin Desalting Columns	Thermo Fisher, Waltham, USA

2.1.9 Cell Lines

Cell line	Source	Origin
A549	Human	Lung carcinoma
cmHsp70.1	Human	Hybridoma
CT26	Mouse	Colon carcinoma
EPLC-272H	Human	Lung carcinoma
H1339	Human	Lung carcinoma
HCT-15	Human	Colorectal carcinoma
HeLa	Human	Cervix carcinoma
LN-229	Human	Glioblastoma
MCF7	Human	Mammary carcinoma
MDA-MB-231	Human	Mammary carcinoma
MIA PaCa	Human	Pancreas carcinoma
PANC-1	Human	Pancreas carcinoma
Sf9	Fall Armyworm	Ovaries
SK-BR-3	Human	Mammary carcinoma
T47D	Human	Mammary carcinoma
U-87	Human	Glioblastoma

2.1.10 Instruments and Equipment

Instrument/Equipment	Company
-20°C comfort	Liebherr, Bulle, Switzerland
4°C refrigerator	Liebherr, Bulle, Switzerland
-80°C Forma 88000 Series	Thermo Fisher Scientific, Waltham, USA
ÄKTAprime plus	GE Healthcare, Chalfont St. Giles, UK
Autoclave Tecnoclav	Integra, Plainsboro, USA
Biotek EL808 Microplate Reader	Biotek, Winooski, USA
Corning Stripettor plus pipetting controller	Corning, Amsterdam, Netherlands
Cryogenic storage system Biosafe	Cryotherm, Kirchen/Sieg, Germany
Direct Q3 ultrapure water system	Millipore, Billerica, USA
DynaMag-15	Thermo Fisher Scientific, Waltham, USA
DynaMag-2	Thermo Fisher Scientific, Waltham, USA
Electrophoresis Power Supply EPS 301	Amersham Biotech, Uppsala, Sweden
FACS Calibur	BD Biosciences, San Jose, USA
Freezing Container Mr. Frosty	Thermo Fisher Scientific, Waltham, USA
Gel electrophoresis system	Peqlab, VWR, Radnor, USA
Hemocytometer	Carl Roth, Karlsruhe, Germany
Heraeus Fresco 17	Thermo Fisher Scientific, Waltham, USA
Heraeus Multifuge 3S-R	Thermo Fisher Scientific, Waltham, USA
Hettich Zentrifugen Mikro 22R	Hettich Lab Technology, Tuttlingen, Germany
Ice machine AF100	Scotsman, Milan, Italy
Incubator Heraeus BBD 6220	Thermo Fisher Scientific, Waltham, USA
Incubator TECO 20	Selutec, Hechingen, Germany
Magnetic Stirrer	Heidolph, Schwabach, Germany
Mini Extruder	Avanti Polar Lipids, Alabaster, USA
Multichannel pipette	Eppendorf, Hamburg, Germany
Pipettes	Eppendorf, Hamburg, Germany
Rotator Intellimixer RM-2	Omnilab, Bremen, Germany
Scale EW620-3NM	Kern, Balingen, Germany
Scanner Bear Paw 2400 TA Plus	Mustek, Hsinchu, China
Shaker 3015	GFL, Burgwedel, Germany

Sorvall Discovery M120 SE Micro-Ultracentrifuge	Kendro Laboratory Products (Newtown, Connecticut, USA)
Sorvall S52-ST Swinging Bucket Rotor	Kendro Laboratory Products (Newtown, Connecticut, USA)
Sorvall S55-A Fixed Angle Rotor	Kendro Laboratory Products (Newtown, Connecticut, USA)
Thermo Scientific Megafuge 1.0 R	Thermo Fisher Scientific, Waltham, USA
Tilting shaker PMR-30	Thermo Fisher Scientific, Waltham, USA
Vortex-Genie 2	Carl Roth, Karlsruhe, Germany
WB Development machine	Kodak, Rochester, USA
Western blot system Hoefer Semiphor	GE Healthcare, Chalfont St. Giles, UK
Zeiss Axio Imager.M2	Zeiss, Jena, Germany
Zeiss Axio Observer.Z1	Zeiss, Jena, Germany
Zeiss Axiovert 135	Zeiss, Jena, Germany
Zeiss Axiovert 40C	Zeiss, Jena, Germany

2.1.11 Software

Software	**Company**
Adobe Photoshop Elements 12	Adobe Systems, San Jose, USA
AxioVision SE64 Rel. 4.9	Zeiss, Jena, Germany
CellQuest Pro 6.0	BD, San Jose, USA
ImageJ 1.49h	Wayne Rasband National Institute of Health, USA
Microsoft Office 2013	Microsoft, Redmond, USA
Sigma Plot 12.5	Systat Software, San Jose, USA

2.2 Methods

2.2.1 Cells

2.2.1.1 Culture of Cancer Cell Lines

Human and murine cancer cell lines were cultivated under standard conditions (37°C, 5% CO_2 and 95% humidity) in 25 cm^2 or 75 cm^2 cell culture flasks. Media and additives were adjusted to the respective cell line as specified in 2.1.4. Cells were split regularly every three to four days as follows: Old medium was removed from the flask and the cell layer was washed twice with PBS. Trypsin/EDTA was added and the cells were incubated at 37°C as recommended for each cell line (Table 1). The reaction was stopped with cell culture medium and the detached cells were resuspended evenly. An appropriate number of cells in new medium were then transferred into a new cell culture flask (Table 1) and cultivated under the conditions described above.

Table 1: Human and murine cancer cell lines with appropriate trypsinization times and cell numbers for seeding

Cell Line	Trypsinization	Cells per T75
A549	3 min	1 Million
CT26	1 min	0.5 Million
EPLC-272H	8 min	2 Million
H1339	4 min	1 Million
HCT-15	2 min	1 Million
HeLa	2 min	1 Million
LN-229	1 min	0.5 Million
MCF7	2.5 min	1 Million
MDA-MB-231	1.5 min	0.5 Million
MIA PaCa	2 min	0.5 Million
PANC-1	1 min	1 Million
SK-BR-3	3 min	0.4 Million
T47D	4 min	1 Million
U-87	1 min	0.5 Million

For experiments, cells were seeded at slightly higher cell numbers and usually used on day two or three after seeding. At that time point, the cells were in an exponential growth phase and confluence of the monolayer was about 80-90%. Cells were regularly tested for mycoplasma contamination and only clean cell cultures were used in experiments.

To determine the cell number, 20-30 µl of a cell suspension were transferred to a 96 well plate and mixed with an equal amount of trypan blue solution. The suspension was then pipetted into a Neubauer hemocytometer. Blue cells were counted as damaged or dead; only bright, clear cells were counted as intact and viable. The cell number was calculated according to the following equation: Cells/ml = n*d*10,000/q where n is the number of viable cells, d is the dilution factor (usually 2) and q is the number of quadrants (consisting of 4x4 smaller quadrates).

2.2.1.2 Cryoconservation

To sustain the cell bank stock and save cells for later experiments, cell cultures were expanded and frozen. For that purpose, cells were harvested as described in 2.2.1.1 and then washed once by centrifugating the cells at 500 g for 5 min and resuspending the pellet in PBS. After a second centrifugation step, the cells were resuspended in FCS and mixed with an equal amount of freezing medium. The suspension was then transferred to 2 ml cryo tubes. All steps were carried out on ice to minimize cell damage by DMSO in the freezing medium. The cryo tubes were put into a freezing container and stored at -80°C for at least 4 h. Isopropanol in the container leads to a constant decrease of the temperature at approximately 1°C per hour. For long term storage, cells were kept in a cryogenic storage system with liquid nitrogen.

To thaw cells, cryo tubes were briefly placed in a water bath and the cell suspension was then transferred into precooled cell culture medium. Cells were washed once with cell culture medium and pelleted by centrifugation. After resuspension in fresh medium, cells were seeded in cell culture flasks. Cells were allowed to recover for at least two to three passages before using them in further experiments.

2.2.1.3 Culture of Sf9 Insect Cells

Sf9 cells are derived from the ovarian tissue of the fall armyworm (*Spodoptera frugiperda*). They grow as a mixture of adherent cells and cells in suspension and are commonly used for recombinant protein production via transfection with baculovirus.

Cells were seeded at $3*10^6$ cells per T75 culture flask and grown in TNM-FH medium at 27°C without need for additional CO_2. The culture was expanded by splitting the cells every three to four days. Detachment of cells was achieved by rapping the flask sharply against the palm of the hand several times. Cells were then counted and seeded into new cell culture flasks.

For Hsp70 production, cells were transfected at seeding with 3 ml of supernatant from previous transfection experiments. The supernatant contained baculovirus coding for the Hsp70 protein. Cells were grown for four days and adherent as well as floating cells were harvested. After centrifugation at 500 g for 5 min, cells were washed once with cold PBS and the supernatant was removed completely. Finally, the dry cell pellet was frozen at -20°C and collected for later protein isolation and purification.

2.2.1.4 Isolation of PBMCs and Tumor Cells with Ficoll

Blood was collected from healthy volunteers in K3 EDTA tubes to prevent coagulation and mixed with at least an equal amount of RPMI 1640 medium. For bead experiments, cells from tumor cell culture were washed once with PBS and mixed into the blood at appropriate concentrations. Peripheral blood mononuclear cells (PBMCs) and tumor cells were isolated using a lymphocyte separation medium (LSM 1077) made with Ficoll density gradient medium. 10 ml of the LSM were pipetted into a 50 ml Falcon tube and the mixture of blood, tumor cells and medium was carefully layered above the LSM. The components were then separated by density centrifugation at 850 g and room temperature (RT) for 20 min. In order to avoid disruption of the layers, the break of

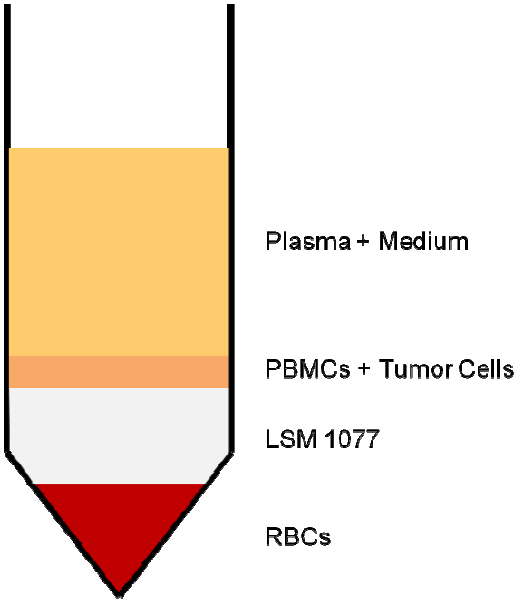

Figure 6: Cell layers after density centrifugation of blood and tumor cells with lymphocyte separation medium

the centrifuge was turned off. PBMCs and tumor cells were carefully extracted from the interphase between the plasma and the separation solution using a pipette (Figure 6). The cells were washed twice in medium (50 ml and 5 ml, respectively) with centrifugation at 700 g for 10 min. For further experiments, cells were allowed to recover under rotation in FACS buffer for 4 h.

For ELISA validation, erythrocytes from the lowest layer were isolated.

2.2.2 Proteins

2.2.2.1 SDS Polyacrylamide Gel Electrophoresis (SDS-PAGE)

Polyacrylamide gels were cast according to Table 2. The separating gel was covered with isopropanol and left to polymerize for 60 min. The stacking gel was added, a comb for the desired number of wells was inserted and the gel was allowed to polymerize for 30 min. Samples were mixed with a reducing loading buffer and incubated at 95°C for 10 min. After loading of the samples and an appropriate molecular weight marker, the gels were run at 20 mA per gel and 220 V for 1-1.5 h, separating the proteins according to their molecular weight.

Table 2: Composition of 10% separating and 5% stacking gels for SDS-PAGE

Component	Amount for one 10% Separating Gel (5 ml)	Amount for one 5% Stacking Gel (2.5 ml)
H_2O dd	2 ml	1.4 ml
Rotiphorese 40	1.65 ml	415 µl
Buffer (see 2.1.3)	1.25 ml	650 µl
10% SDS	50 µl	25 µl
10% APS	50 µl	25 µl
TEMED	2 µl	2.5 µl

After gel electrophoresis, gels were either stained with Coomassie blue solution or processed further for western blot analysis.

2.2.2.2 Coomassie Staining

For the analysis of protein content and purity of fractions after Hsp70 purification, SDS gels were stained with the Coomassie stain Roti-Blue. After SDS-PAGE, gels were incubated over night in Coomassie solution on a shaker. To reduce background staining, the gels were then incubated with destaining solution for several hours with repeated exchange of the solution. For documentation purposes, the gels were first scanned and then dried for long term storage. For that, the gel and two cellophane sheets were soaked in gel drying solution for 30 min, assembled in a drying frame and allowed to dry over night.

2.2.2.3 Western Blot

For specific identification, proteins were transferred from SDS gels to nitrocellulose membranes. Gel, membrane and four pieces of Whatman paper were soaked in transfer buffer for 15 min and assembled in a semi-dry western blot system. Blotting was carried out at 0.8 mA per cm^2 and 50 V for 45 min. Membranes were blocked with 5% milk powder in TPBS at RT for 1 h and then incubated with the primary antibody (1 µg/ml cmHsp70.1) in 1% milk powder in TPBS at 4°C over night. After three 10 min washing steps with TPBS, membranes were incubated with a horseradish peroxidase-conjugated secondary antibody (1:1000 Rabbit-anti-mouse-HRP) in 1% milk powder in TPBS at RT for 1 h. After another three washing steps, ECL substrate was pipetted onto the membrane and protein bands were visualized on hyperfilm at various exposure times.

2.2.2.4 Purification of Hsp70

Frozen pellets of transfected Sf9 cells containing His-tagged Hsp70 (2.2.1.3) were resuspended in ice cold insect cell lysis buffer at $4*10^6$ cells per ml. Cells were lysed for 45 min on ice with occasional vortexing. The lysate was transferred to 2 ml tubes and centrifuged at 10,000 g and 4°C for 30 min. The supernatant was collected, pooled and filtered through a 0.2 µm syringe filter to remove residual particles. After cleaning of the Äkta system, a 1 ml HisTrap column was installed and the whole system was rinsed with binding buffer. The lysate was loaded onto the column at 0.7 ml/min and the system was washed with binding buffer until the conductibility signal was stable. Hsp70 protein was eluted with an elution buffer gradient from

0-100% over 20 ml and fractions of 1 ml were collected. Finally, the system was washed with water and then ethanol.

Fractions were tested for protein content by mixing 10 µl of the respective fraction with 200 µl of a 1:5 dilution of Bradford dye in water. Samples with a color change to blue were analyzed with SDS-PAGE followed by Coomassie staining (2.2.2.1, 2.2.2.2). Fractions with high protein content and purity were pooled and dialyzed over night in Spectra/Por dialysis tubing in PBS with a buffer change after 4 h. After the buffer exchange the protein solution was filtered through a 0.2 µm syringe filter and protein concentration was determined with a BCA kit. Aliquots were stored at -20°C.

2.2.2.5 Labeling of Hsp70 with FITC

Hsp70 protein was labeled with FITC using the FluoReporter FITC Protein Labeling Kit. 1-2 mg of Hsp70 in PBS was labeled with a 40-fold molar excess of FITC by incubating the protein with the dye for 1 h at RT under continuous stirring. After preparation of a purification spin column, the sample was carefully loaded onto the column for the removal of remaining free dye. The protein was eluted by centrifugation at 1,100 g for 5 min. Estimated protein concentration was calculated according to the following equation: $c = m_0*0.85/V$ where m_0 is the amount of protein before the labeling process, 0.85 is the estimated yield (usually 80-90%) and V is the volume after purification with the spin column. Aliquots were stored at 4°C.

2.2.2.6 Labeling of cmHsp70.1 with Biotin

The mouse monoclonal antibody cmHsp70.1 was labeled with biotin using EZ-link sulfo NHS-LC-biotin. 1 mg of the antibody was labeled with a 40-fold molar excess of biotin in a total volume of 400 µl by incubating the mixture for 1 h at RT. Excessive biotin was removed using a Zeba Spin Desalting Column. Protein concentration was determined using a BCA kit and aliquots were stored at 4°C.

2.2.2.7 Protein Quantification

Protein concentration was determined using a BCA protein assay kit. A 2 mg/ml BSA stock solution was diluted for a nine point standard curve ranging from 0-1,000 µg/ml. AB solution was prepared by diluting solution B 1:50 in solution A. 25 µl of each standard or sample were pipetted into a 96 well plate and 200 µl of AB solution were

added to each well. After incubation at 37°C for 30 min, absorbance was measured at 550 nm in a microplate reader and the sample concentration was calculated from the standard curve.

2.2.2.8 Preparation of Lipid Vesicles with Hsp70

Lipid vesicles were prepared as described previously (Schilling *et al.*, 2009). Two lipids, 1-palmitoyl-2-oleoyl-*sn*-glycero-3-phosphocholine (POPC) and 1-palmitoyl-2-oleoyl-*sn*-glycero-3-phospho-L-serine (POPS), dissolved in chloroform, were mixed in a molar ratio of 8:2 and dried under nitrogen gas. The lipids were rehydrated at 10 mg lipid per ml of buffer for 1.5 h at RT under continuous rotation. Any precipitate was dissolved by vortexing. The Mini Extruder was assembled according to the manufacturer's instructions and the lipid suspension was loaded into one of the Hamilton syringes. The lipid suspension was then pushed through a 100 nm polycarbonate membrane 13 times to achieve uniformly sized vesicles. Vesicle concentration was adjusted to 1 mg/ml and 100 µl of the suspension were incubated with 1 µg recombinant Hsp70 for 30 min at RT. An equal amount of ultrapure water was added and the suspension was centrifuged at 200,000 g and 4°C for 2 h in an ultracentrifuge. The pellet was resuspended in PBS and stored at 4°C. As a control, empty vesicles were prepared accordingly.

2.2.3 Cell Biology

2.2.3.1 Flow Cytometry

To investigate the expression of various cell surface markers, cells were analyzed using flow cytometry. Cells were seeded two to three days before the experiment, harvested according to 2.2.1.1 and washed with cold FACS buffer. For each sample, 100,000 cells were transferred to a 1.5 ml reaction tube and washed again with cold FACS buffer. All steps were performed on ice. Cells were pelleted by centrifugation at 500 g and 4°C for 5 min and the supernatant was aspirated completely. Appropriate antibodies with fluorescent labeling were added and the mixture was incubated for 30 min on ice in the dark. Unbound antibody was removed in an additional washing step. Finally, the cell pellet was resuspended in 300-500 µl FACS buffer and the suspension was transferred to 5 ml FACS tubes. To distinguish between vital and dead cells, PI was added at a final concentration of 1 µg/ml and

only vital cells were gated in the analysis. Matched isotype controls were used as a negative control while MHCI was used as a positive control for human tumor cell lines. Samples were measured on a FACS calibur.

2.2.3.2 Prestaining of Cells with CFSE

CFSE staining of tumor cells was performed using the Vybrant CFDA Cell Tracer Kit. CFSE leads to an intracellular staining. The dye diffuses passively into the cell. It is colorless and non-fluorescent until its acetate groups are cleaved by intracellular esterases. The resulting succinimidyl ester groups react with intracellular amines, retaining the dye in the cell. Excess dye and by-products diffuse back into the surrounding medium and can be washed away (Wallace *et al.*, 2008). A 10 mM stock solution of the dye was prepared by dissolving the content of one vial from kit in 90 µl DMSO. The stock solution was then diluted to a 10 µM working solution with 0.1% BSA in PBS. Cells were harvested and washed once with PBS. Cell pellets smaller than 50 µl were resuspended in 600 µl, cell pellets larger than 50 µl were resuspended in 1000 µl of the dye. The suspension was incubated at 37°C for 15 min with occasional agitation of the vial for an even distribution of the cells throughout the incubation. The reaction was stopped with a tenfold excess of FACS buffer and the cells were pelleted at 500 g for 5 min. After two additional washing steps with PBS, the cells were resuspended in PBS and kept at 4°C for further experiments.

2.2.3.3 Prestaining of Cells with PKH26 Red

Tumor cells were stained with the PKH26 Red Fluorescent Cell Linker Kit. PKH26 Red is a lipid-like molecule with fluorescent head groups and long aliphatic tails. These tails integrate into the plasma membrane and are retained by strong non-covalent interactions with the surrounding lipids. Excess dye can be washed away after the staining reaction (Wallace *et al.*, 2008). The working solution of the dye was prepared by mixing 4 µl of the stock solution with 1 ml Diluent C. Cells were harvested, washed once with PBS and $20*10^6$ cells were resuspended in 1 ml Diluent C. The cell suspension was mixed with 1 ml of the working solution and incubated at RT for 5 min with periodic mixing. The reaction was stopped by adding 12 ml of FACS buffer and the cells were pelleted at 400 g and RT for 10 min. Excess dye was removed by washing the cells three times with FACS buffer and once with PBS. The cells were resuspended in PBS and kept at 4°C for further experiments.

2.2.3.4 Microscopy

For fluorescence microscopy, samples were analyzed using the Zeiss Axio Imager.M2 or the Axio Observer.Z1. Pictures were taken. Both microscopes were equipped with 10x, 20x, 40x and 100x objectives and standard filters. Image analysis and processing was performed using AxioVision SE64 Rel. 4.9 and Adobe Photoshop software.

2.2.4 ELISA Development

2.2.4.1 Commercial Hsp70 ELISA

As a control for the ELISA development, Hsp70 content of samples was analyzed in parallel with the DuoSet IC Human/Mouse/Rat Total Hsp70 ELISA (R&D Systems) according to the manufacturer's instructions. Briefly, 96 well plates from Costar were coated over night with 2 µg/ml capture antibody in PBS. After washing three times with 0.05% Tween-20 in PBS, the wells were blocked with Diluent #1 for 1.5 h at 27°C. Following another washing step, serum or other samples diluted in Diluent #4 were added to the wells for 2 h at 27°C. Then the wells were washed again and incubated with 100 ng/ml Detection Antibody in Diluent #1 for 2 h at 27°C. Finally, after another washing step, horseradish peroxidase-conjugated streptavidin in Diluent #1 was added for 20 min at 27°C. Binding was quantified by adding substrate reagent for 20 min at 27°C and absorbance was read at 450 nm, corrected by absorbance at 570 nm, in a microplate reader. An Hsp70 eight point standard was included into each ELISA test using 0-10 ng/ml recombinant Hsp70 diluted in Diluent #4.

2.2.4.2 LipHsp70 ELISA

The final protocol after Hsp70 ELISA development established as follows: 96 well MaxiSorp Nunc-Immuno plates were coated over night with 2 µg/ml rabbit polyclonal antibody, directed against human recombinant Hsp70, in sodium carbonate buffer. After washing three times with 0.05% Tween-20 in PBS, the wells were blocked with 2% milk powder in PBS for 1.5 h at 27°C. Following another washing step, serum samples diluted 1:5 in CrossDown Buffer were added to the wells for 2 h at 27°C. Then the wells were washed again and incubated with 4 µg/ml of the biotinylated mouse monoclonal antibody cmHsp70.1 in 2% milk powder in PBS for 2 h at 27°C.

Finally, after another washing step, 0.2 µg/ml horseradish peroxidase-conjugated streptavidin in 1% BSA was added for 1 h at 27°C. Binding was quantified by adding substrate reagent for 30 min at 27°C and absorbance was read at 450 nm, corrected by absorbance at 570 nm, in a microplate reader. An eight point Hsp70 standard was included into each ELISA test using 0-50 ng/ml recombinant Hsp70 diluted in CrossDown Buffer.

2.2.4.3 ELISA Validation

Linearity was evaluated according to the Clinical Laboratory Standards Institute (CLSI) guideline EP6-A. Briefly, six solutions of different Hsp70 concentrations were analyzed with the ELISA and their relative concentration was plotted against the system output (concentration according to ELISA measurement). First-, second- and third-order models were then fitted to the data and a *t*-test was applied to the non-linear coefficients of the second- and third-order models using SigmaPlot software. If none of the non-linear coefficients were significant ($p > 0.05$), the dataset was considered linear.

To determine intra-assay precision, control serum samples from two different donors were run in 20 replicates on a single plate. Inter-assay precision was assessed by running control serum samples in duplicate on three different days. The concentration was determined for each sample and the coefficients of variation (CVs) were calculated.

The limit of detection (LoD) was established according to the Clinical Laboratory Standards Institute (CLSI) guideline EP17-A as summarized by Arbruster and Pry (Armbruster & Pry, 2008). Briefly, optical density (OD) values of 36 blank samples and 36 samples with a low Hsp70 concentration (0.63 ng/ml) were converted to concentrations by back-calculating against the standard curve. The limit of blank (LoB) was calculated according to the following equation: $LoB = \mu_B + 1.645\sigma_B$, where μ_B and σ_B are the mean and standard deviation of the blank measurements, respectively. Finally, the LoD was calculated according to the following equation: $LoD = LoB + 1.645\sigma_S$, where σ_S is the standard deviation of the low sample measurements.

Recovery was assessed by spiking defined amounts of the respective standard Hsp70 into 1:5 diluted serum samples. The Hsp70 concentration of the serum alone was subtracted from the measured value and recovery was calculated as the ratio of observed concentration versus expected.

2.2.4.4 Collection of Serum and Plasma Samples

Blood samples were taken from 114 healthy human volunteers and patients with head and neck cancer (n=23), lung cancer (n=22), colorectal cancer (n=44), pancreatic cancer (n=46), glioblastoma (n=30) or hematological malignancies (n=32), who provided informed, written consent. Patient characteristics are summarized in Table 4. Blood was collected in one EDTA KE tube and one serum separator tube and mixed by gently inverting the tube. For plasma separation, EDTA blood was centrifuged at 1,500 g for 15 min. For serum collection, blood was allowed to clot for 15 min at RT and serum was separated by centrifugation at 750 g for 10 min. Serum from leukemia patients was allowed to clot for two to three hours and separated by centrifugation at 380 g for 5 min. Serum and plasma were stored in aliquots at -80°C. Approval of the study was obtained by the Ethics Committees of the universities who provided samples. All procedures were in accordance with the Helsinki Declaration of 1975 as revised in 2008.

To validate the ELISA, the interference factors food intake of the blood donor, repeated freezing and thawing and hemolysis of the serum samples were tested. To test the influence of food intake, serum samples were collected from healthy individuals before and 2 h after intake of a high-fat diet. Repeated freezing and thawing procedures of up to ten cycles were performed on some of the serum samples. In order to study the impact of hemolysis on the assay, erythrocytes were isolated from the blood of healthy donors by density gradient centrifugation using LSM1077 (2.2.1.4). Erythrocytes were lysed by applying shear stress and the corresponding serum samples were spiked with increasing amounts of the lysed erythrocytes. The hemoglobin content of the spiked serum samples was analyzed by measuring the absorbance of the samples at 562 nm, 578 nm and 598 nm. The hemoglobin concentration was calculated as described elsewhere (Kahn *et al.*, 1981).

2.2.5 Development of a CTC Detection Method

2.2.5.1 Coupling of cmHsp70.1 to Dynabeads MyOne Tosylactivated

Coupling of cmHsp70.1 antibody to Dynabeads MyOne Tosylactivated was carried out according to the manufacturer's protocol. All steps were performed in 1.5 ml reaction tubes. Briefly, 500 µl beads (corresponding to 50 mg) were washed twice by placing them in the DynaMag for 2 min, removing the supernatant and resuspending the beads in coating buffer. In addition to the 50 mg beads, the coating mixture contained 1 M ammonium sulphate and 2 µg antibody (corresponding to 40 µg per mg beads). Appropriate volumes for the coating buffer, the antibody and the 3 M ammonium sulphate stock solution were calculated for a total volume of 1250 µl. The mixture was prepared by resuspending the beads in coating buffer, followed by addition of the antibody and the ammonium sulphate stock solution. After thorough resuspension, the mixture was incubated for 16-24 h at 37°C with slow rotation. The tube was then placed in the DynaMag for 2 min and the supernatant was removed. After resuspension of the beads in 1250 µl blocking buffer, the beads were blocked over night at 37°C with rotation. Finally, the beads were washed three times and resuspended in 1 ml washing/storage buffer with 0.02% sodium azide. Aliquots of 50 µl were stored at 4°C.

Success of the coupling reaction was tested with FITC-labeled Hsp70. A 10 µl aliquot of the beads was washed three times with 0.1% BSA in PBS and incubated with 5 µg FITC-labeled Hsp70 in a total volume of 250 µl for 30 min at 4°C with rotation. The beads were washed again three times and then analyzed in a fluorescence microscope.

2.2.5.2 Cell Isolation with Dynabeads MyOne Tosylactivated

A 50 µl aliquot of beads was washed three times with 0.1% BSA in PBS. Tumor cells or a mixture of tumor cells and lymphocytes after Ficoll (2.2.1.4) were resuspended in 0.1% BSA in PBS. The beads and 500,000 tumor cells were mixed in a total volume of 250 µl and incubated at 37°C for 1 h. The tube was placed in a DynaMag and beads were separated from the supernatant. The cell number in both fractions was counted and compared as percentage of the total number of cells.

2.2.5.3 Binding of Cells to CTC Wire

2 ml reaction tubes were blocked with 3% BSA in PBS for 30 min and the lid was cut off. Tumor cells were harvested and washed twice with PBS. The cell number was adjusted to 100,000 cells/ml in PBS or EDTA blood and the reaction tubes were filled to the top. A detector was placed in a silicone stopper by sticking an injection needle into the stopper and inserting the wire into the needle. The needle was carefully removed, leaving the wire secured in the silicone stopper. The silicone stopper with the detector was then carefully placed on the reaction tube without touching the tube wall with the wire. To avoid shear stress, remaining air bubbles were removed from the tube. For that purpose, a few milliliters of the cell suspension were transferred to a 5 ml syringe with an injection needle and the needle was stuck into the silicon stopper. With a second needle as an outlet valve, the cell suspension was inserted into the tube until all air bubbles were removed. The wire was cut with pliers to fit into the rotator and the tube was incubated at 2 rpm and RT for 30 min. For some experiments the tubes were incubated on a tilting shaker at 30 rpm.

2.2.5.4 Staining of Cells on CTC Wire

After binding of tumor cells, the detector was washed four times by twirling it carefully twice in 1.6 mg/ml EDTA in PBS twice in PBS. For further experiments the detector was stored in PBS at 4°C. Cells were fixed by placing the detector in -20°C acetone for 30 s and then dried for 5 min at RT. The acetone also leads to a permeabilization of the cells. The detector was then blocked in 3% BSA for 30 min. Staining of the cells with a cocktail of different cytokeratin antibodies was performed at RT for 30 min in the dark. Afterwards, the detector was washed for 1 min in PBS and the cell nuclei were stained with Hoechst 33342 for 5 min at RT. After a final washing step the detector was stored in PBS at 4°C for a maximum of 6 h or dry at -20°C for a maximum of 7 days before analysis with fluorescence microscopy. For long term storage after analysis, detectors were stored dry at -80°C.

2.2.5.5 Counting and Documentation of Cells on CTC Wire

For fluorescence microscopy, the detector was secured on a microscopy slide with Parafilm or modeling clay in a way that the functional part protruded over the edge of the slide. The wire was brought into focus with the 10x objective and cells were located by Hoechst staining in the DAPI channel. For a definite identification, the

microscope was switched to the GFP channel for analysis of the CK staining. Representative pictures were taken with the 10x or 20x objective in both channels. The functional part of the detector was analyzed from the tip to the base, counting all events that could be identified as cells by their size, morphology and staining. Then, the wire was turned by 180° and the process was repeated.

2.2.5.6 Staining of Cells in Chamber Slides

Tumor cells were seeded in 8 well chamber slides at different cell numbers (5,000, 10,000, 20,000 and 40,000 per well). Two days after seeding, the wells with the optimal degree of confluence were selected for staining. Staining was performed as described in 2.2.5.4 with 200 µl of each reagent per well. Washing and blocking steps were performed with 300 µl per well. To avoid detachment of the cells, all reagents were pipetted against the wall of the wells and then aspirated carefully. Finally, wells were filled with PBS and analyzed with a fluorescence microscope.

2.2.5.7 Staining of Cells on Poly-Lysin Slides

Tumor cells were harvested and washed with PBS. The cell number was adjusted to 100,000 cells/ml and 20 µl of the suspension were applied to a poly-lysin coated slide. The surface tension of the liquid leads to a circular spot on the slide. To avoid disruption of the spots in later incubation steps, the spot was additionally encircled with a PAP pen. After incubation at RT for 30 min, the PBS was carefully removed with a Kimwipe and the cells were fixed with -20°C acetone. The cells were now firmly attached to the slide and could be frozen at -20°C for later use. Staining was carried out as described in 2.2.5.4. For fixation and washing steps, the whole slide was submerged into the liquid. Blocking and staining steps were performed by applying 20 µl and 10 µl spots to the slide, respectively. Finally, the spots were covered with PBS and cover slips and analyzed with a fluorescence microscope.

3 Results

3.1 The lipHsp70 ELISA

The following chapter contains figures and a supplemented version of the paper Breuninger *et al*., which was published in advance in the *Journal of Clinical & Cellular Immunology* (Breuninger *et al.*, 2015), as well as data from a paper in preparation.

3.1.1 ELISA Development and Optimization

Hsp70 is frequently overexpressed in tumor cells and can be actively released in lipid vesicles by viable tumor cells. Therefore, elevated Hsp70 serum levels have potential utility as biomarkers for the detection of viable tumor mass and to measure the response to therapeutic interventions. However, commercially available Hsp70 ELISAs are neither optimized for the measurement of Hsp70 in serum nor of lipid-associated Hsp70. Therefore, a novel Hsp70 ELISA based on the cmHsp70.1 antibody was established and blocking reagents, antibody combinations and serum diluent were optimized. The performance of the ELISA, termed lipHsp70 ELISA, was then compared to a commercially available ELISA kit.

For the eight point calibration curve, recombinant Hsp70 was isolated from baculovirus-transfected Sf9 insect cells and purified with a HisTrap column. To minimize the background, different blocking reagents were tested. When comparing 1% BSA, 1% FCS, 1% Casein and 2% milk powder in PBS, the lowest background could be achieved with milk powder. It was therefore chosen as blocking and dilution reagent. Similarly, matrix effects caused by serum components can significantly influence ELISA measurements, often leading to an underestimation of the analyte concentration. To reduce these unfavorable matrix effects, different sample diluents and ratios were tested. A 1:5 dilution of serum samples in CrossDown buffer was found to be optimal.

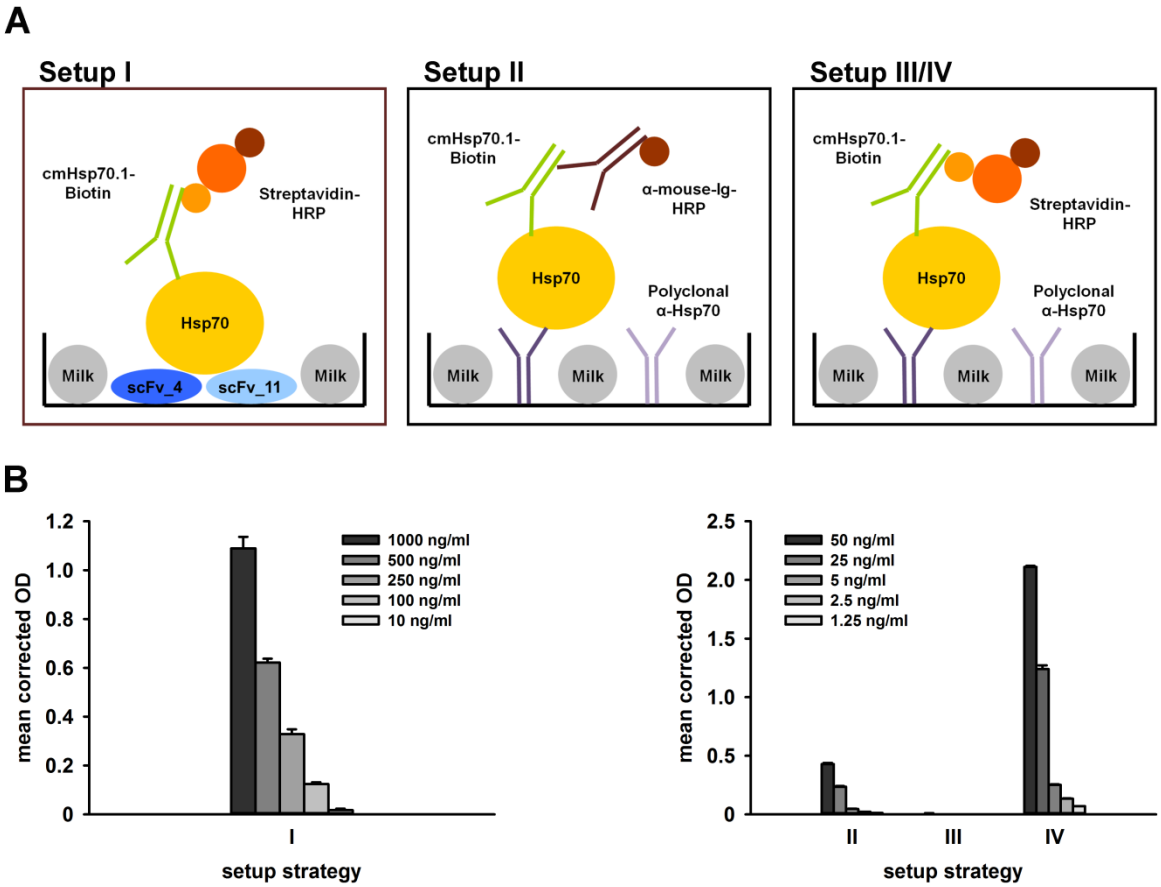

Figure 7: ELISA Development and Optimization. (A) Four different setups of the Hsp70 ELISA were tested. Setup I combined single chain variable segments (scFvs) for protein capture with the cmHsp70.1 antibody for detection. Setup II and Setup III/IV used a polyclonal anti-Hsp70 antibody for protein capture and the cmHsp70.1 antibody for detection, combined with a secondary antibody (Setup II) or biotin-streptavidin binding (Setup III/IV). (B) Setup I with scFvs as a capturing tool could not detect Hsp70 concentrations lower than 10 ng/ml (left panel). Using the polyclonal capture antibody in combination with cmHsp70.1 and a secondary antibody could increase the detection limit to 1 ng/ml, but gave a low signal (right panel, Setup II). The signal could be enhanced significantly by using biotin-streptavidin binding as a secondary detection tool (right panel, Setup IV). To ensure detection was possible, the diluent for streptavidin-HRP had to be changed to 1% BSA, as milk powder interfered with the streptavidin-biotin binding and completely eliminated the signal (right panel, Setup III).

Figure 7 shows a summary of the ELISA development and optimization of the general setup. First experiments were performed using two different single-chain variable fragments for the capture and/or detection of the protein (scFv; #4 and #11), as they have been previously reported as agents for ELISA tests (Griep *et al.*, 2000). Therefore, different setups with the scFvs individually or in combination as well as combined with the cmHsp70.1 antibody were tested. The best results could be obtained with equal parts of the two single chain fragments for Hsp70 capture and a biotinylated cmHsp70.1 with streptavidin-HRP as a detection tool. However, even this

optimized setup was not sensitive enough to distinguish Hsp70 concentrations lower than 10 ng/ml from background (Figure 7B, left panel).

For the new setup, a polyclonal coating antibody was produced in rabbits by Davids Biotechnologie, using the purified Hsp70 protein for immunization of the animals. Coating with this polyclonal antibody and detection with the cmHsp70.1 antibody in combination with a secondary antibody gave good results down to 1 ng/ml but a low signal (Figure 7B, right panel, Setup II). To enhance the signal, the cmHsp70.1 antibody was coupled to biotin and tested in the same setup, which led to a complete elimination of the signal (Figure 7B, right panel, Setup III). Testing of each ELISA step revealed that the milk powder in the diluent interfered with the biotin-streptavidin binding. Replacing the milk powder with 1% BSA for the dilution of streptavidin-HRP could restore the signal, resulting in a fivefold increased signal compared to cmHsp70.1 without biotin (Figure 7B, right panel, Setup IV). This setup was found to be optimal and was used for all further experiments.

3.1.2 ELISA Validation

3.1.2.1 Calibration Curve and Linearity

To quantify Hsp70 in various samples, an eight point standard consisting of recombinant Hsp70 was included into each ELISA test, ranging from 0-50 ng/ml. The Hsp70 concentration was plotted against the background-corrected OD values and a four-parameter fit model was applied to obtain the function describing a sigmoid curve, which gave excellent results. In 20 independent experiments, the highest concentration of the standard yielded a mean OD value of 2.82 and a standard deviation of 0.34. A representative calibration curve and the fitting equation are shown in Figure 8A.

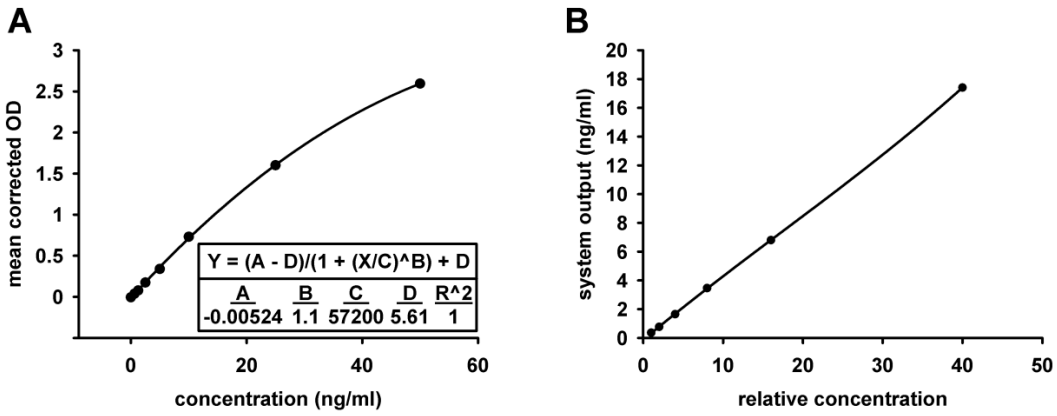

Figure 8: Validation of the lipHsp70 ELISA. (A) Representative eight point calibration curve obtained from the lipHsp70 ELISA using a four-parameter fit model (inset). The OD (mean corrected) is indicated on the Y-axis and the Hsp70 concentration (ng/ml) on the X-axis. (B) Linearity of the lipHsp70 ELISA was assessed by comparing first-, second- and third-order model fits of a relative concentration vs. system output plot. Linearity was shown within a concentration range of 0.36-17.4 ng/ml (Breuninger *et al.*, 2015).

A quantitative analytical method is linear when there exists a mathematically verified straight-line relationship between the observed values and the true concentrations of the analyte. Linearity usually refers to the overall system response (e.g. concentration as determined with the instrument) rather than the raw instrument output (e.g. OD). A linear relationship facilitates a simple interpolation of results and is especially important for a reliable determination of concentrations. If a dataset is not linear, a visual examination of the plot can identify outliers. If an outlier is at either end of the concentration range, the data point can be removed and the statistical analysis repeated. The linear range is reduced accordingly, excluding the outlier. Sample concentrations should be adjusted by dilution to lie within the linear range. Linearity of the ELISA was assessed by comparing linear and nonlinear polynomial fitting of the relationship between true and observed concentrations of six Hsp70 samples (Figure 8B). The lipHsp70 ELISA was linear in a concentration range from 0.36-17.41 ng/ml. All samples that were tested with the ELISA were within the linear range or were diluted if necessary.

3.1.2.2 Assay Precision and Limit of Detection

To determine assay precision, intra- and inter-assay runs were performed with control serum samples from two and five healthy donors, respectively, and the

coefficients of variation (CVs) were calculated. For intra-assay precision, serum samples were applied in 20 replicates on a single plate; CVs ranged from 5.2% to 8.1%. For inter-assay precision, serum samples were tested in duplicates on three different days; CVs varied between 1.0% and 18.0% with a mean of 10.9%.

The limit of detection (LoD) is the smallest amount of analyte that a method can reliably detect to determine its presence or absence. Knowledge of the LoD is necessary to define a lower cutoff for quantitative measurements. The LoD for the lipHsp70 ELISA was 0.3 ng/ml. To enable reliable results, protein concentrations in measured samples were kept well over the LoD.

3.1.2.3 Recovery

Spike and recovery experiments are used to determine whether the analyte detection is affected by the difference between the diluent used to prepare the standard curve and the sample matrix. Especially serum components may affect binding of the antibody or background detection, and therefore influence the detection of the analyte.

Recovery was determined by spiking recombinant Hsp70 protein in buffer and serum samples and comparing results from the lipHsp70 ELISA with the widely used commercially available ELISA as a control. For the spiking experiments in buffer, an Hsp70 protein from Enzo Life Sciences was used as a control that was independent from both ELISAs. When 2.5 ng/ml of the protein were spiked into dilution buffer, the lipHsp70 ELISA recovered significantly higher amounts of the expected Hsp70 protein (2.53±0.09 ng/ml, 101±3% recovery) compared to the control ELISA (1.43±0.07 ng/ml, 57±3% recovery) (Figure 9A).

To determine the recovery of Hsp70 in serum samples, Hsp70 (2.5 ng/ml and 5 ng/ml) of the respective standards was spiked into 1:5 diluted serum samples derived from four different healthy volunteers. With an average recovery of 78±3%, the lipHsp70 ELISA showed a significantly higher recovery of the spikedHsp70 compared to the control ELISA with 50±3% (Figure 9B).

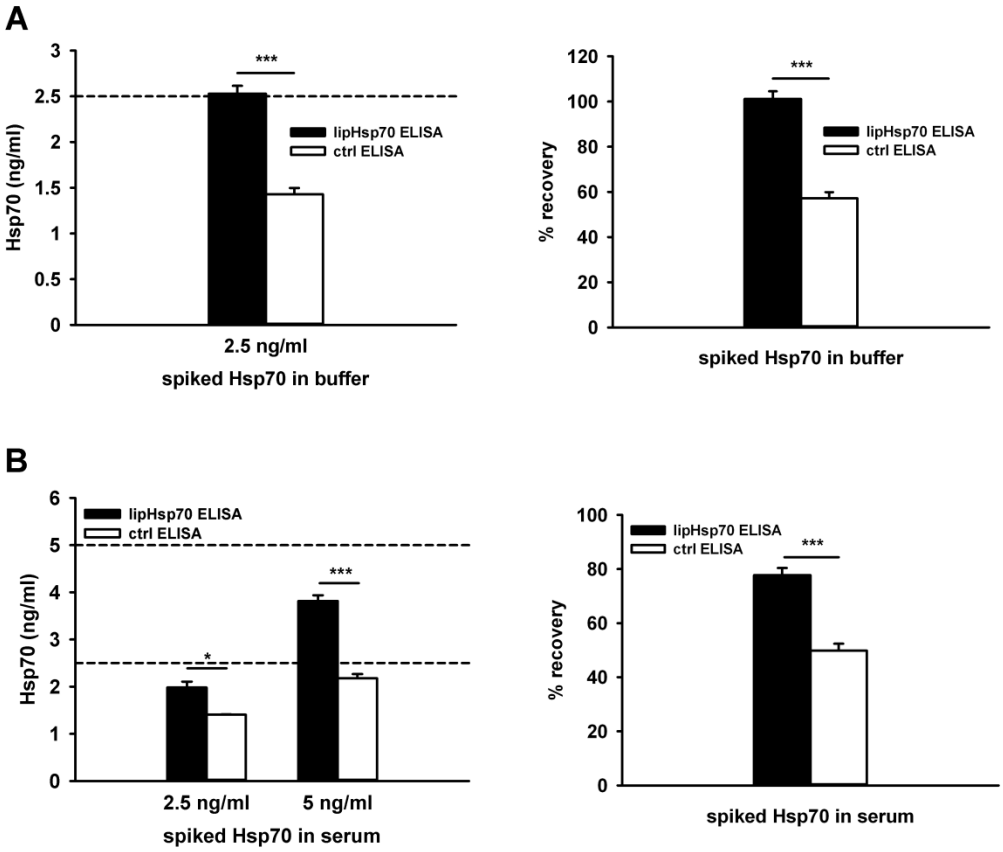

Figure 9: Recovery of spiked Hsp70 protein. (A) Recovery of free Hsp70 in buffer: 2.5 ng/ml Hsp70 was spiked into dilution buffer. The lipHsp70 ELISA recovered 2.53 ± 0.09 ng/ml (left panel) and thus revealed a significantly better recovery (101 ± 3%, right panel) compared to the control ELISA (1.43 ± 0.07 ng/ml, left panel; 57 ± 3%, right panel). The data show the mean of n=20 tests. (B) Recovery of free Hsp70 in serum: 2.5 ng/ml and 5 ng/ml Hsp70 were spiked into serum (diluted 1:5). The lipHsp70 ELISA recovered 1.98 ± 0.12 ng/ml and 3.82 ± 0.12 ng/ml for 2.5 and 5 ng/ml (left panel) and thus revealed a significantly better recovery (mean 78 ± 3%, right panel) compared to the control ELISA (1.41 ± 0.07 ng/ml and 2.18 ± 0.09 ng/ml, left panel; mean 50 ± 3%, right panel). Black bars: lipHsp70 ELISA, white bars: control ELISA, dashed line: expected amount of Hsp70. *p<0.05, ***p<0.001 (t-test) (Breuninger *et al.*, 2015).

The details of the lipHsp70 assay performance are summarized in Table 3.

Table 3: Assay performance characteristics of the lipHsp70 ELISA

Parameters	Performance
Linear range (ng/ml)	0.36-17.41
Intra-assay precision (%CV)	5.2-8.1
Inter-assay precision (%CV)	1.0-18.0
Recovery (%): Buffer/Serum	101±3/78±3
Limit of Detection (ng/ml)	0.31

3.1.3 Hsp70 Serum Levels in Healthy Human Volunteers

In order to establish a control group for Hsp70 serum concentrations, serum samples from 114 healthy volunteers were analyzed. The age of the donors ranged from 20-74 years, with a mean of 42.9 and a median of 41.5 years. These samples were used to determine the basal Hsp70 levels in human blood. To minimize matrix effects and to keep concentrations within the linear range, serum was diluted 1:5 in CrossDown Buffer prior to analysis.

Significantly higher basal levels (6.4±2.7 ng/ml) could be detected with the lipHsp70 ELISA compared to the control ELISA (2.8±1.3 ng/ml). The 25th and 75th percentiles were 4.5 ng/ml and 7.7 ng/ml for the lipHsp70 ELISA and 2.0 ng/ml and 3.1 ng/ml for the control ELISA, respectively (Figure 10A). For both ELISAs, no correlation was found between the basal Hsp70 serum levels and the age of the donors (Figure 10B).

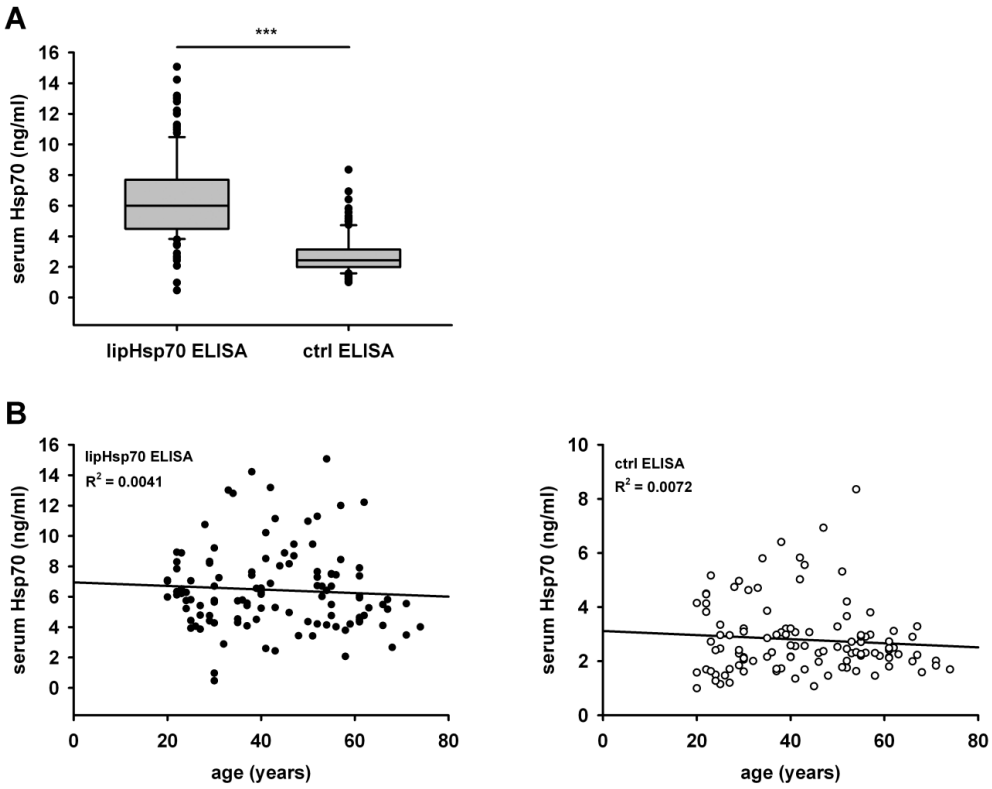

Figure 10: Hsp70 serum levels in healthy human volunteers determined with the lipHsp70 and control Hsp70 ELISA. (A) Serum samples were taken from 114 healthy human volunteers and Hsp70 levels were determined comparatively with the lipHsp70 and the control Hsp70 ELISA (ctrl ELISA). The lipHsp70 ELISA detected significantly higher Hsp70 concentrations (6.4 ± 2.7 ng/ml) in the serum than the ctrl ELISA (2.8 ± 1.3 ng/ml). Lines inside the box plots show the median value, upper/lower boundaries indicate the 25th and the 75th percentile, whiskers indicate the 10th and the 90th percentile, respectively. ***p<0.001 (B) The Hsp70 serum levels determined with the lipHsp70 (left) and the control ELISA (right) showed no correlation with the age of the donors. (Breuninger *et al.*, 2015).

3.1.4 Comparison of Serum and Plasma

Both serum and plasma are routinely used in the analysis of blood samples. However, protein levels may differ depending on whether they were measured in serum or plasma, which can be collected in various anticoagulants. Anticoagulants as well as activation processes during clot formation could influence the protein pattern.

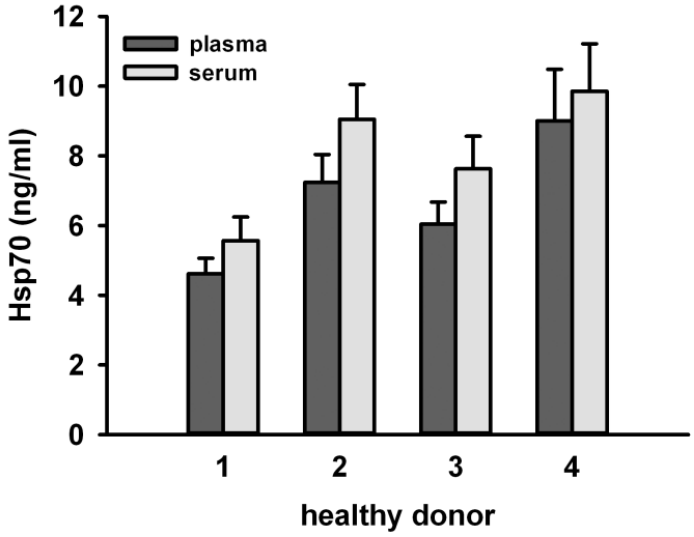

Figure 11: Comparison of the detection of Hsp70 in serum and plasma. Plasma (dark grey) and serum (light grey bars) were taken in parallel from four healthy donors with different basal Hsp70 serum levels. No significant differences could be detected between the Hsp70 values derived from plasma and serum (Breuninger *et al.*, 2015).

To test whether the lipHsp70 ELISA is suitable for measuring Hsp70 levels in both sample types, samples were taken in parallel from four healthy donors. For this experiment, donors with different basal levels of Hsp70 were chosen. For all four donors, the Hsp70 levels in plasma did not differ significantly from those in the corresponding serum samples (Figure 11). These data indicate that both serum and plasma can be used to measure Hsp70 levels with the lipHsp70 ELISA.

3.1.5 Influence of Interference Factors

Different factors in the donor's lifestyle or in the sample preparation process could have an impact on the measurement of Hsp70 in serum. The robustness of the lipHsp70 ELISA towards such interference factors was determined by testing the

influence of food intake of the donor, repeated freezing and thawing of the serum sample and hemolysis.

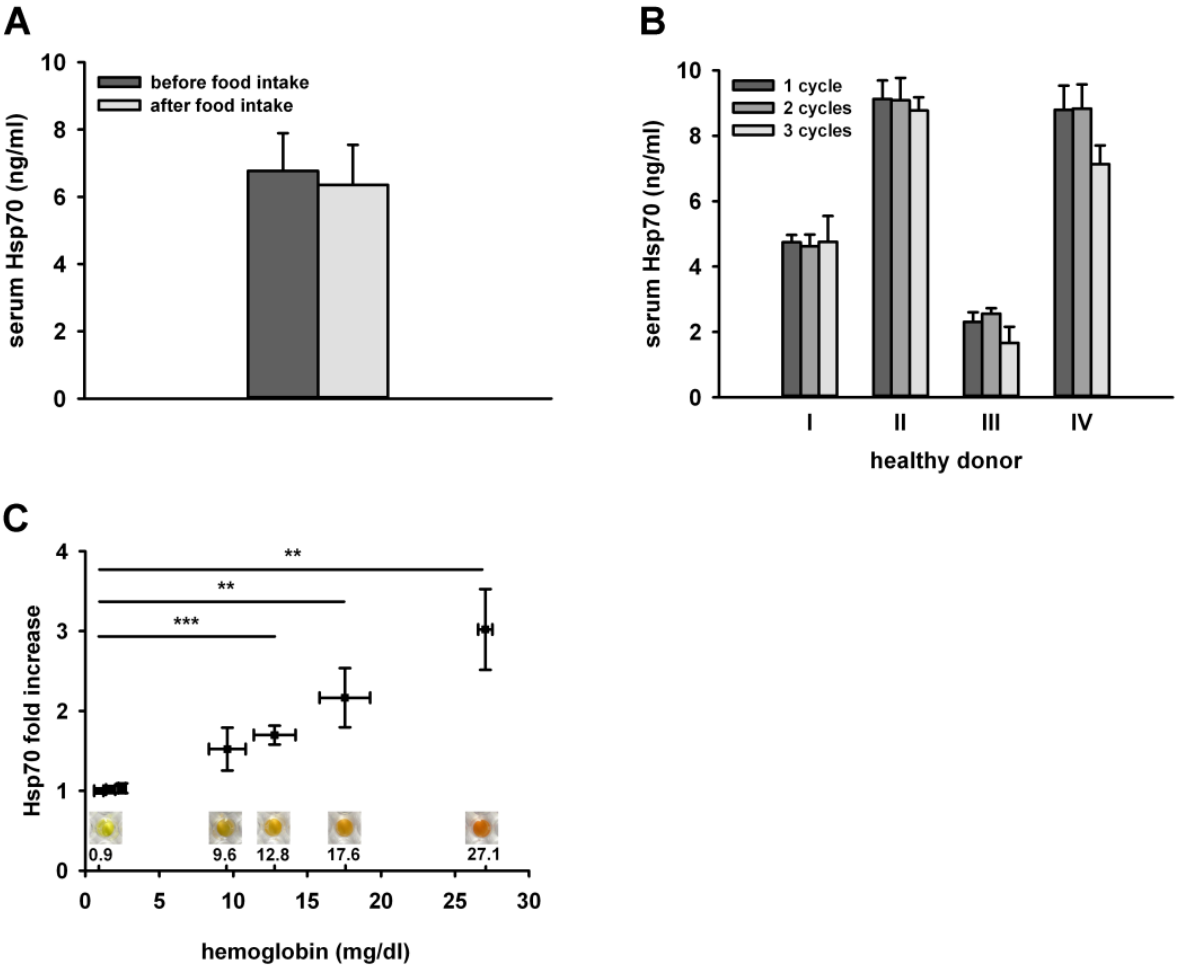

Figure 12: Influence of interference factors on the detection of Hsp70 in serum using the lipHsp70 ELISA. (A) Serum samples of seven healthy individuals were taken before (dark grey bar) and two hours after intake of a high-fat diet (light grey bar). Hsp70 serum levels were determined using the lipHsp70 ELISA. No significant differences in the Hsp70 serum values were detected before and after food intake. (B) Serum samples were subjected to three repeated cycles of freezing and thawing and Hsp70 levels were determined after each cycle. No significant differences in the Hsp70 values were detected after repeated freezing and thawing using the lipHsp70 ELISA. (C) Serum samples were spiked with increasing amounts of lysed, autologous erythrocytes and Hsp70 levels were determined using the lipHsp70 ELISA (n=3). Up to a hemoglobin concentration of 9.6 mg/dl in the serum the Hsp70 values remained unaffected; higher serum hemoglobin concentrations resulted in a significant increase in the Hsp70 values. **p<0.01, ***p<0.001 (t-test) (Breuninger *et al.*, 2015).

Serum samples from seven healthy individuals were taken before and two hours after intake of a high-fat diet. Some of the samples showed a visible increase in turbidity after the food intake. However, Hsp70 serum levels in all donors did not differ significantly before and after food intake (Figure 12A).

Serum samples from four healthy individuals with different basal levels of Hsp70 were subjected to three cycles of freezing and thawing and Hsp70 levels were determined after each cycle. No significant changes were detected (Figure 12B). Even after ten cycles, the measured Hsp70 values did not change significantly.

To test the influence of free hemoglobin on the ELISA measurements, serum derived from three healthy individuals was spiked with increasing amounts of lysed erythrocytes. The hemoglobin content of the samples was analyzed and plotted against the measured Hsp70 values. Free hemoglobin at a concentration of up to 9.6 mg/dl did not significantly change the measured Hsp70 values. In contrast, hemoglobin concentrations above 9.6 mg/dl resulted in a non-specific increase of the Hsp70 values (Figure 12C).

3.1.6 Detection of Lipid-Bound Hsp70

As a major proportion of Hsp70 is released in lipid vesicles, the ability of both ELISAs to detect lipid-bound protein was analyzed. For that purpose, artificial POPS/POPC lipid vesicles were produced and loaded with recombinant Hsp70.

To monitor the success of vesicle formation, samples were analyzed with a Zetasizer. Analysis of the sample before homogenization shows an 85% majority of vesicles with a diameter of approximately 590 ± 40 nm. After processing with the Mini Extruder, 87% of vesicles had a diameter of around 150 nm with a standard deviation of 50 nm, making them comparable to natural vesicles like exosomes (Figure 13A).

The amount of lipid-associated Hsp70 that was determined with the lipHsp70 ELISA showed an excellent correlation with the Hsp70 concentration that was determined by Western blotting. However, a comparison of the levels of liposomal Hsp70 determined with the lipHsp70 ELISA and the control ELISA revealed large differences. The recovery of liposomal Hsp70 using the lipHsp70 ELISA was 76±5%, whereas that of the control ELISA was only 7±1% (Figure 13B).

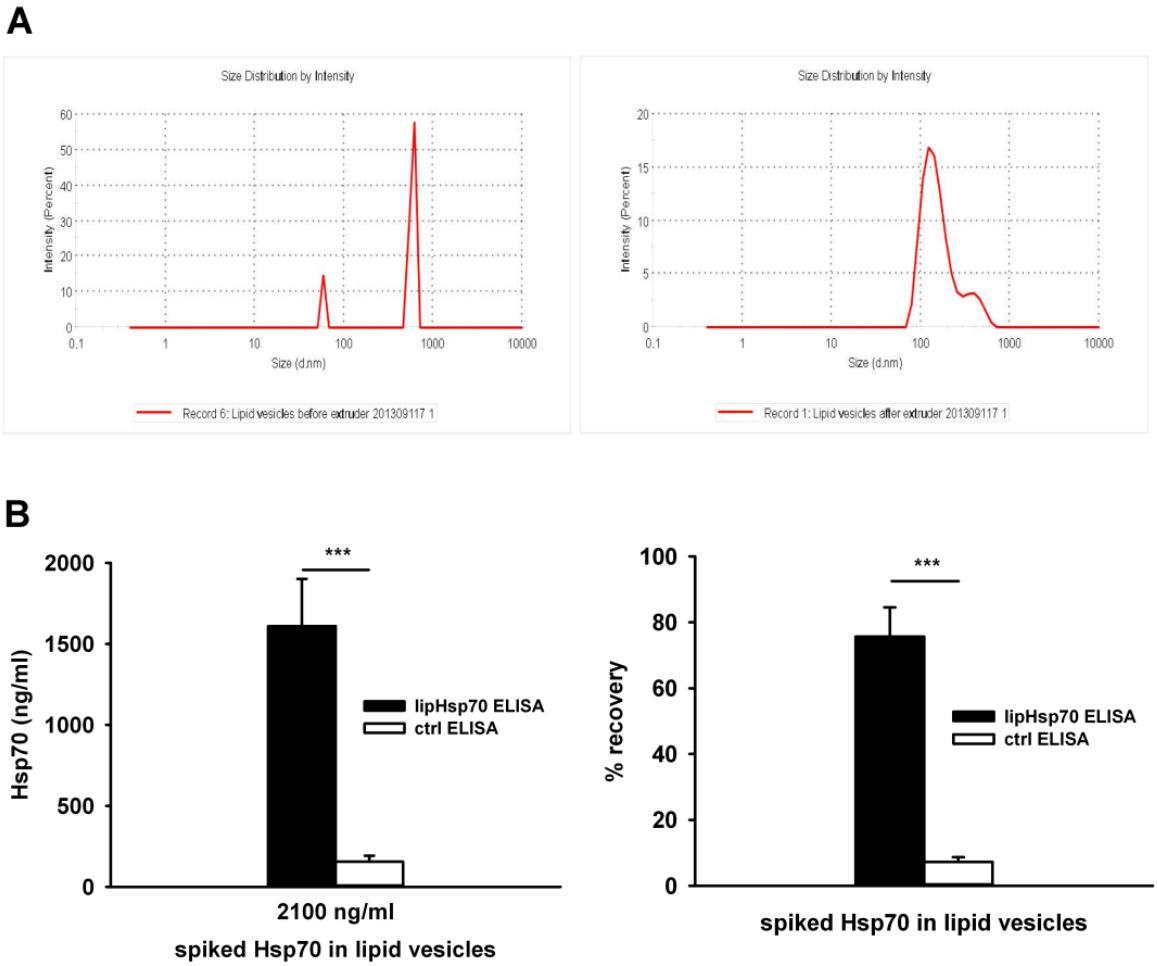

Figure 13: Production and recovery of lipid vesicles loaded with Hsp70 (A) Artificial POPS/POPC lipid vesicles were produced and analyzed with a Zetasizer Before homogenization, an 85% majority of vesicles had a diameter of approximately 590 ± 40 nm (left panel). After homogenization, 87% of vesicles had a diameter of approximately 150 ± 40 nm (right panel), making them comparable to natural vesicles. (B) Recovery of lipid-bound Hsp70 using the lipHsp70 ELISA and the control Hsp70 ELISA. According to quantitative Western blot analysis the lipid vesicles were loaded with 2,100 ng/ml Hsp70. The lipHsp70 ELISA recovered 1,610 ± 292 ng/ml (left panel) and thus revealed a significantly better recovery (76 ± 5%, right panel) compared to the control ELISA (155 ± 36 ng/ml, left panel; 7 ± 1%, right panel). The data show the mean of n=3 tests. Black bars: lipHsp70 ELISA, white bars: control ELISA.***p<0.001 (t-test) (Breuninger *et al.*, 2015).

3.1.7 Hsp70 Serum Levels in Patients with Different Tumor Entities

After optimizing and testing the performance of the lipHsp70 ELISA under various conditions, it was finally used to analyze serum samples from patients with different tumor entities. Hsp70 levels were determined in the serum of patients with head and neck cancer (n=23), lung cancer (n=22), colorectal cancer (n=44), pancreatic cancer (n=46), glioblastoma (n=30) or hematological malignancies (n=32) and compared to

the basal levels in healthy donors. The mean Hsp70 serum levels in patients of all tumor entity groups were significantly higher than those of the healthy donors (Figure 14A).

Receiver operating characteristic (ROC) curve analysis was performed by comparing serum Hsp70 levels of healthy donors with those of the different patient cohorts (Figure 14B). The curve is derived from plotting the true positive rate against the false positive rate (or sensitivity against 1-specificity) at various threshold settings. It indicates the performance of a binary classifier system, in this case the presence or absence of cancer. An area under the curve (AUC) of 0.5 indicates a random process. The more the AUC approaches 1, the more reliable is the classification of samples into the positive or negative group. The area under the curve (AUC; CI 95%) and sensitivity for a cut-off value of 7.7 ng/ml (derived from the 75th percentile of the healthy donors) is summarized in Table 4. The specificity was 75% for all patient groups.

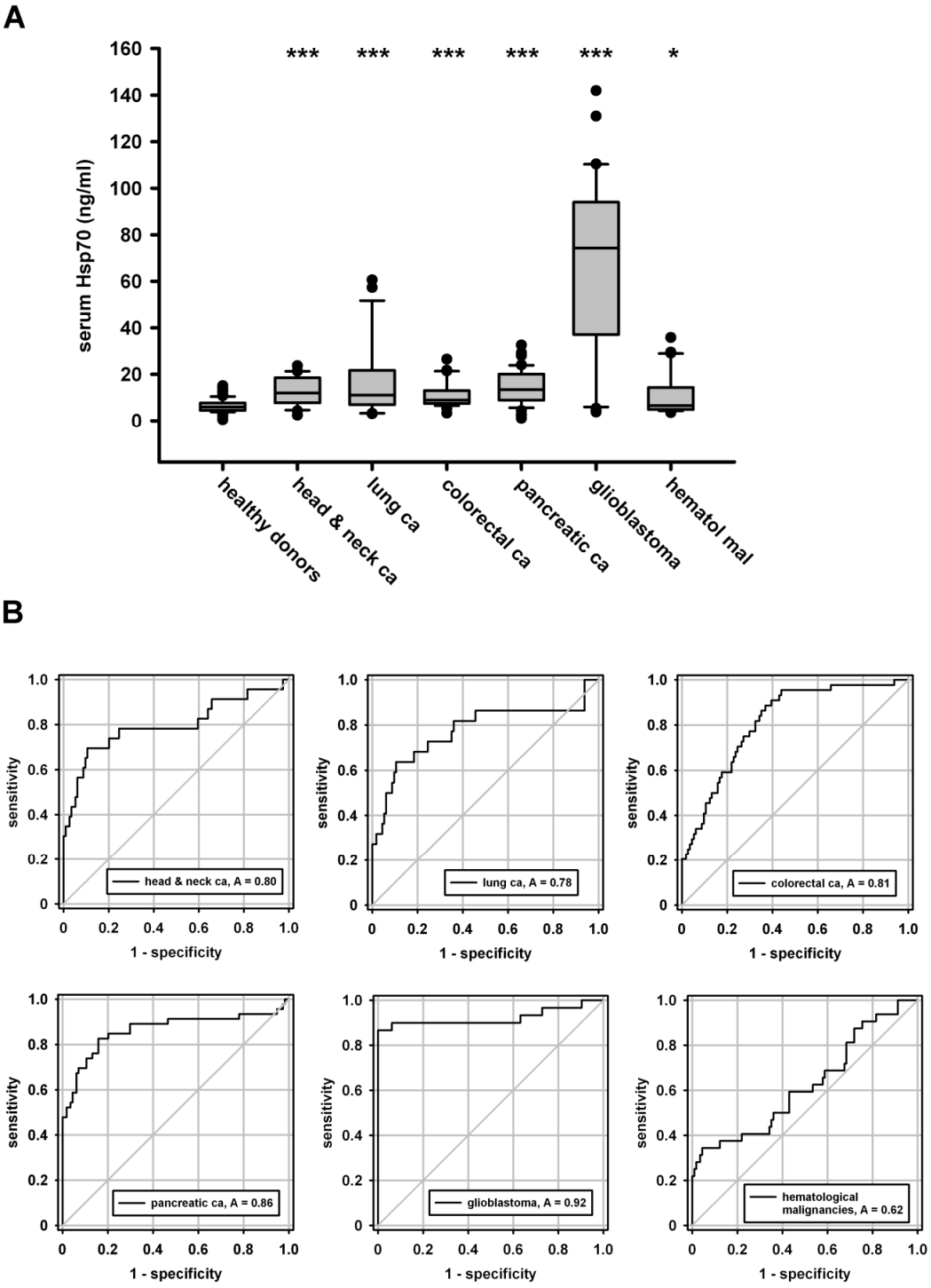

Figure 14: Hsp70 serum levels in patients with different tumor entities compared to healthy controls. (A) Serum samples were taken from healthy human volunteers (n=114) and patients with squamous carcinomas of the head and neck (n=23), lung cancer (n=22), colorectal cancer (n=44), pancreatic cancer (n=46), glioblastoma (n=30) or haematological malignancies (n=32). Patient characteristics are summarized in Table 4. Significantly higher Hsp70 levels were found in all tumor patient cohorts compared to the healthy controls. Lines inside the box plots show the median value, upper and lower boundaries indicate the 25th and the 75th percentile, whiskers indicate the 10th and the 90th percentile, respectively. *p<0.05, ***p<0.001 (Mann-Whitney Rank Sum Test). (B) ROC curve analysis was performed on the data shown in (A). AUC, sensitivity and specificity data are summarized in Table 4 (Breuninger *et al.*, 2015).

Table 4: Age, gender and Hsp70 levels of healthy donors and patients. AUC: Area Under the Curve, M: Male, F: Female, CI: Confidence Interval, ROC: Receiver Operating Characteristic, SD: Standard Deviation, (Breuninger *et al.*, 2015).

		Healthy Donors	Head & Neck Cancer	Lung Cancer	Colorectal Carcinoma	Pancreatic Cancer	Glioblastoma	Hematological Malignancies
Number (n)		114	23	22	44	46	30	32
Gender (M/F)		67/47	21/2	16/6	26/18	26/20	14/16	25/7
Age	Mean	42.9	62.5	66.1	64.2	69.8	56.2	41.7
	Range	20-74	36-83	48-88	29-81	44-90	25-77	19-64
	SD	14.6	12.2	10.3	13.0	40.6	14.1	12.2
	Median	41.5	61.0	66.5	67.5	73.0	59.0	42.0
lipHsp70 ELISA	Mean Hsp70 (ng/ml)	6.4	12.4	16.8	11.0	14.8	67.6	11.1
	SD	2.7	6.1	16.2	5.2	7.3	37.5	9.0
ROC	AUC (CI 95%)	-	0.80	0.78	0.81	0.86	0.92	0.62
	p-value	-	<0.0001	<0.0001	<0.0001	<0.0001	<0.0001	0.03
	Sensitivity (%)	-	78	73	70	85	90	41
	Specificity (%)	-	75	75	75	75	75	75

3.2 Circulating Tumor Cells

Circulating tumor cells (CTCs) are an important biomarker for prognosis and therapy response of cancer patients. Hsp70 has been found on the membrane of a wide variety of tumor entities (Hantschel *et al.*, 2000; Pfister *et al.*, 2007) and is known to be upregulated in metastases (Farkas *et al.*, 2003), which makes it a promising target. The aim of this project was therefore to establish a detection/isolation system for circulating tumor cells based on the cmHsp70.1 antibody.

3.2.1 Tumor Cell Capture with Magnetic Beads

3.2.1.1 Selection of a Bead System

Magnetic bead systems are widely used for the isolation or separation of proteins and cells from body fluids and primary cell material. A variety of bead systems with different capture principles can be purchased from many different companies. To find a system suitable for CTC isolation, four different types of magnetic beads were tested.

In the first setup, the mouse antibody cmHsp70.1, which binds to Hsp70 on the membrane of tumor cells, is captured by beads coupled to a sheep-anti-mouse IgG secondary antibody. The system supports a direct or an indirect approach. In the direct approach, cmHsp70.1 is first bound to the secondary antibody on the beads and then added to the cells. In the indirect approach, cmHsp70.1 is first incubated with the cells, before the beads are added. The mixture is then separated in a DynaMag magnet (Figure 15A).

Anti-FITC beads are coupled to an anti-FITC antibody and can be used to capture a FITC-conjugated cmHsp70.1. The separation is carried out in columns that are attached to a magnet and captured cells are later eluted from the column (Figure 15B).

In the Dynabeads FlowComp Flexi system, cmHsp70.1 is labeled with biotin, added to cells and captured with streptavidin-coated beads. The DynaMag magnet is then

used for the separation step. The advantage of this system is that cells can be easily eluted by streptavidin-biotin competition (Figure 15C).

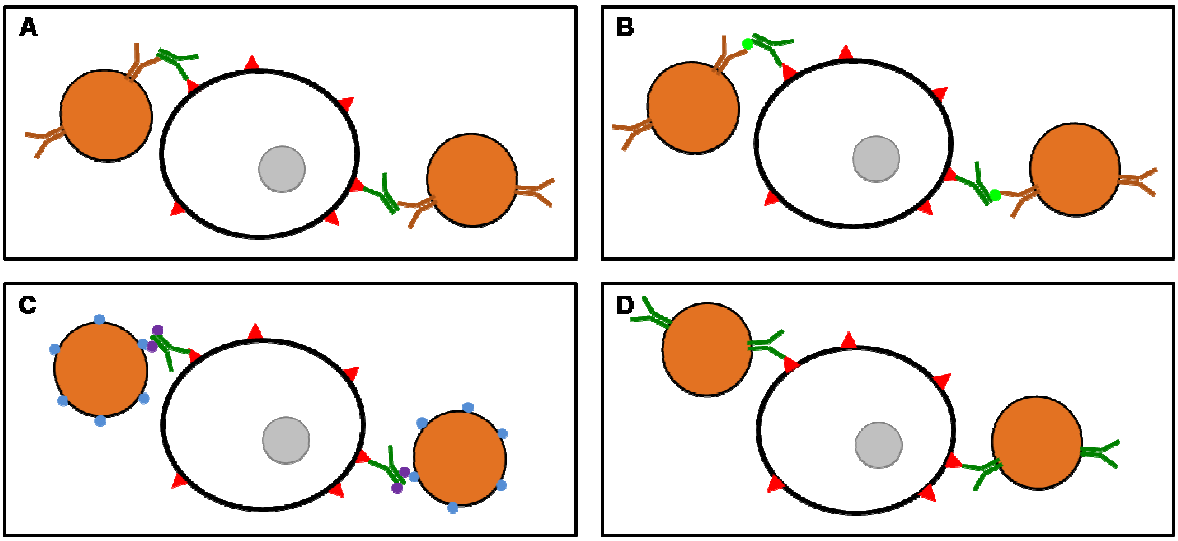

Figure 15: Selection of a magnetic bead system for tumor cell capture from blood. (A) In the first system, beads coupled to a sheep-anti-mouse IgG secondary antibody bind to the cmHsp70.1 antibody. The system allows for a direct or indirect approach. (B) In the second system, anti-FITC beads bind to a FITC-conjugated cmHsp70.1. (C) The Dynabeads FlowComp Flexi system contains streptavidin-coated beads that bind to a biotinylated cmHsp70.1. The cells can later be eluted by streptavidin-biotin competition. (D) The fourth system, which was determined to be optimal and used in all later bead experiments, was the Dynabeads MyOne Tosylactivated system. These are superparamagnetic beads that can be directly coupled to the cmHsp70.1 antibody.

All three bead systems were tested on Hsp70-positive tumor cell lines, but the recovery with these techniques was very low. However, the insights gained from these experiments suggested that a direct coupling of the capture antibody to the magnetic beads would be preferable in order to reduce possible breaking points of the capturing. Therefore, the Dynabeads MyOne Tosylactivated bead system was tested (Figure 15D).

Dynabeads MyOne Tosylactivated are uniform, superparamagnetic polystyrene beads with a diameter of 1 µm. Hydroxy groups on the polyurethane coating can be activated by reaction with p-toluenesulfonyl chloride. The resulting sulfonyl ester can subsequently react covalently with amino or sulfhydryl groups on antibodies.

The beads were coupled to the cmHsp70.1 antibody as described in 2.2.5.1 and stored in aliquots for further experiments. To test the success of the coupling, the beads were incubated with FITC-labeled Hsp70 protein and analyzed with a

fluorescence microscope. A green signal indicated capture of the protein by the antibody on the beads and therefore a successful coupling process.

3.2.1.2 Tumor Cell Capture with Beads from Buffer and Blood

To establish the capturing of tumor cells with beads, first experiments were carried out in buffer. Different tumor cell lines were used in the experiments. To test the specificity of the system, a tumor cell line with a high Hsp70 membrane expression was compared to a tumor cell line with a low Hsp70 membrane expression. For that purpose, the human mammary carcinoma cell lines SK-BR-3 and T47D were chosen. Around 90-95% of SK-BR-3 cells are positive for Hsp70, while only around 30-40% of T47D are Hsp70 positive, as determined by flow cytometry (Figure 18). In addition, SK-BR-3 are widely used as a model cell line for CTC detection/isolation systems.

The cells were incubated with magnetic beads for 1 h at 37°C with rotation and separated in a DynaMag magnet. Cells that were captured on the beads as well as cells left in the supernatant were then counted. For the Hsp70-positive cell line SK-BR-3, 80±11% of the cells could be captured with the beads, while only 38±13% of T47D could be isolated (Figure 16A). These numbers are in good agreement with the Hsp70 status of the cells. The results of these experiments show that isolation of tumor cells based on their Hsp70 membrane expression is possible.

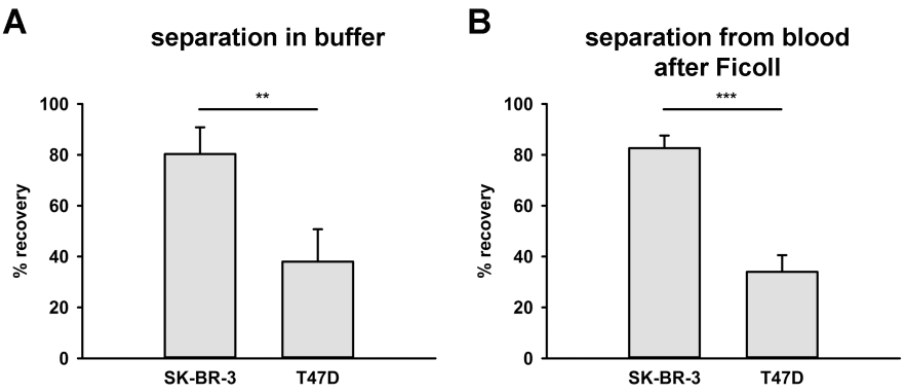

Figure 16: Recovery of tumor cells from buffer and a mixture with blood. Two breast cancer cell lines were chosen for the recovery experiments with the MyOne Tosylactivated bead system: SK-BR-3 with a high surface expression of Hsp70 and T47D with a low surface expression of Hsp70. (A) Tumor cells were spiked into buffer and incubated with the beads for 1 h at 37°C. The percentage of recovered cells was in good agreement with the Hsp70 status of the cells, as determined by flow cytometry, with 80±11% of SK-BR-3 and 38±13% of T47D being recovered. (B) Tumor cells were spiked into blood from healthy donors and preselected with Ficoll. After a recovery step, they were incubated with the beads for 1 h at 37°C. Recovery was very similar to the results in buffer, with 83±5% for SK-BR-3 and 34±7% for T47D.

The next step was to isolate tumor cells from a mixture with blood. For that purpose, tumor cells were spiked into blood from healthy human volunteers. To minimize the interference of blood components with the cell capture, different approaches were tested.

In the first approach, the mixture of tumor cells and blood was subjected to erythrocyte lysis prior to cell capture with the beads. When the cells were analyzed afterwards, only a small proportion of tumor cells could be found in the bead fraction, which was highly contaminated with blood cells. Flow cytometry analysis of whole blood revealed that lymphocytes, which are normally negative for Hsp70 staining, showed up to 30% positivity when they were exposed to lysis buffer prior to antibody staining (Figure 17). This led to the conclusion that erythrocyte lysis damaged the lymphocytes to an extent that they started to unspecifically bind Hsp70 antibody. The same effect could have resulted in unspecific binding to the antibody-coupled beads, which were thus blocked, leading to a reduced capacity to bind tumor cells. The binding of tumor cells to the beads itself was not impaired by the lysis buffer, as tested in the absence of blood cells (data not shown).

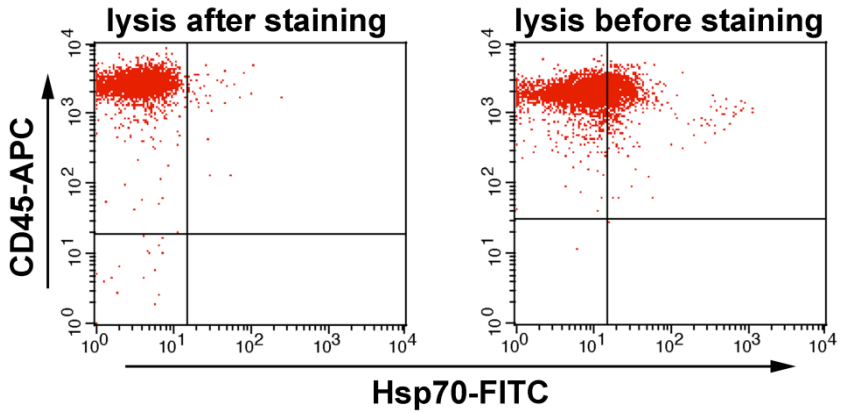

Figure 17: Lymphocyte damage after erythrocyte lysis. Lymphocytes, which are normally negative for surface Hsp70 (left panel), showed up to 30% positivity after exposure to lysis buffer. This unspecific binding could also lead to blocking of the magnetic beads during tumor cell capture.

In the second approach, the mixture of tumor cells and blood was preselected with Ficoll. Previous experiments had shown that tumor cells are enriched in the same density layer as PMBCs (see 2.2.1.4). To reduce the risk for unspecific binding, the cells were allowed to recover in FACS buffer for 1 h after the isolation procedure. After that, beads were added to the cells and the separation was carried out as

described above. Similar to the results in buffer, 83±5% of SK-BR-3 cells could be recovered with the beads while only around 34±7% of T47D cells were captured (Figure 16B).

3.2.2 Tumor Cell Capture with the GILUPI CellCollector®

The main disadvantage of most existing isolation methods for circulating tumor cells, including magnetic bead separation, is the restricted blood volume. The medical device company GILUPI therefore developed a functionalized structured medical wire for the direct isolation of cells from the blood stream (Saucedo-Zeni *et al.*, 2012). The aim of this collaboration with GILUPI was to establish the cmHsp70.1-coupled version of their CellCollector® for the isolation of tumor cells.

3.2.2.1 Screening and Selection of Cell Lines

For the development of the Hsp70-based CellCollector® isolation system, a membrane Hsp70-high and a membrane Hsp70-low tumor cell line was needed, as described in 3.2.1.2. However, the final objective of this project is to study the performance of the Hsp70 detector in comparison with the preexisting EpCAM detector. For this, three cell lines with specific characteristics are required. One cell line needs to have a high Hsp70 expression and a low EpCAM expression, so it can be captured with the Hsp70 collector but not with the EpCAM collector. A second cell line needs to have the opposite properties, and finally a cell line with a similarly high expression of both markers needs to be chosen. Therefore, a large number of tumor cell lines were screened for their Hsp70 and EpCAM expression. Hsp70 and EpCAM status are summarized in Figure 18. From these, three cell lines with the appropriate marker composition were chosen: SK-BR-3 with a high membrane expression of both markers, T47D with a low Hsp70 and a high EpCAM expression and the glioblastoma cell line U-87 with a high Hsp70 and no EpCAM expression.

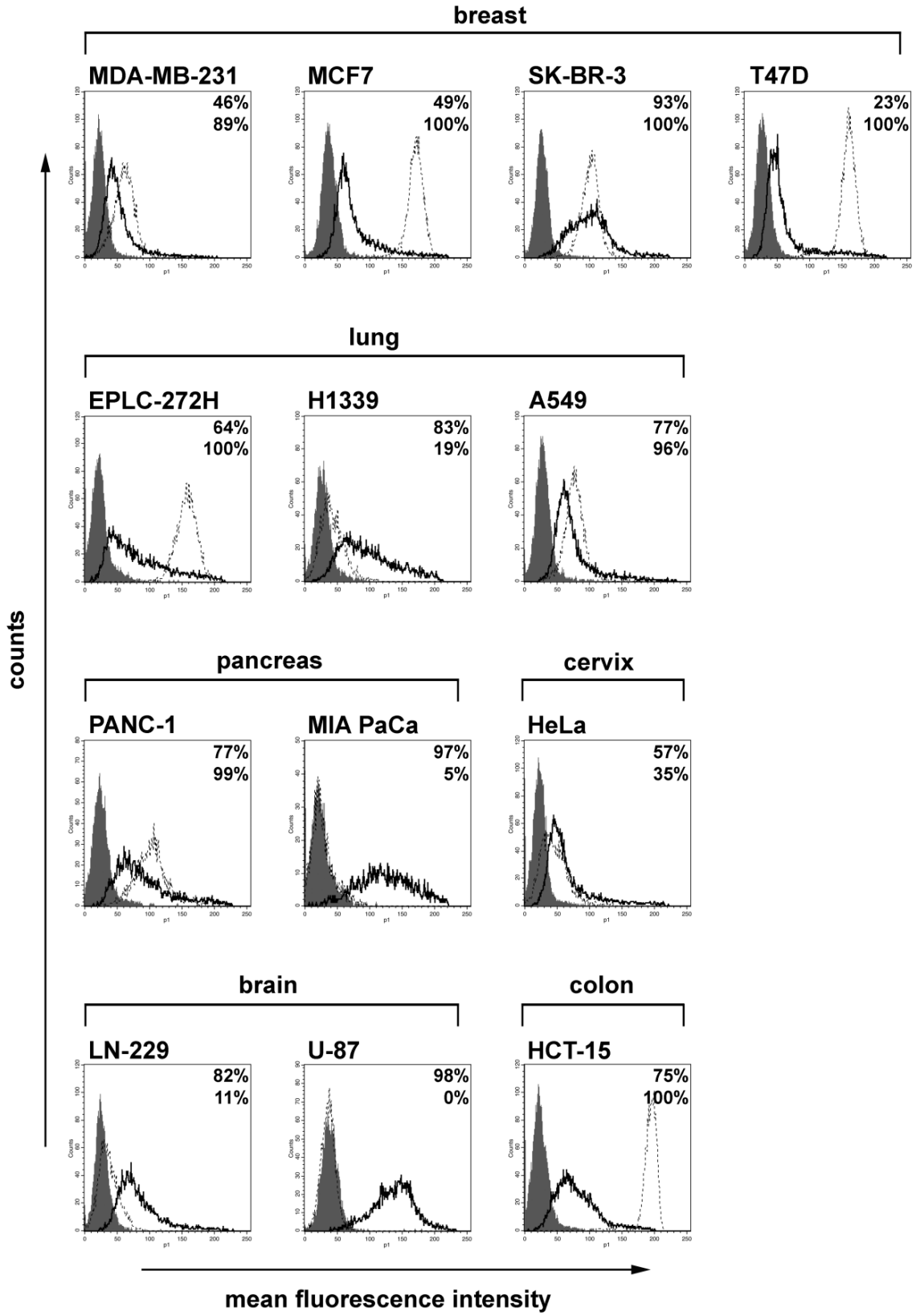

Figure 18: Screening and selection of tumor cell lines for CellCollector® experiments. Cell lines from various different cancer entities were screened for their Hsp70 and EpCAM surface expression using flow cytometry. Grey histograms represent isotype control, white histograms (solid line) Hsp70 staining and white histograms (dashed line) EpCAM staining. The numbers in the histograms indicate the proportion of cells stained positive for Hsp70 (top) and EpCAM (bottom). SK-BR-3, T47D and U-87 were chosen for further experiments.

3.2.2.2 CFSE Staining vs. PKH26 Red Staining

For first *in vitro* test experiments, tumor cell lines had to be prestained prior to isolation with the detector. Thus, the detectors could be analyzed directly after the capturing procedure without further need for fluorescence staining based on molecular markers.

Two different dyes were tested for the prestaining: CFSE, which is an intracellular dye, and PKH26 Red, which integrates into the plasma membrane of the cell. One limiting factor of fluorescence dyes is photobleaching, since the collectors need to be exposed over a certain time period to count and document captured cells. SK-BR-3 cells were stained with CFSE or PKH26 Red and photos were taken every 30 s over several minutes. As shown in Figure 19A, PKH26 Red staining was very stable while the CFSE signal faded more rapidly. However, when PKH26 Red-stained SK-BR-3 cells were stained with the FITC-conjugated cmHsp70.1 and analyzed with flow cytometry, the Hsp70 signal was dramatically reduced from 91% for unstained cells to 51% (Figure 19B). Similarly, the capability of cmHsp70.1-coated Dynabeads to recover the prestained cells was reduced to 45%. In contrast, the results for capturing CFSE-stained cells with Dynabeads were similar to those of unstained cells. As the integration of the PKH26 Red dye into the membrane might interfere with the binding of the antibody to membrane Hsp70, PKH26 Red was replaced with CFSE for further experiments.

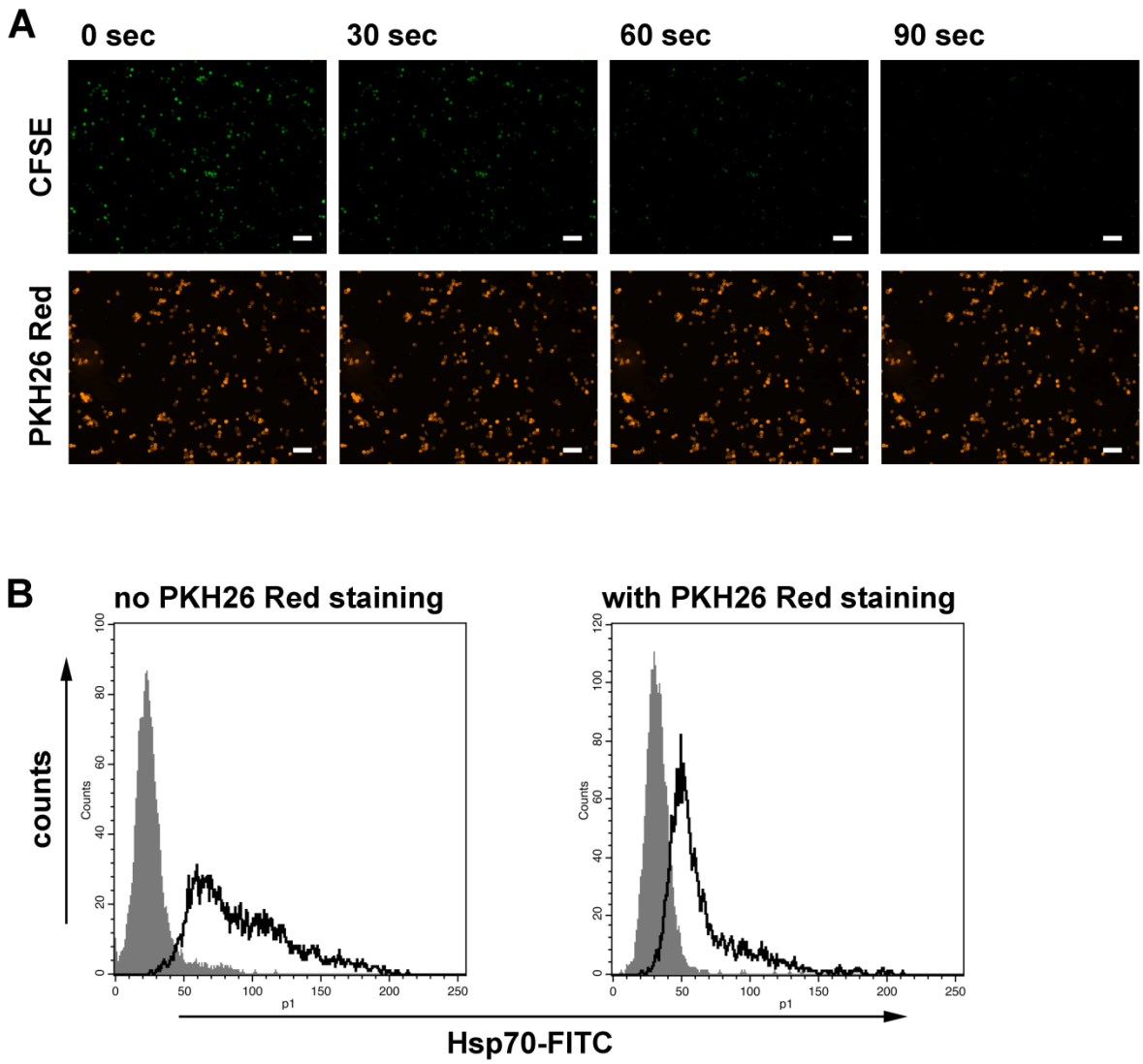

Figure 19: Comparison of CFSE staining and PKH26 Red Staining. (A) SK-BR-3 cells were stained with CFSE or PKH26 Red and analyzed with a fluorescence microscope. Photos were taken every 30 seconds. CFSE-stained cells showed rapid bleaching (green, upper row), while the PKH26 Red dye was far more stable (orange, lower row). Scale bar 100 µm. (B) SK-BR-3 cell were stained with PKH26 Red prior to staining with cmHsp70.1 and analyzed with flow cytometry. PKH26 Red Staining reduced the proportion of cells stained positive for Hsp70 from 91% (left panel) to 51% (right panel). As PKH26 Red integrates into the membrane, it likely interferes with antibody binding to membrane proteins. Grey histograms represent isotype control, white histograms represent Hsp70 staining.

In order to reduce the risk of artifacts caused by damaged or dying cells captured on the collector, the influence of CFSE staining on the viability of cells was tested. For that, SK-BR-3, T47D and U-87 cells were stained with CFSE and monitored for several hours. After 0, 60, 120 and 240 min samples were taken and cells were counted and analyzed with trypan blue. Even after 4 h the number of viable cells was not significantly decreased. Photobleaching effects described above could be reduced by microscope settings and fixation of the cells.

3.2.2.3 Test Run with CFSE-Stained Cells

The first collector experiment was performed on the first generation of wires. These are stainless steel wires with a gold coating that covers 2 cm of the tip. The gold layer is covered with a hydrogel that contains functional groups for the coupling with antibodies.

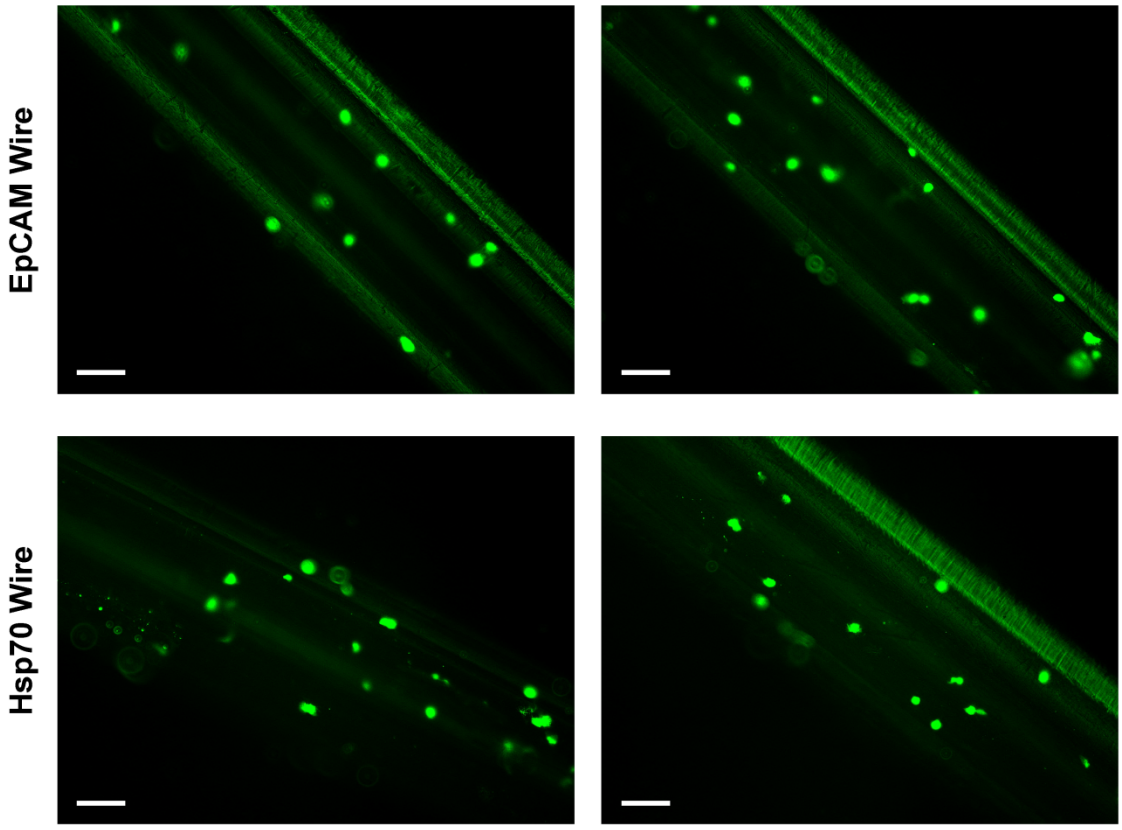

Figure 20: Comparison of the performance of the EpCAM CellCollector® and the Hsp70 CellCollector®. SK-BR-3 cells were stained with CFSE (green) and incubated with an EpCAM (upper row) or Hsp70 (lower row) detector. Captured cells were analyzed with a fluorescence microscope. A similar number of cells could be captured on both detectors. Scale bar 100 µm.

SK-BR-3 cells, which have a similarly high expression of Hsp70 and EpCAM, were prestained with CFSE. The cells were counted and tested for vitality and successful staining before they were approved for the experiment. One Hsp70 and one EpCAM detector were incubated with the cells for 30 min on a tilting shaker. The wire was washed and then analyzed with fluorescence microscopy. For that, the wire was placed in a petri dish with PBS and captured cells on the functional part were counted based on morphology and green staining. After counting of one side of the wire, it was turned by 180° and the second side was analyzed as well. As shown in Figure 20, cells could be collected with both the Hsp70 and the EpCAM detector.

Counting of the cells led to similar results on both wires. 147 cells were detected on the Hsp70 collector, while 154 cells were detected on the EpCAM wire. The cells looked intact and had normal morphological features.

3.2.2.4 Transfer of Captured Cells into Cell Culture

Circulating tumor cells are very rare. To be able to analyze these cells for their molecular characteristics, expansion of the cells in culture would be useful. Therefore, the possibility to transfer cells from the cell collector into cell culture was tested. The cells were prepared under sterile conditions. This time, a mixture of SK-BR-3 cells with blood from healthy human volunteers was tested. After incubation with the cells and washing, the functional parts of the EpCAM and the Hsp70 detector were cut from the wire and placed in cell culture flasks. After a few days, adherent cells started to grow in the culture flasks. The cells were expanded and finally tested for Hsp70 and EpCAM expression with flow cytometry. As shown in Figure 21, the expression pattern of the cells derived from the Hsp70 and the EpCAM collector was identical with that of fresh SK-BR-3 cells.

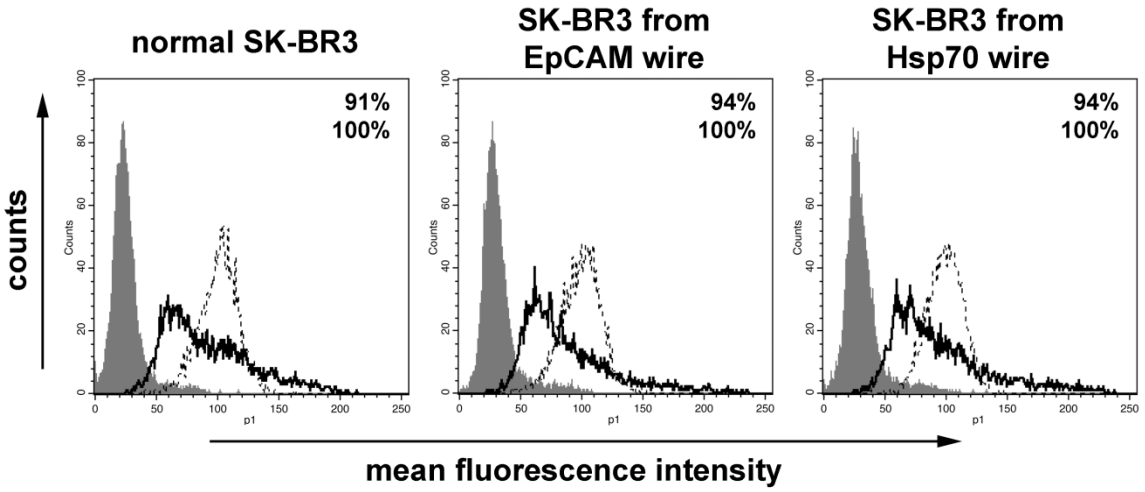

Figure 21: Transfer of captured cells into cell culture. SK-BR-3 cells were captured from a mixture of the tumor cell line with blood. The functional part of the wire was cut from the detector and transferred to a cell culture flask. Cells that became adherent in the flask were expanded and finally analyzed with flow cytometry. Cells captured with the EpCAM wire (middle panel) and the Hsp70 wire (right panel) showed staining for Hsp70 and EpCAM comparable to that of fresh SK-BR-3 cells. Grey histograms represent isotype control, white histograms (solid line) Hsp70 staining and white histograms (dashed line) EpCAM staining. The numbers in the histograms indicate the proportion of cells stained positive for Hsp70 (top) and EpCAM (bottom).

Pre-staining of tumor cells with CFSE is a very useful tool for first proof-of-principle experiments. However, the final goal is the capture and analysis of circulating tumor cells from patient blood. As these cells are of course unstained when they are captured, the staining has to be performed on the wire. Cytokeratins (CK) are present in most tumor cells, if they are derived from epithelial tumors, although different tumors can express different cytokeratins. An antibody cocktail that is directed against multiple different cytokeratins is therefore most suitable for the equal detection of different cell lines. CK staining was established on the same cell lines that were chosen previously.

Cells were grown in 8 well chamber slides and stained on the second day after seeding. After fixation with acetone, the cells were blocked with BSA and stained with a green-labeled CK antibody cocktail and Hoechst 33342 for the cell nucleus. Figure 22A shows a strong and even CK staining of SK-BR-3 and T47D cell. As U-87 is a glioblastoma cell line without epithelial origin, these cells cannot be stained with CK antibodies.

Although the CK staining in chamber slides was successful, it does not accurately reflect the conditions on the wire, where the cells are not adherent like in cell culture but in suspension. The suspension cells are then immobilized on a surface, in this case the detector. To mimic these conditions, cells were immobilized on a poly-lysin-coated slide. Poly-lysin enhances the electrostatic interactions between cell membranes and surfaces. After attachment to the slide, the cells were fixed, blocked and stained with the CK antibody cocktail and Hoechst 33342. Finally, the slides were analyzed with fluorescence microscopy. SK-BR-3 and T47D showed a strong staining, comparable to the staining in chamber slides (Figure 22B). The size, morphology and staining of these immobilized cells could then serve as a reference for the expected appearance of cells captured with the detector.

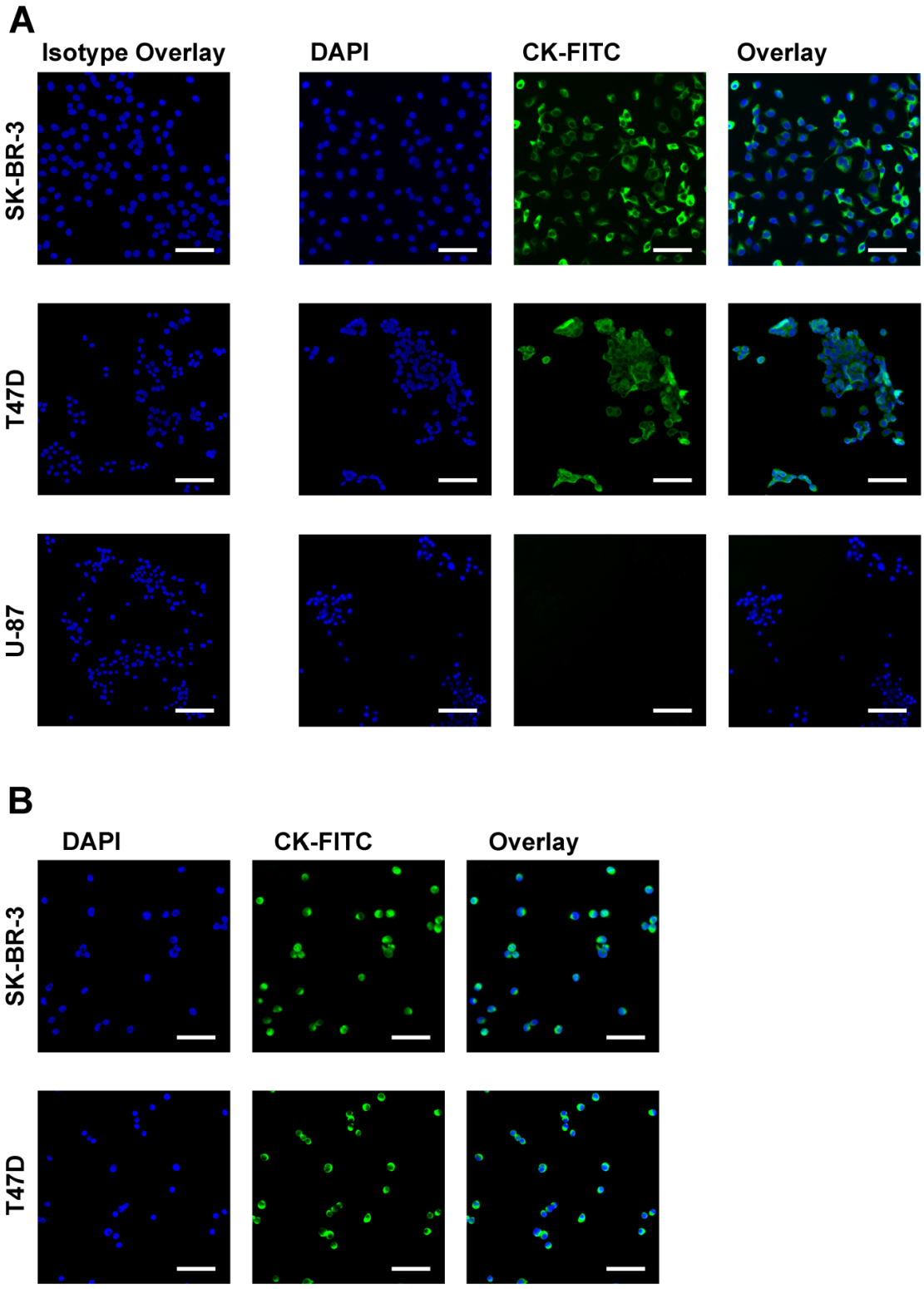

Figure 22: Optimization of the cytokeratin (CK) staining. (A) SK-BR-3, T47D and U-87 cells were grown in chamber slides, fixed and stained with a green-labeled CK antibody cocktail and Hoechst 33342 (blue) for the cell nucleus. SK-BR-3 and T47D cells showed a strong and even CK staining (upper and middle row). Being a glioblastoma cell line, U 87 is negative for cytokeratins (lower row). (B) To accurately reflect the conditions for cells stained on the wire, SK-BR-3 and T47D cells were immobilized on poly-lysin-coated slides, fixed and stained as described above. The size, morphology and staining of these cells was then used as a reference for the cells captured on the CellCollector®. Scale bar 100 µm.

3.2.2.5 Capture of Membrane Hsp70-high and Membrane Hsp70-low Tumor Cells with the Hsp70 CellCollector®

After suitable cell lines were selected and the CK staining was established, the next step was to compare the performance of the Hsp70 CellCollector® on the membrane Hsp70-high and Hsp70-low cell lines. These experiments were performed on the new generation of collectors. Their functional part is 4 cm long and the gold coating is replaced by a special alginate coating. To further increase the functional surface, the tip consists of three intertwined wires instead of one. While cell capture in earlier experiments was performed on a tilting shaker, the incubation was now carried out in a rotator. This prevents cells from settling on the detector solely due to gravity.

SK-BR-3 and T47D cells were incubated with the Hsp70 collectors for 30 min, fixed and stained according to the CK protocol. For each cell line, six detectors were used. The experiments were carried out on two consecutive days to ensure short storage times prior to the microscopic analysis. To avoid bias based on the different days, half of the wires for each cell line were used on each day. The detectors were analyzed directly after staining by counting the captured cells on each wire. Because of the unique properties of the intertwined wires, counting on four sides of the device (90° rotation) resulted in double counting of many of the cells. It was therefore decided to count only two sides of the wires, with a 180° rotation of the device.

Fluorescent events were identified as cells based on their size, morphology and a coinciding signal in the blue (nucleus) and green (cytokeratin) channel. Representative images were taken for both cell lines (Figure 23 and Figure 24). It was noticeable that many of the cells did not display the clear image that was expected from the test staining on poly-lysin slides. In several cases, the whole cell body was evenly stained in blue and green. Other cells appeared to have leaked their contents to the surrounding, resulting in a faint signal in the proximity of the cells. However, many of the cells showed the expected pattern with a distinct staining of nucleus and cytoplasm, especially on the T47D collectors.

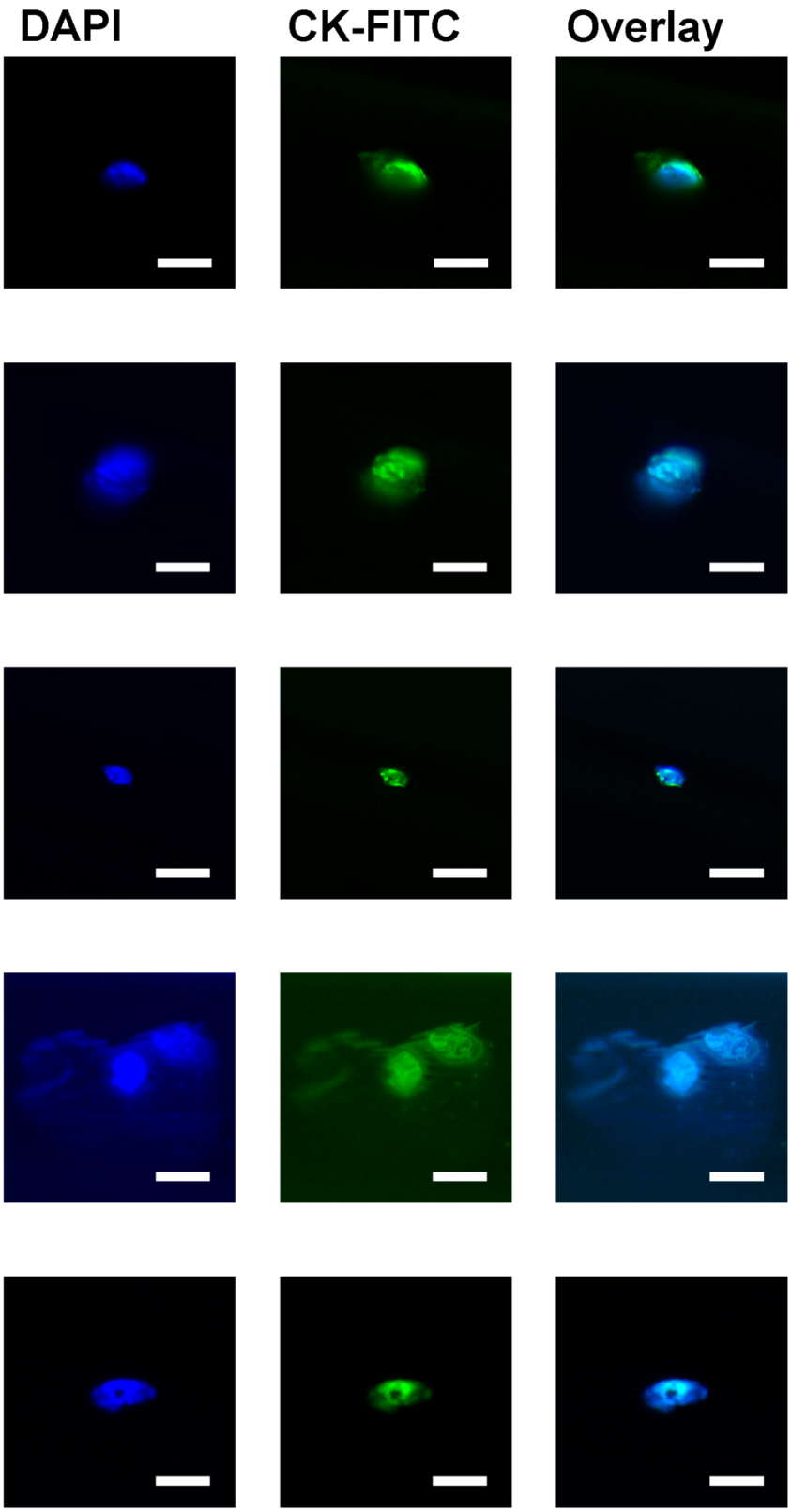

Figure 23: Capture of membrane Hsp70-high SK-BR-3 with the Hsp70 CellCollector®. SK-BR-3 cells were incubated with the Hsp70 CellCollector® for 30 min, fixed and stained with cytokeratin antibodies (green) and Hoechst 33342 (blue). This figure shows representative images taken while counting the captured cells on the wire. It is noticeable that some cells seem to be damaged and have leaked their contents into the surrounding, indicating the staining procedure might have to be further optimized. Scale bar 25 µm.

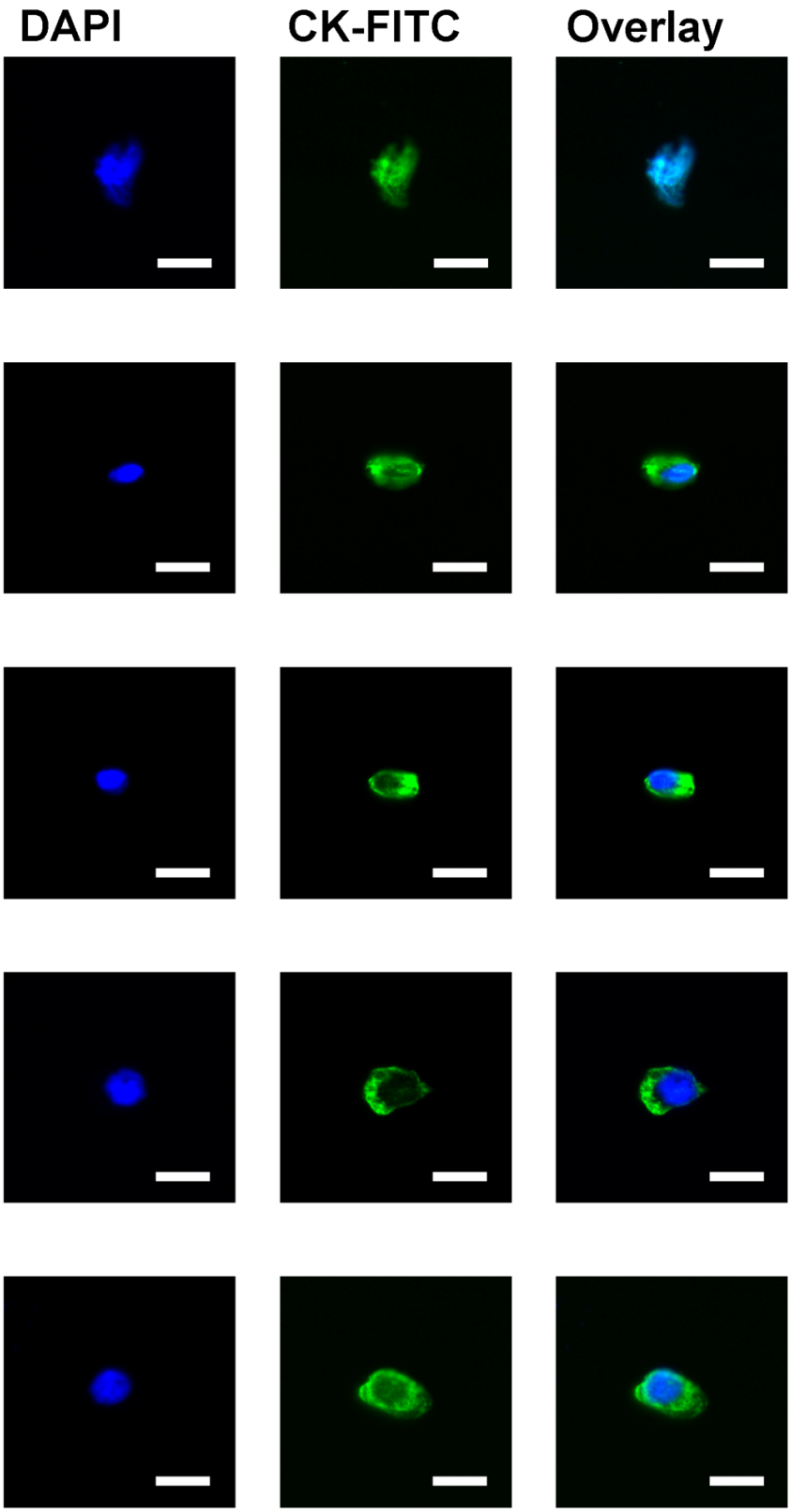

Figure 24: Capture of membrane Hsp70-low T47D with the Hsp70 CellCollector®. T47D cells were incubated with the Hsp70 CellCollector® for 30 min, fixed and stained with cytokeratin antibodies (green) and Hoechst 33342 (blue). This figure shows representative images taken while counting the captured cells on the wire. The T47D cells show a much more intact morphology compared to the SK-BR-3 cells, indicating they might be more resistant to the staining procedure. Scale bar 25 µm.

Counting of the captured cells resulted in a mean cell number of 117 cells on the SK-BR-3 collectors and 87 cells on the T47D collectors (Figure 25). This means that, as expected, more cells are captured in the case of a highly Hsp70-positive cell line than for a cell line with low Hsp70 expression, although the data set was not significant. An increase in n numbers and optimization of the fixation process should improve the result.

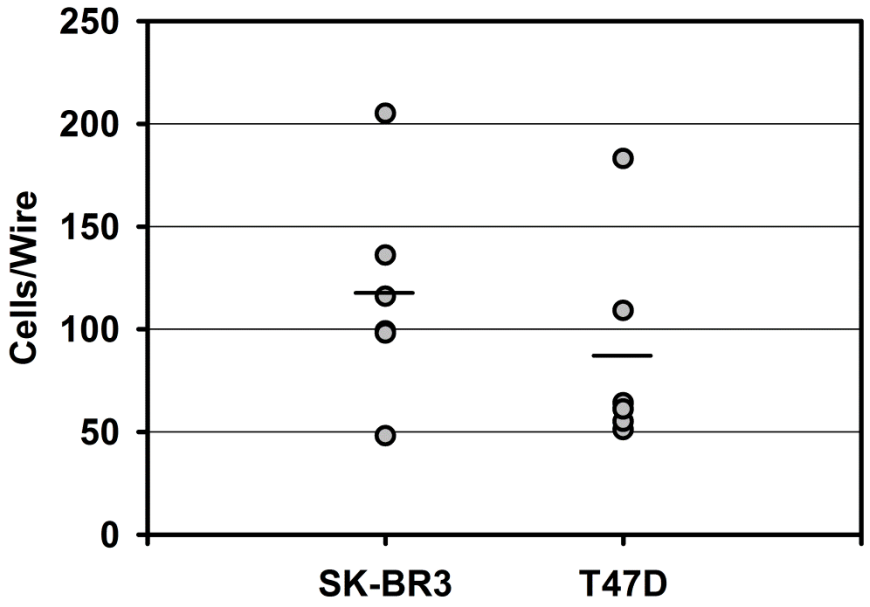

Figure 25: Comparison of high- and low-expressing tumor cells captured with the Hsp70 CellCollector®. Six detectors each were incubated with the Hsp70-high SK-BR-3 cells and Hsp70-low T47D cells, respectively. After fixation and staining of the cells, the detectors were analyzed with a fluorescence microscope. Cells were counted on one side of the wire, which was then turned by 180° and cells were counted on the other side. With a mean of 117 captured cells, the recovery of SK-BR-3 cells was higher than that of the T47D cells with a mean of 87 captured cells. Most likely due to the small sample number, the result was not significant. (Solid Line: Mean of six experiments.)

4 Discussion

4.1 Development of the lipHsp70 ELISA

Blood-borne biomarkers have been a useful tool in the detection and monitoring of diseases for many years. Similarly, they have shown growing potential for the detection of tumors, monitoring of tumor growth and assessing the outcome of antitumor therapies (Alvarez-Chaver *et al.*, 2014; Hirales Casillas *et al.*, 2014; Madu & Lu, 2010). However, many tumor markers have been criticized for their lack of specificity and selectivity, and the need for a universal and specific tumor biomarker is still unmet (Grunnet & Sorensen, 2012; Hayes & Barry, 2014; Loeb, 2014).

Although heat shock (stress) proteins are commonly considered as being intracellular molecules, elevated levels of Hsp70 have been detected in the supernatants of cultured tumor cells (De Maio, 2011) and also in the peripheral circulation of patients with cancer (Pockley *et al.*, 2014). Levels of circulating heat shock proteins, including Hsp70, might therefore serve as useful biomarkers for disease in a number of clinical settings.

Extracellular Hsp70 exists in two different versions. It can be a free protein or a protein that is bound to lipid vesicles such as exosomes (Gastpar *et al.*, 2005) and lysosomal endosomes (Mambula & Calderwood, 2006). Other groups, including ours, have shown an interaction of Hsp70 with cholesterol-rich microdomains (Broquet *et al.*, 2003; M. Gehrmann, Liebisch*, et al.*, 2008). The minor part of extracellular Hsp70 is free Hsp70, which is mostly derived from dying cells. Certain combined treatment modalities such as radiation plus hyperthermia have been shown to increase the release of free Hsp70 by dying cells (Schildkopf *et al.*, 2011). The major proportion of extracellular Hsp70, which is derived from living, metabolically active tumor cells, is bound to small lipid vesicles such as exosomes, which are actively released by a large variety of human tumor cell types (Gastpar *et al.*, 2005; Vega *et al.*, 2008). Lipid-bound, exosomal Hsp70 could therefore serve as an interesting novel biomarker, which might better reflect the presence and size of viable tumor masses in patients and their response to treatment. However, most commercially available Hsp70 ELISA systems are optimized and validated for the analysis of free Hsp70 protein in aqueous buffer systems. It is therefore not surprising that different “in-

house" and commercially available Hsp70 assays have reported different Hsp70 levels in blood samples (Fredly *et al.*, 2012; Lebherz-Eichinger *et al.*, 2012; Lee *et al.*, 2015; Lichtenauer *et al.*, 2014; Njemini *et al.*, 2005; Pockley *et al.*, 1998). A prerequisite for measuring the absolute levels of Hsp70 in patient blood is therefore an assay that reliably quantitatively detects both free and liposomal Hsp70.

Our group has previously reported on the development and validation of a mouse monoclonal antibody (cmHsp70.1), which is able to bind to a form of Hsp70 that is located in the plasma membrane of viable tumor cells (Stangl *et al.*, 2011), but also detects free Hsp70 in Western blots. Thus, this antibody is an ideal tool for the detection of both liposomal and free Hsp70. The cmHsp70.1 antibody therefore provided the basis for the development of the novel lipHsp70 ELISA in this project.

Single-chain variable fragments (scFv) have been reported to be promising agents in therapeutics and diagnostics. Their main advantage is their easy and fast production and optimization via phage display. They contain the complete antigen binding site of an antibody, including the variable heavy and light domains (Weisser & Hall, 2009). However, different ELISA setups with a combination of the anti-Hsp70 single-chain fragments and the cmHsp70.1 antibody could not detect Hsp70 at concentrations below 10 ng/ml. A possible explanation is that the scFvs are relatively small in comparison to full-length antibodies. This might lead to an increased blocking of the antigen binding site when they are absorbed to an ELISA plate, thus hindering the specific detection of the antigen.

Milk powder proved to be the blocking agent resulting in the lowest background. This is most likely due to the fact that it contains a mixture of large and small proteins that are able to block gaps of different sizes in the ELISA well. Dilution of the sample in CrossDown buffer reduced the matrix effects that are often observed with serum samples. The final, optimized lipHsp70 ELISA was set up using a polyclonal coating antibody, a biotinylated cmHsp70.1 as detection tool and streptavidin-HRP for signal enhancement.

4.2 Performance of the lipHsp70 ELISA

The novel lipHsp70 ELISA was tested and validated for a variety of circumstances. It allows for the quantification of Hsp70 in both serum and plasma at equal levels. These results are in contrast to Lee *et al.*, who found lower Hsp70 levels in serum than plasma when comparing two commercial ELISA kits (Lee *et al.*, 2015). The lipHsp70 ELISA might therefore also be less susceptible to matrix effects that are often caused by serum components. The validation experiments (summarized in Table 3) indicate a high assay precision and linearity in the relevant concentration range. Hsp70 levels in all measured samples were well above the limit of detection.

The recovery of spiked Hsp70 in buffer and serum samples was significantly higher with the lipHsp70 ELISA compared to that of the commercially available ELISA test. The most prominent differences in the recovery of Hsp70 were detected with respect to liposomal Hsp70 from artificial exosomes, in that the lipHsp70 ELISA recovered tenfold more of the liposomal Hsp70 than the commercial ELISA. An explanation for this observation is the capacity of the monoclonal antibody cmHsp70.1 to recognize the lipid-associated form of Hsp70 as outlined schematically in Figure 26.

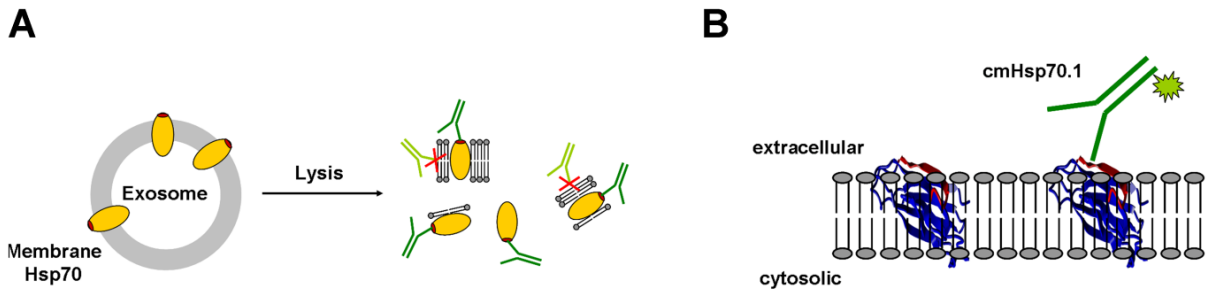

Figure 26: Lipid-association of Hsp70 in exosomes and in the plasma membrane of living tumor cells. (A) An incomplete solubilization of lipid vesicles such as exosomes with detergents used in ELISA tests can lead to Hsp70-lipid complexes. Lipid-bound Hsp70 that exerts a different conformation can only be detected by the cmHsp70.1 antibody but not by other Hsp70-specific antibodies. (B) The cmHsp70.1 antibody detects Hsp70 on the plasma membrane of living tumor cells. This lipid-bound conformation of Hsp70 in the plasma membrane is similar to that of lipid-bound Hsp70 in exosomes. Therefore, the recovery of lipid-bound Hsp70 with the lipHsp70 ELISA is better than with the control ELISA (Breuninger *et al.*, 2015).

Membrane-bound Hsp70 is often located in detergent-resistant microdomains or lipid rafts (Brown & London, 2000; Vega *et al.*, 2008). As most commercially available sample dilution buffers for ELISAs contain non-ionic detergents to dissolve lipid vesicles, it is likely that a proportion of serum Hsp70 remains associated with lipids after treatment (Figure 26A). The continued association of Hsp70 with lipid components could inhibit the binding of Hsp70-specific antibodies that are used in

commercial kits or influence the conformation of Hsp70 such that binding of the antibody does not occur. In contrast, the documented ability of the cmHsp70.1 antibody to detect the membrane-bound conformation of Hsp70 on viable tumor cells (Figure 26B) suggests that it can also recognize lipid-associated Hsp70 from exosomes. Since a major proportion of serum-derived Hsp70 is bound to lipid vesicles, the lipHsp70 ELISA is more appropriate for the measurement of circulating Hsp70 derived from viable tumor cells.

4.3 Hsp70 Levels in Healthy Donors and Cancer Patients

In a final step, the novel lipHsp70 ELISA was evaluated as a tool for the detection and quantification of Hsp70 as a biomarker in the blood of cancer patients. First, the normal serum Hsp70 levels in the blood of healthy donors were determined and tested with respect to different interference factors. The basal levels of Hsp70 in the serum of 114 healthy human donors were found to be significantly higher when measured with the lipHsp70 ELISA compared to the commercial R&D ELISA, as well as two other commercially available ELISA kits that were tested by Lee et al. (Lee *et al.*, 2015). These results are most likely due to the fact that hematopoietic cells (such as B cells and T cells), dendritic cells, Schwann cells, neuronal cells, adipocytes and fibroblasts are able to release exosomes that contain low amounts of Hsp70 in their lumen (Record *et al.*, 2011).

Hsp70 levels did not change with the age of the donors. The results obtained with the lipHsp70 ELISA remained unaffected by food intake of the blood donor, thereby facilitating the use of this assay in a clinical setting, where examination and treatment of patients occur throughout the whole day. Similarly, repeated freezing and thawing of the serum samples up to ten times did not influence the results of the assay, which allows for storage and reuse of the samples. The lipHsp70 ELISA also tolerated moderate hemolysis up to a hemoglobin concentration of 9.6 mg/dl. Concentrations above this level resulted in a non-specific increase of the measured Hsp70 values. This means that macroscopically visibly red sera should be treated with caution.

Finally, the novel lipHsp70 ELISA was used to analyze the serum Hsp70 levels of patients with six different tumor entities, including head and neck, lung, colorectal, pancreatic cancer, glioblastoma and hematological malignancies. Significantly higher Hsp70 levels were detected in the serum of those patients compared to healthy

controls. This is in agreement with the fact that tumor cells exhibit higher cytosolic Hsp70 levels and actively release high amounts of Hsp70 in lipid vesicles.

Notably, distinct differences could be observed with elevated concentrations of circulating Hsp70 in patients with different tumor entities, with the highest Hsp70 serum levels in patients with glioblastoma. Although these data require further analysis and validation with extended cohorts of patients, these relationships may provide evidence on different expression patterns not only between individual patients, but also between different tumor entities. They are also in agreement with previous findings showing that more aggressive tumor types express and release higher levels of Hsp70 (Botzler, Schmidt*, et al.*, 1998; Farkas *et al.*, 2003; M. Gehrmann, Specht*, et al.*, 2014; Pfister *et al.*, 2007).

Previous studies in our group could show a correlation between gross tumor volume (GTV) and blood Hsp70 levels (obtained with the commercial Hsp70 ELISA), as well as a reduction of blood Hsp70 levels after therapy in mice (Bayer *et al.*, 2014). Similar results were found in patients with squamous cell carcinoma of the head and neck (M. Gehrmann, Specht*, et al.*, 2014). As the major part of circulating Hsp70 is actively released in lipid-associated form by viable tumor cells, the novel lipHsp70 ELISA could further improve our ability to assess these relationships. First results with the lipHsp70 have been obtained by our group in non-small cell lung cancer (NSCLC) patients. It could be shown that a small GTV was associated with low serum Hsp70 and a large GTV with high serum Hsp70 levels in a patient cohort with 55 NSCLC patients. In addition, a slight but not significant drop in serum Hsp70 levels directly after therapy could be observed in a group of six NSCLC patients (Gunther *et al.*, 2015). Additional studies with larger patient populations and later follow-up time points are ongoing.

4.4 Tumor Cell Capture with Magnetic Beads

Circulating tumor cells, like proteins, constitute a valuable blood-borne cancer biomarker. They can provide information on various clinical parameters like prognosis and therapy response, as well as give us insights into the mechanisms of metastasis development (Alix-Panabieres & Pantel, 2012). To increase our understanding of metastases is essential, given that in 90% of the cases metastases rather than the primary tumor are the cause of death from cancer (Gupta & Massague, 2006). A

major part of existing detection and isolation methods relies on the expression of the epithelial cell adhesion molecule EpCAM (Alix-Panabieres & Pantel, 2014). However, EpCAM is known to be downregulated during epithelial-mesenchymal transition (EMT), which is an important process that many tumor cells undergo during their transition into the blood stream (Hanahan & Weinberg, 2011).

Hsp70 has been found on the membrane of a wide variety of tumor entities (Hantschel *et al.*, 2000; Pfister *et al.*, 2007) and is known to be upregulated in metastases (Farkas *et al.*, 2003). This makes it a promising target for the isolation of circulating tumor cells and could enable us to catch cells that might be lost in EpCAM-based approaches due to EMT. Our group's antibody cmHsp70.1 has the unique ability to bind Hsp70 located on the cell membrane, and therefore provides us with the ideal tool for this approach.

Many antibody-based CTC detection techniques use magnetic beads or particles for capture and isolation of the cells, including the current "gold standard" of isolation techniques, the CellSearch® system (Coumans & Terstappen, 2015). Four different systems were tested in this project, each of them with individual advantages and disadvantages, as described in 3.2.1.1. By far the best results could be obtained with the Dynabeads MyOne Tosylactivated, which are covalently coupled to the capture antibody, and thus reduce the points where the binding between bead and cell can be interrupted to a minimum.

Proof-of-principle experiments with these beads in buffer gave excellent results, yielding recovery fractions comparable to the Hsp70 status of the respective high and low expressing cancer cell lines. As CTCs are very rare cells, the main challenge with magnetic bead isolation is the limited blood volume that can be analyzed (Alix-Panabieres & Pantel, 2012). An enrichment step prior to the isolation from blood can therefore significantly improve the yield and at the same time reduce interference by the very abundant erythrocytes. Two approaches were tested. Lysing of erythrocytes prior to cell capture resulted in significant damage of the lymphocytes, which lead to unspecific binding and blocking of the antibody-coated beads and almost completely abolished tumor cell capture. In contrast, enrichment of the cells with Ficoll and subsequent magnetic bead separation resulted in recovery yields very similar to the isolation in buffer, which makes this a very promising approach. However, it does not completely solve the underlying problem of the limited blood volume.

4.5 Tumor Cell Capture with the GILUPI CellCollector®

The GILUPI CellCollector® was developed to overcome the restrictions caused by attempting to find extremely rare cells in a blood sample of only a few milliliters. The antibody-coated wire is inserted directly into the bloodstream for 30 min, increasing the blood volume to be analyzed to several liters. It has been extensively studied for biocompatibility and is well tolerated by the patients (Saucedo-Zeni *et al.*, 2012). Like most of the CTC detection methods, the CellCollector® uses an EpCAM antibody for the capture of the tumor cells. The aim of this project was therefore to explore whether an Hsp70-based cell capture could further improve this system by sidestepping the problem of downregulated EpCAM due to EMT.

From a panel of tumor cells lines, three cell lines were chosen that would later allow a comparison of the performance and specificity of the EpCAM versus the Hsp70 wire: SK-BR-3 with a similarly high expression of both markers, T47D with a high EpCAM and a low Hsp70 expression and U-87 with opposite characteristics. Staining of these cells was optimized for pre-staining with CFSE, as well as for cytokeratin staining after cell capture, reducing bleaching and damaging of the cells as far as possible. Test runs with the previously developed bead separation technique could show that the pre-staining did not interfere with subsequent antibody binding. The glioblastoma cell line U-87 is not of epithelial origin and can therefore not be stained with cytokeratin antibodies. It should therefore be considered to replace this cell line for further experiments that use cytokeratin for cell staining. As shown in the cell line screening (Figure 18), the pancreas tumor cell line MIA PaCa also has a high Hsp70 and a low EpCAM expression. Alternatively, a different staining procedure would have to be chosen for the U-87 cells.

A first comparison between the Hsp70 wire and the EpCAM wire revealed a similar capacity to capture SK-BR-3 cells from buffer, as would be expected based on their expression of both markers. It was possible to transfer the captured cells back into cell culture in order to analyze them further. This may become important when the rare circulating tumor cells need to be expanded to study their characteristics. In the same experiment it could be shown that the cells can be isolated from a mixture with blood.

In the final validation step, the second generation Hsp70 wire was tested on the two breast cancer cell lines SK-BR-3 and T47D, with high and low Hsp70 expression, respectively. Cells were fixed and stained with DAPI and a CK antibody cocktail directly on the wire. As expected, more cells could be found on the wire when SK-BR-3 cells were captured compared to T47D cells. However, due to the small sample size, the results were not significant.

4.6 Conclusion and Future Perspectives

Hsp70 has been shown to be present on the cell surface of a large variety of different tumor cell lines, primary tumors and metastases. Comparative studies have demonstrated that more aggressive primary tumors, as well as metastases, often express even higher levels of Hsp70. In addition to that, tumors actively release Hsp70 in lipid vesicles into the extracellular space. This makes circulating as well as membrane-bound Hsp70 a promising biomarker, as well as a target for tumor detection and therapy. The antibody cmHsp70.1, with its ability to bind to free and lipid-bound Hsp70, provides us with an ideal tool to explore these possibilities.

In this project, cmHsp70.1 was used to develop the novel lipHsp70 ELISA for the detection of free and lipid-bound Hsp70 and a method to isolate circulating tumor cells. Both parameters could serve as important biomarkers in the blood of cancer patients.

The reliability and robustness of the lipHsp70 ELISA together with its ability to detect higher levels of Hsp70 in the circulation of patients with cancer makes this method a promising tool for monitoring the presence and size of viable tumor mass, as well as measuring the therapeutic outcome.

Combining the GILUPI CellCollector® – a functionalized medical wire suitable for direct insertion into the patient's blood stream – with the cmHsp70.1 antibody has provided us with first promising results for capturing circulating tumor cells. This approach needs further optimization. Staining of the cells on the wire, with and without fixation, should be improved in order to reduce cell damage and to allow for subsequent use of the captured CTCs in cell culture and for analyzing their characteristics. It should also be considered to establish staining of the cells for

different markers. In another step, the performance of the Hsp70 wire will have to be compared with the EpCAM version of the wire in more detail.

In summary, the data presented in this thesis provide a strong basis for using extracellular Hsp70 and membrane Hsp70 on circulating tumor cells as a novel universal biomarker for future clinical applications.

5 References

Aceto, N., Bardia, A., Miyamoto, D. T., Donaldson, M. C., Wittner, B. S., Spencer, J. A., Yu, M., Pely, A., Engstrom, A., Zhu, H., Brannigan, B. W., Kapur, R., Stott, S. L., Shioda, T., Ramaswamy, S., Ting, D. T., Lin, C. P., Toner, M., Haber, D. A., and Maheswaran, S. (2014). Circulating tumor cell clusters are oligoclonal precursors of breast cancer metastasis. *Cell,* **158**(5), 1110-1122. doi: 10.1016/j.cell.2014.07.013

Alix-Panabieres, C., and Pantel, K. (2012). Circulating Tumor Cells: Liquid Biopsy of Cancer. *Clin Chem*. doi: 10.1373/clinchem.2012.194258

Alix-Panabieres, C., and Pantel, K. (2014). Technologies for detection of circulating tumor cells: facts and vision. *Lab Chip,* **14**(1), 57-62. doi: 10.1039/c3lc50644d

Alvarez-Chaver, P., Otero-Estevez, O., Paez de la Cadena, M., Rodriguez-Berrocal, F. J., and Martinez-Zorzano, V. S. (2014). Proteomics for discovery of candidate colorectal cancer biomarkers. *World J Gastroenterol,* **20**(14), 3804-3824. doi: 10.3748/wjg.v20.i14.3804

American Society of Clinical Oncology. (2016). Practice & Guidelines - Assays and Predictive Markers. Retrieved 07-Oct-2016, from https://www.asco.org/practice-guidelines/quality-guidelines/guidelines/assays-and-predictive-markers

Anand, P. K. (2010). Exosomal membrane molecules are potent immune response modulators. *Commun Integr Biol,* **3**(5), 405-408. doi: 10.4161/cib.3.5.12474

Arispe, N., Doh, M., Simakova, O., Kurganov, B., and De Maio, A. (2004). Hsc70 and Hsp70 interact with phosphatidylserine on the surface of PC12 cells resulting in a decrease of viability. *FASEB J,* **18**(14), 1636-1645. doi: 10.1096/fj.04-2088com

Armbruster, D. A., and Pry, T. (2008). Limit of blank, limit of detection and limit of quantitation. *Clin Biochem Rev,* **29 Suppl 1**, S49-52.

Baccelli, I., Schneeweiss, A., Riethdorf, S., Stenzinger, A., Schillert, A., Vogel, V., Klein, C., Saini, M., Bauerle, T., Wallwiener, M., Holland-Letz, T., Hofner, T., Sprick, M., Scharpff, M., Marme, F., Sinn, H. P., Pantel, K., Weichert, W., and Trumpp, A. (2013). Identification of a population of blood circulating tumor cells from breast cancer patients that initiates metastasis in a xenograft assay. *Nat Biotechnol*. doi: 10.1038/nbt.2576

Barber, C. J. (1989). Central venous catheter placement for intravenous digital subtraction angiography: an assessment of technical problems and success rate. *Br J Radiol,* **62**(739), 599-602. doi: 10.1259/0007-1285-62-739-599

Bausero, M. A., Gastpar, R., Multhoff, G., and Asea, A. (2005). Alternative mechanism by which IFN-gamma enhances tumor recognition: active release of heat shock protein 72. *J Immunol,* **175**(5), 2900-2912.

Bayer, C., Liebhardt, M. E., Schmid, T. E., Trajkovic-Arsic, M., Hube, K., Specht, H. M., Schilling, D., Gehrmann, M., Stangl, S., Siveke, J. T., Wilkens, J. J., and Multhoff, G. (2014). Validation of heat shock protein 70 as a tumor-specific biomarker for monitoring the outcome of radiation therapy in tumor mouse models. *Int J Radiat Oncol Biol Phys,* **88**(3), 694-700. doi: 10.1016/j.ijrobp.2013.11.008

Bertelsen, E. B., Chang, L., Gestwicki, J. E., and Zuiderweg, E. R. (2009). Solution conformation of wild-type E. coli Hsp70 (DnaK) chaperone complexed with ADP and substrate. *Proc Natl Acad Sci U S A,* **106**(21), 8471-8476. doi: 10.1073/pnas.0903503106

Botzler, C., Issels, R., and Multhoff, G. (1996). Heat-shock protein 72 cell-surface expression on human lung carcinoma cells in associated with an increased sensitivity to lysis mediated by adherent natural killer cells. *Cancer Immunol Immunother,* **43**(4), 226-230.

Botzler, C., Li, G., Issels, R. D., and Multhoff, G. (1998). Definition of extracellular localized epitopes of Hsp70 involved in an NK immune response. *Cell Stress Chaperones,* **3**(1), 6-11.

Botzler, C., Schmidt, J., Luz, A., Jennen, L., Issels, R., and Multhoff, G. (1998). Differential Hsp70 plasma-membrane expression on primary human tumors and metastases in mice with severe combined immunodeficiency. *Int J Cancer,* **77**(6), 942-948.

Bratt, O., and Lilja, H. (2015). Serum markers in prostate cancer detection. *Curr Opin Urol,* **25**(1), 59-64. doi: 10.1097/MOU.0000000000000128

Breuninger, S., Erl, J., Knape, C., Gunther, S., Regel, I., Rödel, F., Gaipl, U. S., Thorsteinsdottir, J., Giannitrapani, L., and Dickinson, A. M. (2015). Quantitative analysis of liposomal heat shock protein 70 (Hsp70) in the blood of tumor patients using a novel lipHsp70 ELISA. *Journal of Clinical & Cellular Immunology,* **2014**.

Broquet, A. H., Thomas, G., Masliah, J., Trugnan, G., and Bachelet, M. (2003). Expression of the molecular chaperone Hsp70 in detergent-resistant microdomains correlates with its membrane delivery and release. *J Biol Chem,* **278**(24), 21601-21606. doi: 10.1074/jbc.M302326200

Brown, D. A., and London, E. (2000). Structure and function of sphingolipid- and cholesterol-rich membrane rafts. *J Biol Chem,* **275**(23), 17221-17224. doi: 10.1074/jbc.R000005200

Calderwood, S. K., Xie, Y., Wang, X., Khaleque, M. A., Chou, S. D., Murshid, A., Prince, T., and Zhang, Y. (2010). Signal Transduction Pathways Leading to Heat Shock Transcription. *Sign Transduct Insights,* **2**, 13-24. doi: 10.4137/STI.S3994

Chambers, A. F., Groom, A. C., and MacDonald, I. C. (2002). Dissemination and growth of cancer cells in metastatic sites. *Nat Rev Cancer,* **2**(8), 563-572. doi: 10.1038/nrc865

Cho, E. H., Wendel, M., Luttgen, M., Yoshioka, C., Marrinucci, D., Lazar, D., Schram, E., Nieva, J., Bazhenova, L., Morgan, A., Ko, A. H., Korn, W. M., Kolatkar, A., Bethel, K., and Kuhn, P. (2012). Characterization of circulating tumor cell aggregates identified in patients with epithelial tumors. *Phys Biol,* **9**(1), 016001. doi: 10.1088/1478-3975/9/1/016001

Ciocca, D. R., and Calderwood, S. K. (2005). Heat shock proteins in cancer: diagnostic, prognostic, predictive, and treatment implications. *Cell Stress Chaperones,* **10**(2), 86-103.

Cohen, S. J., Punt, C. J., Iannotti, N., Saidman, B. H., Sabbath, K. D., Gabrail, N. Y., Picus, J., Morse, M. A., Mitchell, E., Miller, M. C., Doyle, G. V., Tissing, H., Terstappen, L. W., and Meropol, N. J. (2009). Prognostic significance of circulating tumor cells in patients with metastatic colorectal cancer. *Ann Oncol,* **20**(7), 1223-1229. doi: 10.1093/annonc/mdn786

Coumans, F., and Terstappen, L. (2015). Detection and Characterization of Circulating Tumor Cells by the CellSearch Approach. *Methods Mol Biol,* **1347**, 263-278. doi: 10.1007/978-1-4939-2990-0_18

Cristofanilli, M., Budd, G. T., Ellis, M. J., Stopeck, A., Matera, J., Miller, M. C., Reuben, J. M., Doyle, G. V., Allard, W. J., Terstappen, L. W., and Hayes, D. F. (2004). Circulating tumor cells, disease progression, and survival in metastatic breast cancer. *N Engl J Med,* **351**(8), 781-791. doi: 10.1056/NEJMoa040766

Daugaard, M., Rohde, M., and Jaattela, M. (2007). The heat shock protein 70 family: Highly homologous proteins with overlapping and distinct functions. *FEBS Lett,* **581**(19), 3702-3710. doi: 10.1016/j.febslet.2007.05.039

De Maio, A. (1999). Heat shock proteins: facts, thoughts, and dreams. *Shock,* **11**(1), 1-12.

De Maio, A. (2011). Extracellular heat shock proteins, cellular export vesicles, and the Stress Observation System: a form of communication during injury, infection, and cell damage. It is never known how far a controversial finding will go! Dedicated to Ferruccio Ritossa. *Cell Stress Chaperones,* **16**(3), 235-249. doi: 10.1007/s12192-010-0236-4

Diamandis, E. P., and Yousef, G. M. (2002). Human tissue kallikreins: a family of new cancer biomarkers. *Clin Chem,* **48**(8), 1198-1205.

Duffy, M. J. (2001). Clinical uses of tumor markers: a critical review. *Crit Rev Clin Lab Sci,* **38**(3), 225-262. doi: 10.1080/20014091084218

Duffy, M. J. (2007). Role of tumor markers in patients with solid cancers: A critical review. *Eur J Intern Med,* **18**(3), 175-184. doi: 10.1016/j.ejim.2006.12.001

Duffy, M. J. (2013). Tumor markers in clinical practice: a review focusing on common solid cancers. *Med Princ Pract,* **22**(1), 4-11. doi: 10.1159/000338393

Duffy, M. J., and Crown, J. (2008). A personalized approach to cancer treatment: how biomarkers can help. *Clin Chem,* **54**(11), 1770-1779. doi: 10.1373/clinchem.2008.110056

Farkas, B., Hantschel, M., Magyarlaki, M., Becker, B., Scherer, K., Landthaler, M., Pfister, K., Gehrmann, M., Gross, C., Mackensen, A., and Multhoff, G. (2003). Heat shock protein 70 membrane expression and melanoma-associated marker phenotype in primary and metastatic melanoma. *Melanoma Res,* **13**(2), 147-152. doi: 10.1097/01.cmr.0000056221.78713.57

Flaherty, K. M., DeLuca-Flaherty, C., and McKay, D. B. (1990). Three-dimensional structure of the ATPase fragment of a 70K heat-shock cognate protein. *Nature,* **346**(6285), 623-628. doi: 10.1038/346623a0

Fredly, H., Reikvam, H., Gjertsen, B. T., and Bruserud, O. (2012). Disease-stabilizing treatment with all-trans retinoic acid and valproic acid in acute myeloid leukemia: serum hsp70 and hsp90 levels and serum cytokine profiles are determined by the disease, patient age, and anti-leukemic treatment. *Am J Hematol,* **87**(4), 368-376. doi: 10.1002/ajh.23116

Fuchs, A. B., Romani, A., Freida, D., Medoro, G., Abonnenc, M., Altomare, L., Chartier, I., Guergour, D., Villiers, C., Marche, P. N., Tartagni, M., Guerrieri, R., Chatelain, F., and Manaresi, N. (2006). Electronic sorting and recovery of single live cells from microlitre sized samples. *Lab Chip,* **6**(1), 121-126. doi: 10.1039/b505884h

Gaca, S., Reichert, S., Multhoff, G., Wacker, M., Hehlgans, S., Botzler, C., Gehrmann, M., Rodel, C., Kreuter, J., and Rodel, F. (2013). Targeting by cmHsp70.1-antibody coated and survivin miRNA plasmid loaded nanoparticles to radiosensitize glioblastoma cells. *J Control Release*. doi: 10.1016/j.jconrel.2013.08.020

Garrido, C., Gurbuxani, S., Ravagnan, L., and Kroemer, G. (2001). Heat shock proteins: endogenous modulators of apoptotic cell death. *Biochem Biophys Res Commun,* **286**(3), 433-442. doi: 10.1006/bbrc.2001.5427

Gascoyne, P. R., Noshari, J., Anderson, T. J., and Becker, F. F. (2009). Isolation of rare cells from cell mixtures by dielectrophoresis. *Electrophoresis,* **30**(8), 1388-1398. doi: 10.1002/elps.200800373

Gastpar, R., Gehrmann, M., Bausero, M. A., Asea, A., Gross, C., Schroeder, J. A., and Multhoff, G. (2005). Heat shock protein 70 surface-positive tumor exosomes stimulate migratory and cytolytic activity of natural killer cells. *Cancer Res,* **65**(12), 5238-5247. doi: 10.1158/0008-5472.CAN-04-3804

Gastpar, R., Gross, C., Rossbacher, L., Ellwart, J., Riegger, J., and Multhoff, G. (2004). The cell surface-localized heat shock protein 70 epitope TKD induces migration and cytolytic activity selectively in human NK cells. *J Immunol,* **172**(2), 972-980.

Gehrmann, M., Liebisch, G., Schmitz, G., Anderson, R., Steinem, C., De Maio, A., Pockley, G., and Multhoff, G. (2008). Tumor-specific Hsp70 plasma membrane localization is enabled by the glycosphingolipid Gb3. *PLoS One,* **3**(4), e1925. doi: 10.1371/journal.pone.0001925

Gehrmann, M., Marienhagen, J., Eichholtz-Wirth, H., Fritz, E., Ellwart, J., Jaattela, M., Zilch, T., and Multhoff, G. (2005). Dual function of membrane-bound heat shock protein 70 (Hsp70), Bag-4, and Hsp40: protection against radiation-induced effects and target structure for natural killer cells. *Cell Death Differ,* **12**(1), 38-51. doi: 10.1038/sj.cdd.4401510

Gehrmann, M., Pfister, K., Hutzler, P., Gastpar, R., Margulis, B., and Multhoff, G. (2002). Effects of antineoplastic agents on cytoplasmic and membrane-bound

heat shock protein 70 (Hsp70) levels. *Biol Chem,* **383**(11), 1715-1725. doi: 10.1515/BC.2002.192

Gehrmann, M., Radons, J., Molls, M., and Multhoff, G. (2008). The therapeutic implications of clinically applied modifiers of heat shock protein 70 (Hsp70) expression by tumor cells. *Cell Stress Chaperones,* **13**(1), 1-10. doi: 10.1007/s12192-007-0006-0

Gehrmann, M., Specht, H. M., Bayer, C., Brandstetter, M., Chizzali, B., Duma, M., Breuninger, S., Hube, K., Lehnerer, S., van Phi, V., Sage, E., Schmid, T. E., Sedelmayr, M., Schilling, D., Sievert, W., Stangl, S., and Multhoff, G. (2014). Hsp70--a biomarker for tumor detection and monitoring of outcome of radiation therapy in patients with squamous cell carcinoma of the head and neck. *Radiat Oncol,* **9**, 131. doi: 10.1186/1748-717X-9-131

Gehrmann, M., Stangl, S., Foulds, G. A., Oellinger, R., Breuninger, S., Rad, R., Pockley, A. G., and Multhoff, G. (2014). Tumor Imaging and Targeting Potential of an Hsp70-Derived 14-Mer Peptide. *PLoS One,* **9**(8), e105344. doi: 10.1371/journal.pone.0105344

Gehrmann, M. K., Kimm, M. A., Stangl, S., Schmid, T. E., Noel, P. B., Rummeny, E. J., and Multhoff, G. (2015). Imaging of Hsp70-positive tumors with cmHsp70.1 antibody-conjugated gold nanoparticles. *Int J Nanomedicine,* **10**, 5687-5700. doi: 10.2147/IJN.S87174

Griep, R. A., Prins, M., van Twisk, C., Keller, H. J., Kerschbaumer, R. J., Kormelink, R., Goldbach, R. W., and Schots, A. (2000). Application of Phage Display in Selecting Tomato spotted wilt virus-Specific Single-Chain Antibodies (scFvs) for Sensitive Diagnosis in ELISA. *Phytopathology,* **90**(2), 183-190. doi: 10.1094/PHYTO.2000.90.2.183

Grosse-Wilde, A., Fouquier d'Herouel, A., McIntosh, E., Ertaylan, G., Skupin, A., Kuestner, R. E., del Sol, A., Walters, K. A., and Huang, S. (2015). Stemness of the hybrid Epithelial/Mesenchymal State in Breast Cancer and Its Association with Poor Survival. *PLoS One,* **10**(5), e0126522. doi: 10.1371/journal.pone.0126522

Grunnet, M., and Sorensen, J. B. (2012). Carcinoembryonic antigen (CEA) as tumor marker in lung cancer. *Lung Cancer,* **76**(2), 138-143. doi: 10.1016/j.lungcan.2011.11.012

Gunther, S., Ostheimer, C., Stangl, S., Specht, H. M., Mozes, P., Jesinghaus, M., Vordermark, D., Combs, S. E., Peltz, F., Jung, M. P., and Multhoff, G. (2015). Correlation of Hsp70 Serum Levels with Gross Tumor Volume and Composition of Lymphocyte Subpopulations in Patients with Squamous Cell

and Adeno Non-Small Cell Lung Cancer. *Front Immunol,* **6**, 556. doi: 10.3389/fimmu.2015.00556

Gupta, G. P., and Massague, J. (2006). Cancer metastasis: building a framework. *Cell,* **127**(4), 679-695. doi: 10.1016/j.cell.2006.11.001

Hanahan, D., and Weinberg, R. A. (2011). Hallmarks of cancer: the next generation. *Cell,* **144**(5), 646-674. doi: 10.1016/j.cell.2011.02.013

Hantschel, M., Pfister, K., Jordan, A., Scholz, R., Andreesen, R., Schmitz, G., Schmetzer, H., Hiddemann, W., and Multhoff, G. (2000). Hsp70 plasma membrane expression on primary tumor biopsy material and bone marrow of leukemic patients. *Cell Stress Chaperones,* **5**(5), 438-442.

Hartl, F. U. (1996). Molecular chaperones in cellular protein folding. *Nature,* **381**(6583), 571-579. doi: 10.1038/381571a0

Hartl, F. U., and Hayer-Hartl, M. (2002). Molecular chaperones in the cytosol: from nascent chain to folded protein. *Science,* **295**(5561), 1852-1858. doi: 10.1126/science.1068408

Hayes, J. H., and Barry, M. J. (2014). Screening for prostate cancer with the prostate-specific antigen test: a review of current evidence. *JAMA,* **311**(11), 1143-1149. doi: 10.1001/jama.2014.2085

Hirales Casillas, C. E., Flores Fernandez, J. M., Camberos, E. P., Herrera Lopez, E. J., Pacheco, G. L., and Velazquez, M. M. (2014). Current status of circulating protein biomarkers to aid the early detection of lung cancer. *Future Oncol,* **10**(8), 1501-1513. doi: 10.2217/fon.14.21

Hou, J. M., Krebs, M. G., Lancashire, L., Sloane, R., Backen, A., Swain, R. K., Priest, L. J., Greystoke, A., Zhou, C., Morris, K., Ward, T., Blackhall, F. H., and Dive, C. (2012). Clinical significance and molecular characteristics of circulating tumor cells and circulating tumor microemboli in patients with small-cell lung cancer. *J Clin Oncol,* **30**(5), 525-532. doi: 10.1200/JCO.2010.33.3716

Husemann, Y., Geigl, J. B., Schubert, F., Musiani, P., Meyer, M., Burghart, E., Forni, G., Eils, R., Fehm, T., Riethmuller, G., and Klein, C. A. (2008). Systemic spread is an early step in breast cancer. *Cancer Cell,* **13**(1), 58-68. doi: 10.1016/j.ccr.2007.12.003

Jaattela, M. (1999). Escaping cell death: survival proteins in cancer. *Exp Cell Res,* **248**(1), 30-43. doi: 10.1006/excr.1999.4455

Jolly, M. K., Boareto, M., Huang, B., Jia, D., Lu, M., Ben-Jacob, E., Onuchic, J. N., and Levine, H. (2015). Implications of the Hybrid Epithelial/Mesenchymal Phenotype in Metastasis. *Front Oncol,* **5**, 155. doi: 10.3389/fonc.2015.00155

Kahn, S. E., Watkins, B. F., and Bermes, E. W., Jr. (1981). An evaluation of a spectrophotometric scanning technique for measurement of plasma hemoglobin. *Ann Clin Lab Sci,* **11**(2), 126-131.

Kharaziha, P., Ceder, S., Li, Q., and Panaretakis, T. (2012). Tumor cell-derived exosomes: a message in a bottle. *Biochim Biophys Acta,* **1826**(1), 103-111. doi: 10.1016/j.bbcan.2012.03.006

Kirkwood, J. M., Butterfield, L. H., Tarhini, A. A., Zarour, H., Kalinski, P., and Ferrone, S. (2012). Immunotherapy of cancer in 2012. *CA Cancer J Clin,* **62**(5), 309-335. doi: 10.3322/caac.20132

Kraan, J., Sleijfer, S., Strijbos, M. H., Ignatiadis, M., Peeters, D., Pierga, J. Y., Farace, F., Riethdorf, S., Fehm, T., Zorzino, L., Tibbe, A. G., Maestro, M., Gisbert-Criado, R., Denton, G., de Bono, J. S., Dive, C., Foekens, J. A., and Gratama, J. W. (2011). External quality assurance of circulating tumor cell enumeration using the CellSearch((R)) system: a feasibility study. *Cytometry B Clin Cytom,* **80**(2), 112-118. doi: 10.1002/cyto.b.20573

Krause, S. W., Gastpar, R., Andreesen, R., Gross, C., Ullrich, H., Thonigs, G., Pfister, K., and Multhoff, G. (2004). Treatment of colon and lung cancer patients with ex vivo heat shock protein 70-peptide-activated, autologous natural killer cells: a clinical phase i trial. *Clin Cancer Res,* **10**(11), 3699-3707. doi: 10.1158/1078-0432.CCR-03-0683

Krebs, M. G., Sloane, R., Priest, L., Lancashire, L., Hou, J. M., Greystoke, A., Ward, T. H., Ferraldeschi, R., Hughes, A., Clack, G., Ranson, M., Dive, C., and Blackhall, F. H. (2011). Evaluation and prognostic significance of circulating tumor cells in patients with non-small-cell lung cancer. *J Clin Oncol,* **29**(12), 1556-1563. doi: 10.1200/JCO.2010.28.7045

Lebherz-Eichinger, D., Ankersmit, H. J., Hacker, S., Hetz, H., Kimberger, O., Schmidt, E. M., Reiter, T., Horl, W. H., Haas, M., Krenn, C. G., and Roth, G. A. (2012). HSP27 and HSP70 serum and urine levels in patients suffering from chronic kidney disease. *Clin Chim Acta,* **413**(1-2), 282-286. doi: 10.1016/j.cca.2011.10.010

Lee, B. J., Sukri, N. M., Ogden, H., Vine, C., Thake, C. D., Turner, J. E., and Bilzon, J. L. (2015). A comparison of two commercially available ELISA methods for the quantification of human plasma heat shock protein 70 during rest and

exercise stress. *Cell Stress Chaperones,* **20**(6), 917-926. doi: 10.1007/s12192-015-0610-3

Lichtenauer, M., Zimmermann, M., Nickl, S., Lauten, A., Goebel, B., Pistulli, R., Yilmaz, A., Figulla, H. R., Ankersmit, H. J., and Jung, C. (2014). Transient hypoxia leads to increased serum levels of heat shock protein-27, -70 and caspase-cleaved cytokeratin 18. *Clin Lab,* **60**(2), 323-328.

Lindquist, S., and Craig, E. A. (1988). The heat-shock proteins. *Annu Rev Genet,* **22**, 631-677. doi: 10.1146/annurev.ge.22.120188.003215

Liotta, L. A., Saidel, M. G., and Kleinerman, J. (1976). The significance of hematogenous tumor cell clumps in the metastatic process. *Cancer Res,* **36**(3), 889-894.

Liu, Z., Fusi, A., Klopocki, E., Schmittel, A., Tinhofer, I., Nonnenmacher, A., and Keilholz, U. (2011). Negative enrichment by immunomagnetic nanobeads for unbiased characterization of circulating tumor cells from peripheral blood of cancer patients. *J Transl Med,* **9**, 70. doi: 10.1186/1479-5876-9-70

Loeb, S. (2014). Guideline of Guidelines: Prostate Cancer Screening. *BJU Int*. doi: 10.1111/bju.12854

Madu, C. O., and Lu, Y. (2010). Novel diagnostic biomarkers for prostate cancer. *J Cancer,* **1**, 150-177.

Mambula, S. S., and Calderwood, S. K. (2006). Heat shock protein 70 is secreted from tumor cells by a nonclassical pathway involving lysosomal endosomes. *J Immunol,* **177**(11), 7849-7857.

Mathivanan, S., Ji, H., and Simpson, R. J. (2010). Exosomes: extracellular organelles important in intercellular communication. *J Proteomics,* **73**(10), 1907-1920. doi: 10.1016/j.jprot.2010.06.006

Mayer, M. P. (2013). Hsp70 chaperone dynamics and molecular mechanism. *Trends Biochem Sci,* **38**(10), 507-514. doi: 10.1016/j.tibs.2013.08.001

Moelans, C. B., de Weger, R. A., Van der Wall, E., and van Diest, P. J. (2011). Current technologies for HER2 testing in breast cancer. *Crit Rev Oncol Hematol,* **80**(3), 380-392. doi: 10.1016/j.critrevonc.2010.12.005

Moon, H. S., Kwon, K., Kim, S. I., Han, H., Sohn, J., Lee, S., and Jung, H. I. (2011). Continuous separation of breast cancer cells from blood samples using multi-

orifice flow fractionation (MOFF) and dielectrophoresis (DEP). *Lab Chip,* **11**(6), 1118-1125. doi: 10.1039/c0lc00345j

Multhoff, G., Botzler, C., Jennen, L., Schmidt, J., Ellwart, J., and Issels, R. (1997). Heat shock protein 72 on tumor cells: a recognition structure for natural killer cells. *J Immunol,* **158**(9), 4341-4350.

Multhoff, G., Botzler, C., Wiesnet, M., Muller, E., Meier, T., Wilmanns, W., and Issels, R. D. (1995). A stress-inducible 72-kDa heat-shock protein (HSP72) is expressed on the surface of human tumor cells, but not on normal cells. *Int J Cancer,* **61**(2), 272-279.

Multhoff, G., and Hightower, L. E. (2011). Distinguishing integral and receptor-bound heat shock protein 70 (Hsp70) on the cell surface by Hsp70-specific antibodies. *Cell Stress Chaperones,* **16**(3), 251-255. doi: 10.1007/s12192-010-0247-1

Multhoff, G., Mizzen, L., Winchester, C. C., Milner, C. M., Wenk, S., Eissner, G., Kampinga, H. H., Laumbacher, B., and Johnson, J. (1999). Heat shock protein 70 (Hsp70) stimulates proliferation and cytolytic activity of natural killer cells. *Exp Hematol,* **27**(11), 1627-1636.

Murakami, N., Kuhnel, A., Schmid, T. E., Ilicic, K., Stangl, S., Braun, I. S., Gehrmann, M., Molls, M., Itami, J., and Multhoff, G. (2015). Role of membrane Hsp70 in radiation sensitivity of tumor cells. *Radiat Oncol,* **10**, 149. doi: 10.1186/s13014-015-0461-1

Murphy, M. E. (2013). The HSP70 family and cancer. *Carcinogenesis,* **34**(6), 1181-1188. doi: 10.1093/carcin/bgt111

Nagrath, S., Sequist, L. V., Maheswaran, S., Bell, D. W., Irimia, D., Ulkus, L., Smith, M. R., Kwak, E. L., Digumarthy, S., Muzikansky, A., Ryan, P., Balis, U. J., Tompkins, R. G., Haber, D. A., and Toner, M. (2007). Isolation of rare circulating tumour cells in cancer patients by microchip technology. *Nature,* **450**(7173), 1235-1239. doi: 10.1038/nature06385

National Academy of Clinical Biochemistry. (2016). Practice Guidelines. Retrieved 07-Oct-2016, from https://www.aacc.org/science-and-practice/practice-guidelines

National Cancer Institute. (2016). Diagnosis and Staging - Tumor Markers. Retrieved 07-Oct-2016, from https://www.cancer.gov/about-cancer/diagnosis-staging/diagnosis/tumor-markers-fact-sheet

Njemini, R., Demanet, C., and Mets, T. (2005). Comparison of two ELISAs for the determination of Hsp70 in serum. *J Immunol Methods,* **306**(1-2), 176-182. doi: 10.1016/j.jim.2005.08.012

Pantel, K., Alix-Panabieres, C., and Riethdorf, S. (2009). Cancer micrometastases. *Nat Rev Clin Oncol,* **6**(6), 339-351. doi: 10.1038/nrclinonc.2009.44

Pfister, K., Radons, J., Busch, R., Tidball, J. G., Pfeifer, M., Freitag, L., Feldmann, H. J., Milani, V., Issels, R., and Multhoff, G. (2007). Patient survival by Hsp70 membrane phenotype: association with different routes of metastasis. *Cancer,* **110**(4), 926-935. doi: 10.1002/cncr.22864

Pockley, A. G., Henderson, B., and Multhoff, G. (2014). Extracellular cell stress proteins as biomarkers of human disease. *Biochem Soc Trans,* **42**(6), 1744-1751. doi: 10.1042/BST20140205

Pockley, A. G., Shepherd, J., and Corton, J. M. (1998). Detection of heat shock protein 70 (Hsp70) and anti-Hsp70 antibodies in the serum of normal individuals. *Immunol Invest,* **27**(6), 367-377.

Record, M., Subra, C., Silvente-Poirot, S., and Poirot, M. (2011). Exosomes as intercellular signalosomes and pharmacological effectors. *Biochem Pharmacol,* **81**(10), 1171-1182. doi: 10.1016/j.bcp.2011.02.011

Ribeiro, A. S., and Paredes, J. (2014). P-Cadherin Linking Breast Cancer Stem Cells and Invasion: A Promising Marker to Identify an "Intermediate/Metastable" EMT State. *Front Oncol,* **4**, 371. doi: 10.3389/fonc.2014.00371

Ritossa, F. (1962). A new puffing pattern induced by temperature shock and DNP in drosophila. *Experientia,* **18**(12), 571-573. doi: 10.1007/BF02172188

Sanger, N., Effenberger, K. E., Riethdorf, S., Van Haasteren, V., Gauwerky, J., Wiegratz, I., Strebhardt, K., Kaufmann, M., and Pantel, K. (2011). Disseminated tumor cells in the bone marrow of patients with ductal carcinoma in situ. *Int J Cancer,* **129**(10), 2522-2526. doi: 10.1002/ijc.25895

Satyal, S. H., Chen, D., Fox, S. G., Kramer, J. M., and Morimoto, R. I. (1998). Negative regulation of the heat shock transcriptional response by HSBP1. *Genes Dev,* **12**(13), 1962-1974.

Saucedo-Zeni, N., Mewes, S., Niestroj, R., Gasiorowski, L., Murawa, D., Nowaczyk, P., Tomasi, T., Weber, E., Dworacki, G., Morgenthaler, N. G., Jansen, H., Propping, C., Sterzynska, K., Dyszkiewicz, W., Zabel, M., Kiechle, M., Reuning, U., Schmitt, M., and Lucke, K. (2012). A novel method for the in vivo

isolation of circulating tumor cells from peripheral blood of cancer patients using a functionalized and structured medical wire. *Int J Oncol*. doi: 10.3892/ijo.2012.1557

Schildkopf, P., Frey, B., Ott, O. J., Rubner, Y., Multhoff, G., Sauer, R., Fietkau, R., and Gaipl, U. S. (2011). Radiation combined with hyperthermia induces HSP70-dependent maturation of dendritic cells and release of pro-inflammatory cytokines by dendritic cells and macrophages. *Radiother Oncol,* **101**(1), 109-115. doi: 10.1016/j.radonc.2011.05.056

Schilling, D., Gehrmann, M., Steinem, C., De Maio, A., Pockley, A. G., Abend, M., Molls, M., and Multhoff, G. (2009). Binding of heat shock protein 70 to extracellular phosphatidylserine promotes killing of normoxic and hypoxic tumor cells. *FASEB J,* **23**(8), 2467-2477. doi: 10.1096/fj.08-125229

Shevtsov, M. A., Nikolaev, B. P., Ryzhov, V. A., Yakovleva, L. Y., Marchenko, Y. Y., Parr, M. A., Rolich, V. I., Mikhrina, A. L., Dobrodumov, A. V., Pitkin, E., and Multhoff, G. (2015). Ionizing radiation improves glioma-specific targeting of superparamagnetic iron oxide nanoparticles conjugated with cmHsp70.1 monoclonal antibodies (SPION-cmHsp70.1). *Nanoscale,* **7**(48), 20652-20664. doi: 10.1039/c5nr06521f

Shi, Y., Mosser, D. D., and Morimoto, R. I. (1998). Molecular chaperones as HSF1-specific transcriptional repressors. *Genes Dev,* **12**(5), 654-666.

Specht, H. M., Ahrens, N., Blankenstein, C., Duell, T., Fietkau, R., Gaipl, U. S., Gunther, C., Gunther, S., Habl, G., Hautmann, H., Hautmann, M., Huber, R. M., Molls, M., Offner, R., Rodel, C., Rodel, F., Schutz, M., Combs, S. E., and Multhoff, G. (2015). Heat Shock Protein 70 (Hsp70) Peptide Activated Natural Killer (NK) Cells for the Treatment of Patients with Non-Small Cell Lung Cancer (NSCLC) after Radiochemotherapy (RCTx) - From Preclinical Studies to a Clinical Phase II Trial. *Front Immunol,* **6**, 162. doi: 10.3389/fimmu.2015.00162

Speicher, M. R., and Pantel, K. (2014). Tumor signatures in the blood. *Nat Biotechnol,* **32**(5), 441-443. doi: 10.1038/nbt.2897

Stangl, S., Gehrmann, M., Riegger, J., Kuhs, K., Riederer, I., Sievert, W., Hube, K., Mocikat, R., Dressel, R., Kremmer, E., Pockley, A. G., Friedrich, L., Vigh, L., Skerra, A., and Multhoff, G. (2011). Targeting membrane heat-shock protein 70 (Hsp70) on tumors by cmHsp70.1 antibody. *Proc Natl Acad Sci U S A,* **108**(2), 733-738. doi: 10.1073/pnas.1016065108

Stangl, S., Varga, J., Freysoldt, B., Trajkovic-Arsic, M., Siveke, J. T., Greten, F. R., Ntziachristos, V., and Multhoff, G. (2014). Selective in vivo imaging of

syngeneic, spontaneous, and xenograft tumors using a novel tumor cell-specific hsp70 peptide-based probe. *Cancer Res,* **74**(23), 6903-6912. doi: 10.1158/0008-5472.CAN-14-0413

Statistisches Bundesamt. (2015). Krebs war 2013 die zweithäufigste Todesursache [Press release] 34/15. *Destatis. Retrieved from: https://www.destatis.de/DE/PresseService/Presse/Pressemitteilungen/2015/02/PD15_034_232.html, Access Date: 02/02/2015*

Stewart, B. W., and Wild, C. P. (2014). World Cancer Report. *International Agency for Research on Cancer, WHO*. ISBN: 978-92-832-0429-9, *URL: http://www.iarc.fr/en/publications/books/wcr/index.php*, *Access Date*: *08/25/2015*

Stott, S. L., Hsu, C. H., Tsukrov, D. I., Yu, M., Miyamoto, D. T., Waltman, B. A., Rothenberg, S. M., Shah, A. M., Smas, M. E., Korir, G. K., Floyd, F. P., Jr., Gilman, A. J., Lord, J. B., Winokur, D., Springer, S., Irimia, D., Nagrath, S., Sequist, L. V., Lee, R. J., Isselbacher, K. J., Maheswaran, S., Haber, D. A., and Toner, M. (2010). Isolation of circulating tumor cells using a microvortex-generating herringbone-chip. *Proc Natl Acad Sci U S A,* **107**(43), 18392-18397. doi: 10.1073/pnas.1012539107

Stott, S. L., Lee, R. J., Nagrath, S., Yu, M., Miyamoto, D. T., Ulkus, L., Inserra, E. J., Ulman, M., Springer, S., Nakamura, Z., Moore, A. L., Tsukrov, D. I., Kempner, M. E., Dahl, D. M., Wu, C. L., Iafrate, A. J., Smith, M. R., Tompkins, R. G., Sequist, L. V., Toner, M., Haber, D. A., and Maheswaran, S. (2010). Isolation and characterization of circulating tumor cells from patients with localized and metastatic prostate cancer. *Sci Transl Med,* **2**(25), 25ra23. doi: 10.1126/scitranslmed.3000403

Stuart, R. A., Cyr, D. M., Craig, E. A., and Neupert, W. (1994). Mitochondrial molecular chaperones: their role in protein translocation. *Trends Biochem Sci,* **19**(2), 87-92. doi: 10.1016/0968-0004(94)90041-8

Tan, S. J., Lakshmi, R. L., Chen, P., Lim, W. T., Yobas, L., and Lim, C. T. (2010). Versatile label free biochip for the detection of circulating tumor cells from peripheral blood in cancer patients. *Biosens Bioelectron,* **26**(4), 1701-1705. doi: 10.1016/j.bios.2010.07.054

Thery, C., Ostrowski, M., and Segura, E. (2009). Membrane vesicles as conveyors of immune responses. *Nat Rev Immunol,* **9**(8), 581-593. doi: 10.1038/nri2567

Tibbe, A. G., Miller, M. C., and Terstappen, L. W. (2007). Statistical considerations for enumeration of circulating tumor cells. *Cytometry A,* **71**(3), 154-162. doi: 10.1002/cyto.a.20369

Vanharanta, S., and Massague, J. (2013). Origins of metastatic traits. *Cancer Cell,* **24**(4), 410-421. doi: 10.1016/j.ccr.2013.09.007

Vega, V. L., Rodriguez-Silva, M., Frey, T., Gehrmann, M., Diaz, J. C., Steinem, C., Multhoff, G., Arispe, N., and De Maio, A. (2008). Hsp70 translocates into the plasma membrane after stress and is released into the extracellular environment in a membrane-associated form that activates macrophages. *J Immunol,* **180**(6), 4299-4307.

Vignot, S., Besse, B., Andre, F., Spano, J. P., and Soria, J. C. (2012). Discrepancies between primary tumor and metastasis: a literature review on clinically established biomarkers. *Crit Rev Oncol Hematol,* **84**(3), 301-313. doi: 10.1016/j.critrevonc.2012.05.002

Vona, G., Sabile, A., Louha, M., Sitruk, V., Romana, S., Schutze, K., Capron, F., Franco, D., Pazzagli, M., Vekemans, M., Lacour, B., Brechot, C., and Paterlini-Brechot, P. (2000). Isolation by size of epithelial tumor cells : a new method for the immunomorphological and molecular characterization of circulatingtumor cells. *Am J Pathol,* **156**(1), 57-63. doi: 10.1016/S0002-9440(10)64706-2

Wallace, P. K., Tario, J. D., Jr., Fisher, J. L., Wallace, S. S., Ernstoff, M. S., and Muirhead, K. A. (2008). Tracking antigen-driven responses by flow cytometry: monitoring proliferation by dye dilution. *Cytometry A,* **73**(11), 1019-1034. doi: 10.1002/cyto.a.20619

Weisser, N. E., and Hall, J. C. (2009). Applications of single-chain variable fragment antibodies in therapeutics and diagnostics. *Biotechnol Adv,* **27**(4), 502-520. doi: 10.1016/j.biotechadv.2009.04.004

Wu, C. (1995). Heat shock transcription factors: structure and regulation. *Annu Rev Cell Dev Biol,* **11**, 441-469. doi: 10.1146/annurev.cb.11.110195.002301

Yang, L., Lang, J. C., Balasubramanian, P., Jatana, K. R., Schuller, D., Agrawal, A., Zborowski, M., and Chalmers, J. J. (2009). Optimization of an enrichment process for circulating tumor cells from the blood of head and neck cancer patients through depletion of normal cells. *Biotechnol Bioeng,* **102**(2), 521-534. doi: 10.1002/bit.22066

Yu, M., Bardia, A., Wittner, B. S., Stott, S. L., Smas, M. E., Ting, D. T., Isakoff, S. J., Ciciliano, J. C., Wells, M. N., Shah, A. M., Concannon, K. F., Donaldson, M. C., Sequist, L. V., Brachtel, E., Sgroi, D., Baselga, J., Ramaswamy, S., Toner, M., Haber, D. A., and Maheswaran, S. (2013). Circulating breast tumor cells exhibit dynamic changes in epithelial and mesenchymal composition. *Science,* **339**(6119), 580-584. doi: 10.1126/science.1228522

Zhang, C., Li, C., He, F., Cai, Y., and Yang, H. (2011). Identification of CD44+CD24+ gastric cancer stem cells. *J Cancer Res Clin Oncol,* **137**(11), 1679-1686. doi: 10.1007/s00432-011-1038-5

Zheng, S., Lin, H. K., Lu, B., Williams, A., Datar, R., Cote, R. J., and Tai, Y. C. (2011). 3D microfilter device for viable circulating tumor cell (CTC) enrichment from blood. *Biomed Microdevices,* **13**(1), 203-213. doi: 10.1007/s10544-010-9485-3

Zhu, X., Zhao, X., Burkholder, W. F., Gragerov, A., Ogata, C. M., Gottesman, M. E., and Hendrickson, W. A. (1996). Structural analysis of substrate binding by the molecular chaperone DnaK. *Science,* **272**(5268), 1606-1614.

6 Appendix

6.1 Patient Characteristics

Table 5: Clinicopathological characteristics of head and neck cancer patients. SCCHN: squamous cell carcinoma of the head and neck.

Patient #	Tumor Location	Histology	Staging			Grading
1	hypopharynx	SCCHN	T1	N0	M0	G2
2	hypopharynx	SCCHN	T3	N2b	M0	G3
3	hypopharynx	SCCHN	T1	N0	M0	G3
4	larynx	SCCHN	T3	N2	M0	G2
5	larynx	SCCHN	T3	N0	M0	G3
6	larynx	SCCHN	T4	N1	M0	G3
7	larynx	SCCHN	T3	N0	M0	G2
8	larynx	SCCHN	T4a	N0	M0	G3
9	naso/oro/hypopharynx	SCCHN	T4c	N2c	M0	G2
10	naso/oro/hypopharynx	SCCHN	T3-4a	N2c	M0	G3
11	nasopharynx	SCCHN	T2	N0	M0	G1
12	oral cavity	SCCHN	T1	N0	M0	G2
13	oro/hypopharynx	SCCHN	T2	N2b	M0	G3
14	oro/hypopharynx	SCCHN	T2	N2a	M0	G2
15	oropharynx	SCCHN	T4a	N2c	M0	G3
16	oropharynx	SCCHN	T3	N0	M0	G3
17	oropharynx	SCCHN	T1	N2b	M0	G2
18	oropharynx	SCCHN	T1a	N0	M0	G2
19	oropharynx	SCCHN	T4	N0	M0	G2
20	oropharynx	SCCHN	T2	N2b	M0	G3
21	oropharynx	SCCHN	T4	N0	M0	G3
22	oropharynx	SCCHN	T2	N1	M0	G3
23	paranasal sinus	SCCHN	T2	N0	M0	G3

Table 6: Clinicopathological characteristics of lung cancer patients. NSCLC: non-small cell lung cancer, SCLC: small cell lung cancer.

Patient #	Histology	Staging			Grading
1	NSCLC adeno	T2	N2	M1	G3
2	NSCLC adeno	T4	N2	M0	G2
3	NSCLC adeno	T2	N2	M0	G3
4	NSCLC adeno	T3	N3	M1	G3
5	NSCLC adeno	T4	N2	M1	G3
6	NSCLC adeno	T2	N0	M0	G2
7	NSCLC adeno	T1	N3	M0	G3
8	NSCLC adeno	T2	N2	M1	G2
9	NSCLC squamous	T3	N3	M1	G3
10	NSCLC squamous	T3	N3	M1	G3
11	NSCLC squamous	T4	N0	M0	G2
12	NSCLC squamous	T1	N0	M0	G3
13	NSCLC squamous	T4	N2	M0	G3
14	NSCLC squamous	T4	N3	M1	G3
15	NSCLC squamous	T3	N3	M0	G3
16	NSCLC squamous	T3	N2	M1	G3
17	NSCLC squamous	T4	N2	M1	G3
18	NSCLC squamous	T3	N2	M1	G2
19	SCLC	limited			-
20	SCLC	extensive			-
21	SCLC	extensive			-
22	SCLC	extensive			-

Table 7: Clinicopathological characteristics of colorectal carcinoma patients. c: stagingby clinical examination, u: staging by ultrasonography

Patient #	Staging			Grading
1	uT3	uN+	MX	G2
2	uT3	uN0	cM0	G2
3	cT3	cN+	cM0	G2
4	cT3	cN1	cM0	G2
5	cT3	cN1	cM1	G2
6	cT3	cN0	cM0	G2
7	cT3	cN0	cM0	G2
8	uT3	uN0	cM0	G2
9	cT3	cN2	cM0	G2
10	cT3	uN0/cN+	M0	
11	cT3	cN+	cM0	G2
12	uT3	cNX	cM0	G2
13	cT3	cN1	cM0	G2
14	uT3	uN1	cM0	G2
15	uT3	cN0	cM0	G2
16	cT2	cN1	cM0	G2
17	cT3	cN2	MX	G2
18	cT3	cN2	cM0	G2
19	cT3a	cN2	cM0	
20	cT3-4	cN+	cM0	G2
21	cT3	cN0	cM0	G2
22	cT3	cN1	cM0	G3
23	uT3c	N0	cM0	G2
24	uT3	uN0	cM0	G2
25	cT4	cN1	cM0	G2
26	uT3	uN2	cM0	G2
27	uT3	uN1	cM0	G2
28	uT3	uN1	cM0	G2
29	uT3	N+	cM0	G2
30	cT3	cN0	cM0	
31	cT3	cN1	cM0	G2
32	cT3	cN2	cM1	G2
33	T3	N2	M0	G2
34	cT3	cN0	M0	G2
35	uT3	uN0	cM0	
36	cT3	cN+	cM0	
37	cT3	cN0	cM0	
38	cT2	uN0	M0	G2
39	cT3	cN+	cM0	G2
40	uT3	uN1	cM0	G2
41	uT3b-4	cN+	cM0	
42	uT3	uN1	cM0	G2
43	cT3	cN+	cM0	G2
44	cT3	uN1	cM0	G2

Table 8: Clinicopathological characteristics of pancreatic cancer patients.

Patient #	Tumor Location	Staging			Grading
1	body	T3	N0	M0	G2
2	body/tail	T2	N1	M1	-
3	body/tail	T4	N2	M1	-
4	body/tail	T4	N2	M1	-
5	body/tail	T1	N1	M1	-
6	body/tail	T4	N2	M1	-
7	body/tail	T3	N1	M0	-
8	body/tail	T4	N2	M1	-
9	body/tail	T4	N3	M1	-
10	head	T3	N1	M0	G2
11	head	T4	N1	M0	G2
12	head	T3	N0	M0	G2
13	head	T3	N1	M0	G1
14	head	T3	N1	M0	G2
15	head	T3	N0	M0	G1
16	head	T3	N1	M0	G2
17	head	T1	N0	M0	G3
18	head	T3	N1	M0	G3
19	head	T3	N1	M0	G3
20	head	T3	N1	M0	G3
21	head	T4	N2	M1	-
22	head	T3	N1	M0	-
23	head	T3	N2	M1	-
24	head	T3	N2	M1	-
25	head	T2	N1	M0	-
26	head	T3	N2	M1	-
27	head	T2	N1	M1	-
28	head	T2	N0	M0	-
29	head	T3	N1	M0	-
30	head	T2	N0	M0	-
31	head	T2	N1	M0	-
32	head	T4	N2	M1	-
33	head	T2	N1	M1	-
34	head	T3	N1	M1	-
35	head/body/tail	T4	N2	M1	-
36	head/tail	T1	N0	M0	G1
37	head/uncinate process	T2	N0	M0	-
38	head/uncinate process	T3	N2	M1	-
39	head/uncinate process	T2	N0	M0	-
40	head/uncinate process	T4	N2	M1	-
41	tail	T4	N1	M0	G3
42	tail	T3	N1	M0	G2
43	tail	T3	N0	M0	G2
44	tail	T4	N3	M1	-
45	uncinate process	T3	N1	M0	-
46	uncinate process	T2	N0	M0	-

Table 9: Clinicopathological characteristics of glioblastoma patients.

Patient #	Tumor Origin	Grading
1	primary	G4
2	primary	G4
3	primary	G4
4	primary	G4
5	primary	G4
6	primary	G4
7	primary	G4
8	primary	G4
9	primary	G4
10	primary	G4
11	primary	G4
12	primary	G4
13	primary	G4
14	primary	G4
15	primary	G4
16	primary	G4
17	primary	G4
18	primary	G4
19	primary	G4
20	primary	
21	secondary	G4
22	secondary	G4
23	secondary	G4
24	secondary	G4
25	secondary	G4
26	secondary	G4
27	secondary	G4
28	secondary	G4
29	secondary	G4
30	secondary	

Table 10: Clinicopathological characteristics of patients with hematological malignancies. ALL: acute lymphoid leukemia, AML: acute myeloid leukemia, BAL: biphenotypic acute leukemia, CML: chronic myeloidleukemia, MDS: myelodysplastic syndrome, MPS: myeloproliferative syndrome, NHL: Non-Hodgkin lymphoma

Patient #	Hematological Disease
1	ALL
2	AML
3	AML
4	AML
5	AML
6	AML
7	AML
8	AML
9	AML
10	AML
11	AML
12	BAL
13	CML
14	Hodgkin lymphoma
15	Hodgkin lymphoma
16	Hodgkin lymphoma
17	MDS & MPS
18	Multiple myeloma
19	Multiple myeloma
20	Multiple myeloma
21	MDS
22	MDS
23	MDS
24	MDS
25	MDS
26	MDS
27	MDS
28	NHL
29	NHL
30	NHL
31	NHL
32	Secondary acute leukemia

6.2 Acknowledgements

At this point I would like to thank all those who have contributed their valuable support to the completion of this work.

I am especially thankful to my supervisor Prof. Dr. Gabriele Multhoff, for giving me the opportunity to work on this interesting project, for her scientific advice and the valuable discussions.

I would like to thank PD Dr. Thomas Schmid for taking over the role of second reviewer and his valuable comments during the completion of this work. My thanks also go to Prof. Dr. Bernhard Küster for agreeing to be Chairman of the Examining Board.

My special thanks go to PD Dr. Mathias Gehrmann, for his guidance and support with the daily struggles of lab work; to Dr. Daniela Schilling for her invaluable time and support during the completion of this work; to Janina Schwarzer for being my partner during all ups and downs of this project; to all former and present members of the group and some of the neighboring groups, especially Andrea Mair, Dr. Andreas Kirschner, Anett Lange, Dr. Annett Kühnel, Dr. Christine Bayer, Jessica Pelzel, Dr. Julia Albrecht, Dr. Michael Düwel, Dr. Stefan Stangl and Dr. Wolfgang Sievert, for their constant support in and outside the lab and their friendship, for making me laugh and keeping me motivated.

Finally my thanks go to my family, especially my parents, sister and husband, for their love, motivation, patience and never-ending support.

6.3 Eidesstattliche Erklärung

Ich, Stephanie Breuninger, erkläre an Eides statt, dass ich die der Fakultät Wissenschaftszentrum Weihenstephan für Ernährung, Landnutzung und Umwelt (WZW) der Technischen Universität München zur Promotionsprüfung vorgelegte Arbeit mit dem Titel:

“Utilizing Heat Shock Protein 70 (Hsp70) as a Tumor-Specific Blood Biomarker and for the Isolation of Circulating Tumor Cells (CTCs)”

am Lehrstuhl für Experimentelle Radioonkologie und Strahlentherapie am Klinikum rechts der Isar der TU München unter der Anleitung und Betreuung durch Frau Prof. Dr. Gabriele Multhoff ohne sonstige Hilfe erstellt und bei der Abfassung nur die gemäß § 6 Abs. 5 angegebenen Hilfsmittel benutzt habe.

Ich habe keine Organisation eingeschaltet, die gegen Entgelt Betreuerinnen und Betreuer für die Anfertigung von Dissertation sucht, oder die mir obliegenden Pflichten hinsichtlich der Prüfungsleistungen für mich ganz oder teilweise erledigt.

Ich habe die Dissertation in dieser oder ähnlicher Form in keinem anderen Prüfungsverfahren als Prüfungsleistung vorgelegt.

Ich habe den angestrebten Doktorgrad noch nicht erworben und bin nicht in einem früheren Promotionsverfahren für den angestrebten Doktorgrad endgültig gescheitert.

Die Promotionsordnung der Technischen Universität München ist mir bekannt.

München, den _____ _____

Stephanie Breuninger